UNIVERSITA' POLITECNICA DELLE MARCHE

SCUOLA DI DOTTORATO DI RICERCA XIII CICLO

FACOLTA' DI MEDICINA E CHIRURGIA

Curriculum in Oncologia, nuove tecnologie in Chirurgia

Dipartimento di Scienze Cliniche Specialistiche ed Odontostomatologiche

CELLULAR EXPRESSION AND TRAFFICKING OF STRESS-INDUCED MOLECULES IN CANCER

Tutor:

Prof.ssa Franca Saccucci

Dottoranda:

Dott.ssa Francesca Leoni

Anno Accademico 2015/2016

TABLE OF CONTENTS

CHAPTER 1: INTRODUCTION

Beside their canonical chaperone function, Heat Shock Protein (HSPs) have been considered stress proteins and cellular signals in communication between cells and their interaction with the immune system need to be addressed more in detail. Although there are increasing evidences that HSPs are associated with plasma membranes and can be actively secreted from stressed cells, there is no agreement in the literature about the mechanism of secretion and the type of stress needed for chaperone induction. Experimental data suggest that HSP movement can be stress and cell type dependent. The work presented here aimed to explore the cytoplasmic stress and the endoplasmic reticulum stress in haematological malignancies and explore possible ways of cellular communication of stress to distant cells, through the investigation of mechanisms of Hsp surface presentation to plasma membrane and release in response to cellular stress such as heat shock. The investigation is focused in the role of extracellular vesicles such as exosomes in cellular crosstalk. The work concentrates in the analysis of the cytoplasmic inducible form of the Hsp72 family, HSPA1A, and the corresponding endoplasmic reticulum protein, Grp78 together with other endoplasmic reticulum stress-related proteins.

1.1 The stress response

The cellular stress response is variety of molecular changes that cells experience in response to environmental stresses such as high temperatures, toxins and oxidative stress, but also internal stresses such as diseases. The mechanisms activated in cells are adaptive and aim to protect the whole organism against unfavourable environmental conditions, through short term responses that control cell damage, and through longer term responses that promote apoptosis of the damaged cells and protect the whole organism. Stress response mechanisms operate in every cellular compartment and many molecules are specifically activated. Between all, chaperones plays a crucial role in cellular stress response. Chaperones are present in every cellular compartment but the cytoplasmic stress response, with Hsp72 activation, and the endoplasmic reticulum stress response, with activation chaperones belonging to the Unfolded Protein response Pathway, are the most important ones. The present study focus its attention on the cytoplasmic stress response, looking at the Hsp72/HSPA1A induction and movement to the extracellular space and the endoplasmic reticulum chaperone Grp78 and its related proteins, looking at unfolded protein response (UPR) activation.

1.2 The heat shock proteins (HSPs) family

Heat Shock proteins (HSPs) are evolutionary conserved protein crucial for cell viability and involved in many cellular processes, and their expression depends on their association with other components and the stress applied. HSPs are well known as chaperones: they refold denatured or damaged proteins in response to many cellular stresses: heat, oxidative stress, chemicals treatments, UV radiation, physiological and psychological stress and when the protein are too damaged, they deliver the impaired proteins to degradation by ubiquitination or lysosomic proteolysis [1]. Although there are constitutively expressed chaperones that regulate normal protein folding, most of the HSPs are induced in response to stress, where a higher amount of intracellular proteins are likely to be denaturated.

HSPs have been classified into families, according to their approximate molecular weight. The five main groups are Hsp100, Hsp90, Hsp70, Hsp60 and the small HSPs that can be expressed in the cytoplasm or in the cellular organelles like mitochondria or endoplasmic reticulum. Members of a given family also possess several other features in common: they show, for example, a high degree of sequence homology among different species [2].

Heat shock protein nomenclature is quite complicated: Hsp70 for example can be named in several ways depending on the cell compartment where is expressed and whether is constitutively expressed or induced by stress: Hsp72-1, Hsp72, HSPA1, Hsp72-2, Grp78, HSC70 and GRP75.

Hence a new nomenclature system established that the gene names can be used for their correspondent protein product: the systematic gene symbol that have been assigned by the HUGO gene nomenclature committee and is the one used in the National Centre of Biotechnology Information Entrez Gene database for the heat shock genes [3].

The present study will focus the attention on two chaperones: the cytoplasmatic inducible form of Hsp72, referring to the HSPA1A gene product (the new protein name is HSPA1A) [3] and the endoplasmic reticulum Hsp72 also called Grp78.

1.3 The cytoplasmic Hsp72/HSPA1A and the importance of its location

Hsp72 can be expressed at low levels in normal cells both *in vitro* and *in-vivo* and their expression and release can be modified with several physiological stresses. However patients with different types of disease or transformed cell lines often present abnormal levels of the protein and strictly associate with the disease like various auto-inflammatory diseases and cancer: this aberrant protein synthesis or release in diseases suggests that heat shock proteins participate in the development of the disease or at least is a direct consequence [1]. In particular Hsp72 has been found to be over-expressed in several human malignant cell lines, in cancer tissues and in the serum of patients [1, 4]. Hsp72 seems to be implicated in tumour cell proliferation, differentiation, invasion, metastasis, death, and recognition by the immune system [1, 5-7]. Hsp72 in cancer cells possess dual contrasting effects depending on the cell localization:

1.3.1 Intracellular Hsp72 overexpression

Intracellular Hsp72 overexpression promotes cancer development by suppression of various anticancer mechanisms, like apoptosis, senescence as well as by facilitating expression of metastatic genes. Hsp72 is a potent anti-apoptotic protein since it interferes at several levels in the different apoptotic pathways and stimulates cell survival of cancer cells. Hsp72 over-expression appears to inhibit FAS-induced apoptosis [8]. Heat shock

proteins bind to pro-caspases, inhibiting their activation [9-11] but interfere with several caspase-independent pathways as well [12]. Hsp72 depletion is sufficient to induce apoptosis through caspase-3 activation in the absence of any additional stress stimulus [6, 13].

1.3.2 Surface Hsp72 overexpression

When Hsp72 is overexpressed on the cell surface it facilitate tumour rejection by immune system, though innate and adaptive immunity. Hsp72 surface expression has been found in many types of cancer such as colon, lung, pancreas, mammary head and neck and in metastases derived from them [1, 14]; high level of surface Hsp72 has also been found in bone marrow from haematological malignancies including acute and chronic myeloid leukemia [15]. Tumour cells that have high levels of surface Hsp72 have an increased immunogenicity compared to a low expressing cells line since they are a target recognised by NK cells [16]. Hsp72 has been demonstrated to be embedded in the cell membrane and the part of the Hsp72 protein that extrudes from the membrane triggers the NK mediated immune response. Incubation of NK cells with cytokines and soluble Hsp72 or TKD peptide, enhance cell surface density of activating NK cells receptors including CD94 [17] which seems to interact with Hsp72 on the surface of tumour released exosomes [18]. The assumption that cells expressing high levels of surface Hsp72 are more sensitive to NK attack is under investigation to test potential therapies to combine with standard chemotherapy [19, 20].

1.3.3 Extracellular Hsp72

Released Hsp72, in combination with the tumour antigens are up-taken by the antigen presenting cells (APC), processed via proteasome TAP-dependent pathway and cross presented on the MHC class I complex [21-23]. The role of Hsp72 is to facilitate the internalization, the processing and the cross presentation of the tumour antigens to the MHC class I on APC. Hsp72 purified from tumours have the ability to cross-present tumour antigens to APCs and activate the immune response: MHC class I presentation determines an antigen specific CD8 T-cell mediated initiation of the immune response in *in vitro* mouse models [22, 24-26].

Hsp72 acts as a potential “danger signal” by interacting with the immune response as the danger model propose [27]. However, despite the classic danger model by Matzinger assuming that endogenous components of the cells are released in the extracellular compartment as a result of necrosis or tissue damage, Hsp72 can be actively secreted from non-dying cells [28]. This would allow the Hsp72 protein to deliver a different message to the organism and cause a differential immune response [28].

Extracellular Hsp72 is not just important for immune system activation but also for cellular protection in response to stress. A direct administration of the protein to cells confered cytoprotection when heat shock was applied [29]. Hsp72 release from glial cells has been showed in conjuntion with an enhanced neuronal stress tolerance [30] and a direct external Hsp72 administration rendered the cells more likely to survive injury than their naïve counterparts [31] and has an hypothermic and somnogenic effects in brain tissues [32]. Extracellular Hsp72 has a protective effect during sepsis [33] suggesting that there is an effective cellular protection against stress. These phenomena have great potential significance in the development of neuroprotective therapeutic strategies utilizing the heat shock protein response.

1.3.4 Extracellular Hsp72 in vesicles

It is currently unclear whether Hsp72 released as free soluble protein, in combination with membranes or in detergent soluble membrane vesicles or even all of the above. There are more evidences that demonstrate that Hsp72 can be actively released from pancreatic and colon tumour cell lines associated with membrane structures called exosomes [18]. Exosomes in some cellular models are efficient transport vesicles for Hsp72 from the endosomal compartment into the extracellular space [18, 34]. Studies have also shown that membrane associated released Hsp72 activate the macrophages *via* TNF-α release with a much higher efficiency than the soluble form [35]. The exosomal surface appears to reflect the markers of the tumour cell from which it was derived, with the same relative levels of Hsp72/Bag4: exosomes surface with high level of Hsp72/Bag4 stimulated the migration of CD94+ NK cells towards the surface Hsp72 positive tumour cells and increased the cytoloytic activity of these NK cells [18]. Membrane associated Hsp72 released from cells has also been demonstrated to activate with more efficiency than the correspondent free form in order to activate the macrophage, measured as TNF-α release [35].

1.3.5 Mechanisms of Hsp72 release

According to the literature, several cells line models have demonstrated the active release of Hsp72. However, the results obtained regarding the mechanisms involved are contrasting and several proposed way have been considered.

- *Necrosis vs Apoptosis*

Early evidences showed that extracellular Hsp72 is a result of necrotic cell death: Hsp72 released from dying cells is a potent inflammatory inducer together with many other cell product released in the extracellular compartment, like cytokines [36, 37].

- *Classical release pathways*

Some groups support the idea that Hsp72 is released following the classical release pathway mainly providing with data where Hsp72 release is blocked by classical pathway transport inhibitors such as Monensin or Brefeldin-A [35]. Despite those findings many other works have shown the opposite results demonstrating that Hsp72 release couldn't be blocked with the classical-release pathway inhibitors. Considering that Hsp72 is a leaderless protein, so it wouldn't necessary need to go for processing through the ER and Golgi as the classical pathway require, it is more likely that the release mechanism follows a non-classical pathway.

- *Non-classical release: lipid rafts associated release*

Hsp72 associates with detergent resistant micro-domains enriched in cholesterol and sphingolipids which form a distinct, liquid ordered phase in the lipid bilayer of membrane that serves as major assembly and sorting platforms for signal transduction complexes: the structures are also called lipid rafts. Hsp72 forms ion channels in *in-vitro* lipid models resembling the plasma membrane structures [38]. *In-vitro* models also showed that Hsp72 can interact with phosphatidylserine (PS), a lipid component of the LR structures [39], and that it can bind to the lipid raft component ganglioside-M1 (GM-1) [40]. Heat shocked cells express surface Hsp72 in relation with lipid rafts and secrete them in the extracellular environment [41]. Monensin and Brefeldin A, drugs used to perturb classical protein traffic, did not reduce this effect, determining the release of Hsp72 from cells is independent of the classical secretory route [41-43]. When a cholesterol disrupting agent, methyl-β-

cyclodextrin, was added to the cells Hsp72 release was abrogated, suggesting that Hsp72 localises preferentially in lipid rafts whose integrity is required for active release [41, 43]. Extracellular Hsp72 was demonstrated to bind the macrophage plasma membrane, specifically on its lipid raft microdomain, which caused a disruption of the lipid rafts and abrogated the Hsp72-mediated increase in phagocytosis and enhanced the processing and presentation of internalised antigens [44]. Endogenous Hsp72, up-regulated following a bacterial attack, also binds to the surface of macrophages through the TLR-4 and CD14 receptors: these associations seems to take place within the lipid rafts structures [45]. All these evidences support the idea that Hsp72 can directly bind to membranes by interacting with lipids. Recently it has being raised the hypothesis, mainly using thermal stress models, that cellular stress is detected by the plasma membrane which modify its fluidity and transduce the stress signal to intracellular pathways involving activation of RAF and PI3K with activation the heat shock factor with consequent HSPs over-expression and membrane insertion [46]; in other words plasma membrane could be considered a cellular stress thermometer and HSPs could act as membrane stabilisers. It's interesting to underline that membrane defects are associated with various physiological states such as ageing and are simultaneous with a deregulation of heat shock protein synthesis [46].

- *Exosomes associated release*

Exosomes represent a specific subtype of extracellular vesicles, between 30 and 100 nm in diameter, especially rich in cytosolic and membrane proteins, nucleic acids such as microRNAs, hormones and growth factors [47]. The exosomes are isolated, as well as from cell cultures, from many biological fluids such as blood, saliva, urine and breast milk. Today they represent one of the latest and more promising discoveries regarding intercellular communication [47, 48] as they are involved in many processes such as regulation of immune system, infectious and autoimmune diseases and cancer [49]. Exosomes are distinguished from other extracellular vesicles [50] for their cellular origin rather than by their size or their shape. Exosomes are vesicles that are released from cells following fusion of multivesicular bodies (MVBs) with the cell membrane [51, 52], while microvesicles are defines as vesicles that form from the plasma membrane. The MVBs are organelles that originate from early endosomes; they are enriched of intraluminal vesicles, (ILVs) that form following endosomal membrane invagination. The MVBs can be considered a sort of late

endosomes involved in the endocytic pathway receptor mediated. Exosomes contribute to the release of Hsp72 from human peripheral blood mononuclear cells (PBMCs) during basal conditions and in response to heat shock cellular stress. Vesicles structure consist of lipid raft regions embedded with ligands common to the original cell membrane. Exosome vesicles released from cancer cells showed the presence of surface Hsp72 in combination with lipid rafts [18, 53] demonstrating that a possible combination of the proposed release pathways could occur in different cell models. Hsp72 can be released from heat shocked PBMCs via an exosome-dependent pathway [18, 34]. Exosomes were produced by B-lymphoblastoid and Jurkat cell lines where a time-dependent increase in Hsp72 could be identified. The Hsp72 was located within the exosome lumen following heat stress with no interaction of Hsp72 with the exosome surface, thus suggesting that such exosomes may not interact with cells through cell-surface Hsp72-receptors and demonstrating that Hsp72 levels increase in proportion to the degree of stress [54]. However different cellular models give differential results. Tumour-derived exosomes containing high levels of Hsp72 in their lumen stimulate NK activation. Examination of the plasma membrane of tumour cells and of the secreted exosomes revealed selective Hsp72/Bag-4 expression, high levels on the exosomal surface of Colo+ pancreas and CX+ colon carcinoma tumour sublines and low levels on Colo- and CX- tumour sublines. Results show identical Hsp72/Bag-4 content in exosomal lumen however on the surface of exosomes the Hsp72/Bag-4 content reflected the tumour cell membranes from which they were derived. Colo+ and CX+ tumour cells expressing high levels of Hp72/Bag-4 were found to be susceptible to cytolytic attack by CD94+ NK cells after stimulation with IL-2 plus TKD, due to the Hsp72/Bag-4 surface-positive exosomes initiating migration in CD94+ NK cells [18].

- *Lysosome pathway*

Hsp72 does not have the consensus secretory signal, so it cannot pass through the plasma membrane using any classical mechanism lead to hypothesise different release pathways, one of which is the endolysomal pathway. Hsp72 has been showed to bind intracellularly with lysosomes membranes in Hsp72 over-expressing colon carcinoma cells and immortalized murine embryonic fibroblasts (MEFs); the Hsp72 protects the lysosomal membrane from permeabilization and cell death induced by tumor necrosis factor, etoposide and H_2O_2 suggesting a lysosomes membrane stabilization role of Hsp72 [5].

Mambula et al demonstrated that Hsp72 release from human prostate cancer cells following heat shock, passes through the endolysosomal compartment: inhibition of lysosomal transport using a lysomotropic compound, blocks Hsp72 secretion. Purified lysosomal compartment possesses high level of Hsp72. The increase of surface Hsp72 after heat shock highly correlates with increase of surface LAMP1, a lysosome marker. The release is quick and occurs before any detectable increase in gene expression suggesting that heat shock directly induces the secretion of Hsp72 without activation of the heat shock factors and seems to be an independent aspect of heat shock response [42].

1.4 Grp78 and the Endoplasmic Reticulum stress response

The endoplasmic reticulum (ER) is an organelle responsible for homeostasis of intracellular calcium, for membrane lipids biosynthesis, folding and transport of proteins. Protein folding is a mechanism which is extremely sensitive to cellular environment alterations. Changes in Ca2 + levels, changes in redox state, increased protein synthesis, pathogenic and inflammatory stimuli can all alter protein folding. When cellular environment change misfolded proteins accumulate and form aggregates that are toxic to cells: this condition is defined as “ER stress". The Unfolded Protein Response (UPR) is the system by which the ER respond to stress and is activated by the accumulation of misfolded proteins [55]. The activation of the UPR involves transient attenuation of protein synthesis, increased protein trafficking through the ER, increased protein folding and transport, activation of pathways involved in protein degradation (ERAD – ER Associated degradation). If these adaptive mechanisms are unable to solve the problem, the cells go through apoptotic pathway.

The activation of this pathway occurs not only in normal cells, but also in cancer cells. Therefore, depending on the context, it is not surprising that the activation of the UPR contributes both to increased survival and cellular apoptosis.

When misfolded proteins accumulate in the ER lumen, two key events are necessary for activation of UPR: first, these misfolded protein aggregates bind and sequester the chaperone BIP (immunoglobulin heavy chain binding protein), also known as Grp78 [55]. Secondly, the consequent reduced levels of Grp78 is a clear pathway activation signal that induce the transcription of BIP, as well as other genes coding for chaperones [55, 56]. This response takes place via the activation of three transmembrane receptors:

• Pancreatic ER kinase (PERK)

• Activating Transcription Factor 6 (ATF6)

• Inositol-Requirng Enzyme 1 (IRE1).

1.4.1 PERK

PERK (Pancreatic ER Kinase) is a type I transmembrane kinase that becomes activated by dimerization and autophosphorylation, after dissociation with Grp78. The activation of this kinase causes phosphorylation of eIF2α, responsible for protein translation inhibition [57]. Activation of PERK-eIF2α reduces the global translation of mRNA, but on the other hand, increases the translation of various mRNA, including ATF4 and ATF5. ATF4 is a transcription factor that induces the expression of genes involved in ER function, in redox reactions, in stress response and protein secretion [58]. ATF4 is also associated with CHOP (C/EBP homologous protein) another transcription factor that induce apoptosis ER-stress-mediated, both *in vivo* and *in vitro* [59]. CHOP transcription is inhibited in the initial phases of the UPR activation, while it is induced when the stress become chronic. Therefore, under stress conditions, PERK is immediately activated and is function is to try to prevent cell damage and promote survival. If stress persists, ATF4 induces transcription of CHOP that induces programmed cell death [60].

1.4.2 ATF6

The activating transcription factor 6 (ATF6) is a transmembrane glycoprotein, whose luminal domain detects protein misfolding. In mammals is present with two isoforms, α and β, both expressed ubiquitously in all the tissues. The cytoplasmic portion of ATF6 act as transcription factor because it contains a DNA binding domain. Following the Grp78 dissociation, ATF6 moves to the Golgi apparatus, where it is activated by a proteolytic cleavage by two serine proteases, sp1 and sp2 [61]. Active ATF6 moves to the nucleus and it induces transcription of genes coding for the chaperones, which have an ER response element (ERSE) in their promoter [62]. This determines an ER increased folding capacity, helping to restore initial homeostasis.

1.4.3 IRE1

IRE1 (Inositol Requiring Enzyme-1) is activated after detachment from GRP78, by dimerization and autophosphorylation. The activation of IRE1 is also affected the fluidity of the membrane, which is modified when oxidative stress occurs. XBP1 is the IRE1 substrate. In normal conditions XBP1 levels are very low; they increase when ER occurs due to ATF6 induction. In the presence of its substrate, IRE1 cut by splicing the XBP1 mRNA, forming its active form (XBP1s) that enters the nucleus and determines the activation of target genes [62, 63] that determine an increase degradation of misfolded proteins accumulated in the ER [64]. Protein degradation could then represent the third stage of the response UPR, following translation block and increase of chaperone synthesis. In addition, XBP1 overexpression induces many genes involved in the secretory pathway and determines the expansion of the ER. However IRE1α activation is attenuated in case of chronic stress, through a mechanism not fully established [65, 66]. In addition to this mechanism, which promotes cell survival, IRE1 can also have a pro-apoptotic role by JNK74 kinase activation. Under normal conditions, the receptors (PERK, ATF6, IRE1) remain inactive through binding with the chaperone Glucose Regulated Protein 78 (Grp78). In stress conditions Grp78 dissociates from them and determines the activation, inducing UPR. In the first instance there is the activation of PERK and ATF6 that try to reduce the stress. Subsequently, the activation of IRE1 appears to have a crucial role in setting up pro-apoptotic signals. If the ER stress persists, PERK and IRE1 pathways converge, enhancing their pro-apoptotic effect, mediated by CHOP and JNK60.

1.4.4 UPR IN CANCER

UPR activation has been found in many human diseases and in mouse models. Cell death is the physiological consequence of chronic stress of the ER, and is the key of the pathogenesis of many diseases, including metabolic diseases, inflammation, neurodegenerative diseases and cancer [55]. Cancer cells are stimulated to produce large amount of proteins in a short time, therefore they are very dependent on the correct function of UPR system. UPR is also important in tumor pathology: it is indeed necessary for cancer cell growth in a hypoxic environment. The inactivation of PERK pathway, impairs cell survival in hypoxia [67]. PERK also promotes the proliferation and growth of cancer cells, limiting the DNA damage from oxidative stress, through ATF4 [68]. Thus, the PERK signaling cascade, phosphorylated eIF2α, ATF4 is essential for cancer proliferation.

The activation of UPR in cancer cells is due to intrinsic and extrinsic factors [69]. The hyper-activation of oncogenes (such as HRAS, MYC, BRCA1 and PTEN) and the loss of tumor suppressor function, increases the synthesis and translocation of proteins in the endoplasmic reticulum, due to the high metabolic demand during neoplastic transformation [70-72]. Consequently UPR pathway is activated to increase the protein folding capacity. In addition, the activation of UPR is required to promote the expansion of the ER for division and transmission to the cells during mitosis [73]. In addition, the hostile environment caused by the rapid proliferation of tumor cells, determines a strong endoplasmic reticulum stress of cancer cells, which results in activation of UPR. In solid tumors, there is a hypoxic environment and a lack of nutrients, such as glucose, due to the rapid growth of the mass and thus poor vascularization.

- *PERK pathway in carcinogenesis*

PERK/phosphorylated eIFα/ATF4 pathway plays a key role in cancer cell survival. The inactivation of PERK, alter the possibility of cell survival hypoxic environment [67]. PERK also promotes cell proliferation by limiting, through ATF4, DNA oxidative damage. The function of CHOP in oncogenesis is to date unknown, however it is repeatedly confirmed that the induction of CHOP in response to a prolonged ER stress, causes pre-malignant cell death, and prevent neoplastic progression [69]. CHOP deletion increases the incidence of malignant lung tumours in mouse models KRAS-induced, suggesting an oncosuppressive role of CHOP [74].

- *ATF6 pathway in carcinogenesis*

The main ATF6 target is Grp78/BIP activation, which plays an important role in protein folding and assembly, in regulating Ca2 + levels in the ER and controlling the activation of transmembrane sensors of stress [69]. It has been shown that Grp78/BIP activation in cancer cells protects them from apoptosis and from immune response [75]. By contrast Grp78/BIP suppression inhibits tumor cell growth, metastases progression and development, both *in vivo* and *in vitro* [76, 77]. Furthermore Grp78/BIP may be considered a marker of cell malignancy: in normal conditions is localized exclusively in ER, while in malignant cells, where it is hyper-expressed, can also be detected on the cell surface. In various tumor sites, such as lung, bladder, stomach and breast, overexpression of

Grp78/BIP confers resistance to chemotherapeutic agents, as well as its suppression sensitizes cancer cells to pharmacological treatment [78].

- *IRE1α pathway in carcinogenesis*

IRE1α - XBP1 pathway is also important for cell survival and tumour growth in hypoxic environment, because it induces the transcription of proangiogenic factors, such as vascular and endothelial growth factors [79]. In a glioma mouse model, IRE1α inhibition reduces of tumour growth, angiogenesis and blood perfusion [80]. XBP1 deletion reduces the tumour formation, and increase cell sensitivity to hypoxia [81]. On the other hand, there are studies that demonstrate an oncosuppressive role of IREα/XBP1 pathway: in many human tumours is was found IRE1α mutations [82], some of which result in a loss of kinase and endoribonucleasic function [83]. In addition, the loss of XBP1 function promotes oncogenesis [84].

AIM OF THE THESIS

The work presented here aimed to explore the cytoplasmic stress and the endoplasmic reticulum stress in haematological malignancies and explore possible ways of cellular communication of stress to distant cells. The work was performed *in vitro* using a cell line of leukemic malignant cells. More work has been done *in vivo*, collecting samples from a haematological disease which is in a pre-malignant state, the Myelodysplastic Syndrome (MDS). We chose a haematological model because much literature has been collected regarding solids tumours and stress response but much work still need to be done regarding neoplastic blood diseases. We chose a disease model that is a pre-malignant state because there is no literature about it, while only few data are already collected for malignant haematological diseases such as acute lymphoid leukaemia or acute myeloid leukaemia and it could be interesting to compare the cytoplasmic stress response and endoplasmic reticulum stress response between the two conditions. We chose to start the investigation studying a family of proteins that more than others are sensitive to stress: the chaperones. These proteins are responsible for protein folding, hence fundamental for a correct growth and cell division: in the absence of chaperones, cells including cancer ones, could not divide. Hsp72 is a molecular chaperone and, in addition to being intracellular, it has been localised to the extracellular environment and the plasma membrane [28, 39, 85, 86]. Grp78 is the corresponding endoplasmic reticulum chaperone and is induced upon stress condition and as Hsp72, can translocate to the plasma membrane and outside cells. Outside the cell Hsp72 has been proposed to have several additional functions, including activation of innate and adaptive immune systems [28, 87], as well as having anti-inflammatory activity [86]. In addition, altered expression of both HSPs, both inside and outside the cell, has been reported in several diseases including many types of cancer [88-91]. It is therefore likely that the translocation of heat shock proteins from inside the cell to the extracellular environment have important consequences. Several workers have demonstrated that Hsp72 can be released from cells, constitutively or after a specific stress depending on the cell type [16, 42, 43, 92-96]. The different routes for HSPA1A insertion into the plasma membrane and how that is linked to secretion is not at present fully understood. In this study we investigated Hsp72 cell surface presentation and secretion

after heat stress induced apoptosis, possible mechanisms that control this movement and discuss the significance of different release mechanisms.

Chaperone location is also crucial for other cellular mechanisms such as immune system modulation, disease progression, and spreading, for this reason HSPs could represent useful targets in cancer treatment. Understanding these mechanisms, specially looking at pre malignant state and see differences between advanced malignant state could represent an important step, for a better definition of cancer pathogenesis, and also in the future, for the development of customized therapies.

Chapter 2: MATERIALS AND METHODS

2.1 Tissue culture

Cell culture conditions and freezing

The cells lines that were used in this studies were both derived from blood malignancies: the E6.1 Jurkat is human leukemic T-cell lymphoblast cell, U937 is human Caucasian histiocytic lymphoma cell line and HUT78 is a cutaneous T cell lymphoma. All of them are suspension cells, which need the same cell culture media, therefore they possess similar procedures for resuscitation and culture. Briefly the cells were purchased frozen and the cryovials containing the cells were removed from the cryostat, soaked with alcohol and quickly placed in a 37°C waterbath. The vial was quickly opened and the content was place in a 25cm^2 flask containing 5ml of pre-warmed RPMI 1940 media with 10% serum. The cells were then counted with the haemocytometer and cell density was adjusted to 3-9x10^{5}cells ml^{-1} for E6.1 Jurkat cells and 2-9x10^{5}cells ml^{-1} for U937 cells. Cells were kept at 37°C in the incubator with 5% CO_2. A cell viability test was performed after 24hours using trypan blue assay on haemocytometer. Both cell lines were passaged every 3 days and viability was always tested by trypan blue assay.

All cell lines were frozen according similar procedures: cell suspension was kept at low density, between 3-5x10^{5}cells ml^{-1} for E6-1 and 2-5x10^5 cells ml^{-1} for U937 cells. At this stage the cells were in the log phase of the growth curve therefore they were actively growing. Cell suspension was centrifuged at low speed of 400*g* for 3 min at 25°C to minimise any damage and chilled freeze media, prepared as described above, was added to each cell pellet, transferred in cryovials and slowly freezed in liquid nitrogen vapour phase for about 2 hours. The liquid nitrogen vapour phase provides a gentle freezing of 1 to 3°C/min. The cryovials were then placed in the cryostat, stored in liquid nitrogen until needed.

U937 transformation into macrophages

U937 cells is a monocytic suspension cell line, however phorbol 12-myristate 13-acetate (PMA) treatment activate and transform U937 cells into macrophages. Cells within 48 hours gradually have a cell cycle arrest, began to adhere to the bottom of the flask, increase their size and present a granules in the inside of the cells, some can also present protrusions of the cytoplasm. Transformation of U937 into macrophages was achieved using a suspension of cells actively growing in the log phase of growth. Cells were counted; viability was tested by trypan blue, and then centrifuged at 500*g* for 3 min at 25°C. Cell pellet was resuspended at concentration of 5*x*10^5 cells*ml^{-1} in RPMI medium with 10% heat-inactivated FBS, containing 10 ng/ml phorbol 12-

myristate 13-acetate (PMA). Cells were plated out in 12-well cell culture plates at 1 ml/well and incubated for 48 hours to enable differentiation of cells. After 48 hours the media was removed and cells rinsed twice with 10 % heat-inactivated-RPMI then 1 ml/well fresh heat-inactivated media was added. U937 macrophages were then ready for experimental treatments.

Cell preparation for experiments

The day before each treatment E6-1, HUT78 and U937 cells were counted and plated into 12, 48, 96 well plates depending on the experiment design. Cells were always plated at concentration of $5x10^5$ cells*$ml^{-1.}$ Regarding the activated macrophages, cells were usually plated 48 hours before into 12-well cell culture plates at concentration of 5 X 10^5 cells/ml (1 ml/well); prior to treatments, once the activation had occurred, cells were washed once with 10 % heat-inactivated-RPMI taking care not to resuspend the attached activated macrophages, then 1 ml 10 % heat-inactivated RPMI was added together with the treatments, and incubated for the desired time.

2.8. Blood processing: plasma collection and cell separation

Whole blood collection

The blood provided for these studies came from either patients with myelodysplastic syndrome (MDS) involved in a medical study or from voluntary healthy people. Local research ethics committee approval was obtained for these studies, and consent forms were completed by each patient or volunteer. Blood samples were collected by venepuncture in 7ml K_2 EDTA vacutainers.

Plasma collection for exosomes purification

Plasma was separated from whole blood by centrifugation at 2000xg for 10 min. Platelets were removed by an additional centrifugation at 2500xg for 15 min. The collected plasma was aliquoted and stored at -80°C for further purifications and analysis.

Cell separation and conservation

Whole blood was washed with two volumes of D-PBS and centrifuged at 500*g* for 5 min at 25°C. The supernatant was discarded and the red blood cells were lysed using 1x lysing buffer. The lysed whole blood was then centrifuged at 500*g* for 5 min and the supernatant discarded. The cell pellet was washed with DPBS and the cells counted using the Trypan Blue exclusion method on a haemocytometer. Cells were centrifuged at 500*g* for 5 min, supernatant was discarded and cell pellets were frozen and kept at -80°C.

2.9. Cell viability and apoptosis determination

Microscopic analysis

Visualization of cells under a microscope allowed to make a qualitative and preliminary analysis of the samples and highlighted the macro changes occurred in cells. From cell morphology it was possible to discriminate between viable cells, necrotic cells with signs of shrinking and nuclei condensation and apoptotic cells that could be identified for their distinctive blebbings also called as apoptotic bodies.

Trypan blue exclusion assay

Trypan Blue is a non-permeable cell membrane DNA dye that was used to discriminate between viable and dead cells and also help the visualization of cell morphology. Viable cells do not take up the dye because of their membrane integrity, whereas necrotic cells have a loss of membrane integrity that allows the dye to stain the DNA inside the cells: therefore viable cells would appear clear white whereas dead cells would show up blue. Haemocytometer was prepared and cover-slip was put in place; 10 µl of the cell suspension was mixed to 10 µl of trypan blue solution, then 10 µl of the suspension mixture was loaded to both chambers of the haemocytometer carefully touching the edge of the cover-slip with the pipette tip and allow each chamber to fill by capillary action. Cells were counted in the 0.04 mm centre square and four 0.04 mm corner squares, as highlighted in the Figure 1, and a separate count of viable and non-viable cells was performed.

Viability and proliferation assay by MTS

The number of viable cells in proliferation was tested using a colorimetric method from Promega: CellTiter ® MTS Aqueous solution. The solution was composed of a tetrazolium compound called MTS (3-(4,5-dimethylthiazol-2yl)-5-(3-carcoxymethoxyphenyl)-2-(4-sulfophenyl)-2H-tetrazolium) and an electron coupling agent PES (Phenazyl-Etho-Sulphate). MTS solution is bio-reduced by dehydrogenases enzymes, which are peculiar in metabolically active cells, into formazan which is soluble and coloured in tissue culture. Therefore absorbance at 490 nm can be read directly into a 96 well plate and the quantity of formazan produced is directly proportional to the number of actively living cells in culture. Briefly MTS working solution was added to the 96 well plates where 100 µl of cells were seeded the day before at cell density as previously described. Cells were undergone the desired treatment and, after the required times, MTS working solution was added. Cells were kept at 37°C with 5% CO_2 for the required time (each cell type requires different incubation times (2.5 hours for Jurkat). Absorbance at 490 nm was recorded and comparison with

control was performed: usually several controls were included such as media control, positive control with viable cells and negative control with dead cells (killed by microwave irradiation for 10 sec).

Necrosis detection with Propidium Iodide fluorescent staining

Propidium Iodide binds to the DNA by intercalating between bases with a steichiometry of one dye per 4-5 base pair. PI is membrane impermeable and is generally exclude from viable cells, for instance PI is commonly used to identify necrotic dead cells. The cells were cultured, and treated in a 96 well plate at concentration of 0.2-0.7x10^6cells*ml^{-1}. The volume of cell used for the assay is 100 µl per well for a 96 well plate. The propidium iodide stock solution was kept at -20°C at 100 µg/ml concentration and a working solution of 5 µg/ml in PBS was prepared before each analysis. The working solution was then added to the cell suspension: 100 µl per well for a 96 well plate. The solution was mixed and incubated at room temperature for 20 min in the dark. The PI fluorescence of the cell suspension was read at excitation 535nm emission 617nm. Suitable controls were added in each experiment: a positive control of necrotic cells obtained irradiating the cell with microwaves for 15 sec, negative control of media only and viable cells.

Controls for apoptotic analysis

The following controls have been used in each assay: viable cell control, necrotic cells control obtained by microwave irradiation for 15 seconds and an apoptosis control by camptothecin treatment for 4 hours.

Caspase-3 fluorimetric assay

Caspase-3 is an effector caspase that plays a key role in several apoptosis pathways, and it has been shown to cleave poly-(ADP ribose) polymerase (PARP), DNA-dependent protein kinase (DNA-PK), topoisomerases, and protein kinase C. The kit chosen for the analysis, from Anaspec, uses the inhibitor (Z-DEVD)$_2$ which is conjugated with the fluorogenic indicator Rh110. When caspase-3 is cleaved it binds to the (Z-DEVD)$_2$-Rh110 that at this condition generates the Rh110 (Rhodamine 110), a fluorophore that can be detected at excitation/emission=496 nm/520 nm and relative quantitation compared to the no treated control was performed. Usually a positive control of cells treated with camptothecin was included.

Caspase-3 FC assay

Active caspase-3 was also tested using a polyclonal antibody-FITC conjugated directed against the active cleaved caspase-3. Cells were harvested and washed with wash buffer, centrifuged at 500*g* for 5 min at 25°C and supernatant discarded. Cell pellet was then carefully resuspended in fix/perm solution to allow the cells to fix and permeabilize; the solution was incubated for 20 min at 4°C. The cell suspension was then washed with wash buffer, centrifuged at 500*g* for 5 min at 25°C and the supernatant removed. Cell pellet was incubated with 20µl/1x10^6cells*ml^{-1} caspase-3-FITC conjugated antibody and incubated for 40 min at 4°C in dark. The unbound antibody was washed with wash buffer, centrifuged at 500*g* for 5 min at 25°C, the supernatant removed and resuspended with fresh D-PBS. Cells were analysed on the Millipore guava easyCyte in the FITC channel and gating of the caspase-3 positive population was performed in each analysis.

Annexin-V FC assay

Phophatidylserine (PS) externalization form the inside of the plasma membrane to the outside of the cell is one of the early event that characterizes apoptotic cell death. Annexin V is a protein that binds to the PS and therefore is a marker for early apoptotic events. The detection of early stage of apoptosis was performed by flow cytometry using the Annexin V/PI kit by BD-Bioscience. Cells were harvested, washed with D-PBS and centrifuged at 500*g* for 5 min at 25°C; supernatant was discarded and cell pellet was resuspended with 1x binding buffer, cells counted and concentration adjusted to be all 1x10^5cells*ml^{-1}. Cell suspension was incubated with Annexin V solution for 15 min at 25°C in the dark. Prior the analysis Propidium Iodide (PI 5µg/ml) solution was added to the cell suspension and samples were then analysed straight away by flow cytometry: Annexin V was detected at ex/em=490/520nm and PI was detected using a >520nm longpass filter; 10000 events were recorded for each samples and compensation controls were applied for each experiment.

Caspase-2 FC assay

Active caspase-2 detection was performed using the fluorescent labelled caspase-2 inhibitor carboxyfluorescein-labelled-fluoromethyl-ketone-peptide (FAM-VDVAD-FMK). The inhibitor is cell permeable and non-cytotoxic and binds covalently to the active cleaved caspase-2 that is undergone to proteolytic maturation; the fluorescent molecule bound to the Caspase-2 can be then detected by flow cytometry together with the necrosis markers PI and detected respectively at ex/em=490/520nm for the active Caspase-2 detection and at ex/em=535/617nm for the PI; commercially available kits from Bachem were used.

2.10 . Gene expression analysis

Total RNA extraction

Purification of total RNA from cells was performed using SV Total RNA Isolation System kit (Promega), using diethyl pyrocarbonate (DEPC) treated equipment. The SV Total RNA Isolation System combine the disruptive and protective properties of guanidine thiocynate (GTC) and β-mercaptoethanol to inactivate the ribonuclease present in cell extracts. GTC, in association with SDS, acts to disrupt nucleoprotein complexes, allowing the RNA to be released into solution and isolated free of protein. Dilution of cell extracts in the presence of high concentrations of GTC cause selective precipitation of cellular proteins to occur, while RNA remains in solution. RNA is then bound to the silica surface of the glass fibers found in the Spin Basket. DNAse treatment digest contaminating genomic DNA. The total RNA is finally eluted with nuclease-free water.

Quantity and purity of the total RNA obtained from the purification was tested reading the absorbance at 260 nm and 260/230 and 260/280 ratio, using Nanodrop instrument.

C-DNA Synthesis

RNA was quantified and retro-transcribed to c-DNA using using ImProm-II ™ Reverse Transcription System kit (Promega) using 2 µg RNA and random hexamers primes $(P(n)_6$ (Promega). The optimized reaction buffer and the reverse transcriptase provided in the kit enable cDNA synthesis Volumes of the reaction used is 20µl. The heteroduplex cDNA/RNA formed was then directly amplified by PCR. Briefly 2µl of random primers were added to the 2µg of total RNA purified as a total volume of 12,2 µl of solution. The samples were the heated at 70°C for 5 min and then let cool on ice for another 5 min. Then the reaction mix with buffer, reverse transcriptase, ribonuclease inhibitor and water was added to the samples and incubated 1 hour at 37°C. The c-DNA obtained was stored at -20°C for further analysis.

Real time PCR

Real-time Polymerase Chain Reaction (PCR) monitor the progress of the PCR as it occurs, in real time. In real-time PCR reactions the threshold cycle (Ct) is the crucial point to analyse: this is the first PCR cycle where amplification of a target gene is first detected by fluorescence emission. The higher is the amount of c-DNA in the reaction, the sooner it will be possible to see an increase in fluorescence. Quantitative qPCR has been performed using *Sybr green* technology. The SYBR Green is a fluorescent molecule that binds to the minor groove of the double DNA helix, emitting fluorescence. At the beginning of amplification cycle, the fluorescence signal is very low, since the

DNA is denaturated and SYBR Green molecules are free. In elongation phase, the fluorescence increases, this corresponds with an increase of copy number of double-stranded amplicon. The reaction curve is represented by a sigmoid curve where the fluorescence intensity is expressed as a function of the number of cycles.

The analysis was made using SsoAdvanced™ SYBR® Green supermix (Bio-Rad), in a CFX96 thermocycler (Bio-Rad). The reaction conditions are summarised below:

- ✓ 95°C for 30 seconds
- ✓ 40 cycles with:
- ✓ 95°C for 30 seconds
- ✓ 60°C for 30 seconds.

Melting curves were analysed after the reaction to assess the specificity of the amplification products. The relative expression of the different gene transcripts are calculated using the ΔΔCt method and converted as ratio of relative expression using the formula $2^{-\Delta\Delta Ct}$ for statistical analysis. All data are normalized according to the expression of the endogenous reference gene, Actin.

Primer design and choice

Primers used for the study were designed using Primer 3 software. Primer sequences are listed below:

HSPA1A fw: TGCGACAGTCCACTACCTTT; rv: AACACTGGATCCGCGAGAA

ATF6 fw: TTCCTCCACCTCCTTGTCAG; rv: ACCCATCCTCGAAGTTCATGA

CHOP fw: TGTTAAAGATGAGCGGGTGG; rv: TGCTTTCAGGTGTGGTGATG

GRP78 fw: TGCCTACCAAGAAGTCTCAGA; rv: ACGAGGAGCAGGAGGAATTC

XBP-1 fw: CTGAGTCCGCAGCAGGTG; rv: CCAAGTTGTCCAGAATGCCC

HERPUD-2 fw: GCTGCTTCTTGAACTGGACC; rv: AGTCTGCCCGAATACACCAA

XLOC_006043 fw: GAAGTCGGGCATTCAGGAGA; rv: CAGGTTCTCAGTGTTCCAGG

b-ACTIN fw: AAATCTGGCACCACACCTTC; rv: CATGATCTGGGTCATCTTCTC

2.11 . Flowcytometric analysis

Surface Hsp72 detection by flow cytometry

Surface anti-Hsp72 cmHsp72.1 was specially produced and purchased from Dr G. Multhoff laboratories of Multimune, Munich, Germany. The use of the cmHsp72.1 antibody in this study insured that surface expression of Hsp72 is membrane embedded and not just receptor attached. Literature evidence showed by western blots that the TKD peptide antibody recognise specifically

the Hsp72 present in association with the membrane fraction of the cells [97]. This unique antibody specifically recognises the TKD peptide region, a 14-mer sequence, situated in the N-terminal region of the Hsp72 protein (aa 450–463; peptide sequence: TKDNNLLGRFELSG) and therefore detects protein which is embedded in the membrane. This has been demonstrated to be presented outside the cell membrane when the protein is embedded and is the target for natural killer (NK) cell anti-tumour responses [97]. Although the epitope for the Stressgen antibody overlaps the TKD region, it contains more amino acid residues (location between the amino acid residues 436 and 503), that become hidden in the membrane when the protein is embedded, making binding by the Stressgen antibody impossible. Cells were purified as described above, and concentration of cells was determined and adjusted to $1x10^5$cells*ml^{-1} prior to the labelling. The cell pellet was washed with wash buffer (5% FBS in PBS), prepared as described above, centrifuged at 500*g* for 5 min and supernatant was discarded. The pellet was then resuspended in antibody solution; samples were incubated for 40 min at 4°C in the dark. The incubation time was followed by a wash with 1 ml of wash buffer, centrifugation at 500*g* for 5 min followed by a discard of the supernatant. In order to discard in the analysis any necrotic cells, 2.5 µl of 100 µg/ml propidium iodide was added to the cell pellet and left for 5 min at 4°C. The cell pellet was then resuspended in 20 µl of wash buffer and analysed straight away to the flow cytometer. Cells negative to PI, therefore viable were the only gated, and the analysis of surface Hsp72 was restricted to them only.

Intracellular Hsp72 detection by flowcytometry

Cells were purified as described above, and concentration of cells was determined and adjusted to $1x10^6$cells*ml^{-1} prior to the labelling. The cell pellet, was washed with wash buffer (5% FBS in PBS), prepared as described above, centrifuged at 500*g* for 5 min and supernatant was discarded. Cells were then fixed and permeabilised with Fix/Perm solution (BD biosciences) and incubated for 20 min at 25°C in the dark. Cells were washed by adding 1ml wash buffer, centrifuged 500*g* for 5 min and supernatant removed. Cells were then labelled for the intracellular Hsp72 antibody (santa scruz), mixed and incubated for 40 min at 25°C in the presence of dark. The incubation time was followed by a wash with 1 ml of wash buffer, centrifugation at 500*g* for 5 min followed by a discard of the supernatant. Cell pellet was resuspended in wash buffer and analysed at the flow cytometer.

CD25 surface detection in HUT78 cells

Cells were prepared as described above, and concentration of cells was determined and adjusted to $1x10^6$cells*ml^{-1} prior to the labelling. The cell pellet, was washed with wash buffer (5% FBS in PBS), centrifuged at 500*g* for 5 min and supernatant was discarded. Cells were then labelled for the surface CD25, mixed and incubated for 40 min at 25°C. Cells were the washed with 1 ml of wash

buffer, centrifuged at 500*g* for 5 min ad secondary antibody FITC labelled was added to the cell pellet and incubated for 30 min at 25°C in the dark. Cell pellet was washed and resuspended in wash buffer and analysed at the flow cytometer.

Cell Cycle analysis by flowcytometry

Cell cycle analysis use the property of certain fluorescence molecules to bind the DNA in a stoichiometric manner, in proportion to the amount of DNA present in the cell. Therefore by looking difference fluorescence emission it is possible to distinguish between the S phase where DNA is more than cells in G1. The cells take up proportionally more dye and will fluoresce more brightly until they have doubled their DNA content. The cells in G2 are approximately twice as bright as cells in G1. The protocol used Propidium Iodide as DNA binding molecule. Briefly cells at concentration of $1x10^6$/ml were washed and resuspended in cold PBS, then fixed using 70% cold ethanol and incubated overnight at -20°C. Cell suspension was centrifuged and PI mastermix at 40µg/ml was added to the cell pellet and incubated at 37°C before the analysis. PI fluorescence was measured by flowcytometry.

2.12 Fluorescence Microscopy methods

Cells cultures were labelled with several antibodies in order to find co-localization of surface and intracellular Hsp72 with cellular and membrane markers. The fluorescence slides produced were analysed with the Nikon Eclipse TE2000-U fluorescence microscopy using IPLAB Suite Software.

Detection of surface Hsp72 and the lysosome marker LAMP-1

LAMP-1 protein is present in lysosome but it has been previously found to be present on the surface of cells in certain conditions; protocol was tested to check plasma membrane LAMP-1 or intracellular, therefore two protocols have been developed in order to check the presence in both locations. Cells at concentration of $1x10^6 cells*ml^{-1}$ were prepared, by washing with PBS, centrifuging at 500*g* 5min and removing the supernatant. Cell pellets were blocked with wash buffer (FBS 5% in PBS) for 30 min at 25°C, then washed by centrifuging at 500*g* for 5 min at 25°C, supernatant removed. Cell pellet was labelled with 100ul of LAMP-1 and Hsp72 mixed at appropriate concentrations diluted in buffer for 1 hour at 25°C in the presence of dark; cells were washed as described above and anti-mouse IgG-Cy3 conjugated was added at appropriate concentration for 1 hour at 25°C in the presence of dark. Unbound antibody was washed away with a washing step and cells were fixed with PFA 4% for 30 min. Cells were then washed and resuspended in 20 µl of PBS; the whole cell solution was added carefully on top of a polylysine-coated glass slides; slides were mounted by dropping anti-fade solution with DAPI on top of the

slides and by placing the cover slip on top taking care of not create any bubbles. Slides were left to recover overnight and fluorescence analysis was performed the following day.

Detection of Hsp72 and Golgi apparatus marker, Golgin 97

Golgin 97 is an antibody that labels Golgi apparatus. The staining protocol was made in conjunction with Hsp72 in order to test intracellular co-localization of Golgi with Hsp72 protein. Cells at concentration of $1x10^6$cells*ml^{-1} were prepared, by washing with PBS, centrifuging at 500*g* 5min and removing the supernatant. Cell pellets were blocked with wash buffer (FBS 5% in PBS) for 30 min at 25°C, then washed by centrifuging at 500*g* for 5 min at 25°C, supernatant removed. The cell pellet was fixed and permeabilised by adding 100 µl of fix/perm solution (BD Biosciences) for 20 min at 25°C. Cells were washed as described above and 100ul of Golgin-97 and Hsp72 was added at appropriate concentrations diluted in buffer for 1 hour at 25°C in the presence of dark; cells were washed as described above and antimouse IgG-Cy3 conjugated was added at appropriate concentration for 1 hour at 25°C in the presence of dark. Unbound antibody was washed away with a washing step as previously described and cells resuspended in 20 µl of PBS; the whole cell solution was added carefully on top of a glass slide; the slide was mounted by dropping antifade solution with DAPI on top of the slides and by placing the cover slip on top taking care of not create any bubble. Slides were left to recover overnight and fluorescence analysis was performed the following day.

Detection of surface Hsp72 and the lipid raft marker GM-1

Lipid rafts are detergent, insoluble, shingolipid-and cholesterols-rich membrane microdomains that assemblies in the plasma membrane. Live cells were first labelled with, cholera toxin subunit B (CT-B)-alexa fluor 555 conjugated which binds to the pentasaccharide chain of plasma membrane ganglioside (GM-1) a component of lipid rafts. An antibody that specifically recognizes CT-B is then used crosslink the CT-B labelled lipid rafts into distinct patches on the plasma membrane, which were visualized by fluorescent microscopy. The lipid raft labelling was coupled with Hsp72 in order to obtain an analysis of co-localization of the protein with these membrane structures. Cells at concentration of $1x10^6$cells*ml^{-1} were prepared, by washing with PBS, centrifuging at 500*g* 5min and removing the supernatant. Cell pellets were blocked with wash buffer (FBS 5% in PBS) for 30 min at 25°C, then washed by centrifuging at 500*g* for 5 min at 25°C, supernatant removed. CT-B conjugate was added at appropriate concentrations for 30 min at 4°C. Cells were washed by centrifugation at 500 g for 5 min at 25°C and anti-CT-B together with Hsp72 antibody was added to the cell pellet at appropriate concentrations for 1 hour at 4°C in the presence of dark. Cells were washed as described above and fixed with 100 µl PFA 4% for 30 min at 4°C in the dark. The cell

suspension was washed and resuspended in 20 µl of PBS; the whole cell solution was added carefully on top of a glass slide; the slide was mounted by dropping antifade solution with DAPI on top of the slides and by placing the cover slip on top taking care of not create any bubble. Slides were left to recover overnight and fluorescence analysis was performed the following day.

2.13 Exosome and microvesicles purification and characterization

Exosome and microvesicles purification

Exosome were purified adapting previously developed methods [98]. Briefly cell culture supernatant, from cell growing at $5*10^5$ c/ml, was collected and centrifuged at 500xg for to remove cells; then the supernatant was centrifuged at 2000xg to remove apoptotic bodies and cellular debris; the supernatant was filtered in a 0.22µm filter, then transferred in a 100KDa Vivaspin tube (Sartorius); the sample was concentrated centrifuging the column at 1000xg; microvesicles were isolated centrifuging the resulting supernatant at 16000xg for 30 minutes, the pellet was recovered and the supernatant was isolated for exosome purification and transferred in a ultracentrifuge tube, at the bottom of the 1ml supernatant it was carefully inserted 300µl of a density gradient (20mM TRIS, 30% sucrose in D_2O). Samples were ultracentrifuged in a Beckton Dickinson ultracentrifuge with TLA.100.3 rotor at 100,000xg a 4°C for 40 minutes. 350 µl of the exosome mix from the bottom of the tube was collected, diluted in 2.5ml of PBS and ultracentrifuged in TLA.100.3 rotor a 100,000xg at 4°C for 70 minutes. The pellet was collected at the bottom of the tube, resuspended in 200 µl of PBS and stored at -80°C for further use.

Transmission electron microscopy method for exosome visualization

Purified exosome were analysed by transmission electron microscopy: briefly exosomes in suspension were fixed with an equal volume of 2 % glutaraldehyde in 0.1 M cacodylate buffer (pH 7.4) and observed in transmission electron microscopy after negative staining conducted as follows: a drop (~20µl) of the sample was left to adsorb for 1 min on a 300 mesh nickel grid coated with formvar /carbon film. The sample was then contrasted with 4 steps of drops of uranyl acetate, 3% water for 30 seconds. The grids were air dried and samples were observed with CM10 electron microscope (Philips) at working voltage of 80 KV. The images of the samples were recorded by CCD camera Veleta 130,000X and the magnification of their diameters, expressed in nm, were measured by software iTEM (TEM Imaging Plaatform, Olympus).

Flowcytometry analysis of exosomes using latex beads

CD81 expression, a surface antigen present in exosomes was tested by flow cytometry coupling the vesicles with 4µm aldehyde sulphate latex beads (Invitrogen). CD81 primary antibody used is a mouse monoclonal was and is a kind gift of Prof. Malavasi (University of Torino); the secondary antibody is an antimouse IgG-FITC conjugate (Abcam). HSPA1A surface presentation on exosome membrane was tested using the same flow cytometric methodology, using the membrane cm-Hsp70.1 antibody (Multimmune).

2.8. Cellular and extracellular vesicles protein analysis

Extraction of samples

Protein analysis require extraction, to discard and remove any residue of membrane and nucleic acid. Cell pellet was extracted for ELISA and Western Blot with RIPA buffer. Cells culture or white blood cells were collected at concentration of $1x10^6$cells*ml^-1; sample pellet was homogenized by adding in the tube 500µl of RIPA extraction buffer; samples were mixed vigorously for 5 min and left at 25°C for 5 min followed by a centrifugation at 13500*g* for 20 min. Supernatant was collected and decanted into a clean tube, while the tube containing pellet was discarded. Samples were finally stored in -80°C freezer until required.

Exosomes were extracted with RIPA buffer. Exosomes were homogenized by adding in the tube 200µl of RIPA extraction buffer; samples were mixed vigorously for 5 min and left at 25°C and sonicated applying 2 pulses for 2 seconds to break the detergent resistant microdomains, followed by a centrifugation at 13500*g* for 20 min. Supernatant was collected and decanted into a clean tube, while the tube containing pellet was discarded. Samples were finally stored in -80°C freezer until required.

Bradford protein assay

In order to calculate the amount of total proteins present in each cell pellet, total plasma or exosome sample and to adjust the protein concentration used in the Western Blot and ELISA, were extracted with the extraction buffer as previously mentioned and Bradford protein assay has been performed. Standards were made using a known amount of bovine serum albumin (BSA) diluted in extraction buffer, mixed for 5 sec and incubated for 5 min at 25°C. After the incubation time, absorbance at 595 nm was collected, standard curve of the known standard was created and concentration of the samples was worked out from the standards.

SDS-PAGE electrophoresis

Protein cell extract was analysed by sodium dodecyl sulphate – polyacrylamide electrophoresis (SDS-PAGE). Solutions for the SDS electrophoresis were prepared in advance, Bio-Rad mini-protean II electrophoresis apparatus was assembled and 1mm thick gel was chosen for the experiments. 12% Acrylamide separating gel was prepared. Once the gel has set the staking gel was prepared and combs were placed on top of the separating gel and the staking gel solution was pipetted carefully to the top of the separating gel taking care of not creating any bubbles. The gel was left to polymerise for about 40 min. Meantime samples were prepared and eventually diluted in extraction buffer in order to have the same amount of total protein in each well (50 µg for exosome samples and cell extract). Samples were as well diluted with sample buffer and heated at 85°C for 10 min to allow denaturation. After the heat treatments they were allow cooling for 5 min on ice and then loaded in the wells. Electrode buffer was poured into the middle of the assembly to the top and in the outer assembly until buffer covered the bottom centimetre of the middle assembly. Samples and Precision Plus® standards as a molecular weight reference were loaded into the gel. The apparatus was assembled and electricity was applied to the chamber: gel run at 20mA when samples run into the stacking and 30mA for about one hour.

Exosomes were characterised using the CD81 antibody: in this case the protein gel was performed under non-reducing conditions, while HSp72 SDS-Page was performed under reducing conditions.

Western blot

Bio-Rad mini-trans blot apparatus was assembled; while the gel is running, sponges, 3 pieces of chromatographic paper and nitrocellulose membrane were soaked in transfer buffer. Once the gel was ready the electrophoresis apparatus was opened and the staking gel was removed with a razor blade. Western chamber was assembled by putting an ice pack inside and by placing the sandwiches into the chamber with black sides to all the left, next to the ice pack. Transfer buffer was poured in the chamber filled up to the level. 100 V electricity was applied for 60 min. Once the run is finished the nitrocellulose paper was removed from the chamber and placed in a container with blocking solution for 60 min. The blot was then incubated with the specific antibody at the appropriate dilution in 10 ml of the antibody buffer overnight at 4°C. Blot was then washed 3 times with wash buffer and an appropriate dilution of secondary antibody was added to the blot in 20 ml antibody buffer. The blot was incubated for 1 hour in orbital shaker, then washed three times with wash buffer then incubated with 2 ml working solution of Supersignal West Pico chemiluminescent substrate (1:1 dilution of the two solutions) for CD81 antibody, for 5 min with a gentle shaking; for Hsp72 detection it was used enhanced SuperSignal West Femto maximum sensitivity

chemioluminescent substrate (Thermo Fisher Scientific). The chemioluminescent signal was acquired using ChemiDoc XRS+ System (Bio-rad Laboratories) and quantified using Image Lab Software (Bio-rad Laboratories).

2.14 ELISA

Intracellular Hsp72 detection by ELISA

Nunc binding plates were coated the with 100 µl solution/well of 2µg/ml of polyclonal affinity purified sheep anti-Hsp72 which was raised against the SIGMA Hsp72; the antibody was diluted in carbonate buffer and incubated overnight at 4°C. Plate was washed 3 times by adding 300 µl of wash buffer, then carefully dried. Plate was then blocked with 300 µl of 0.5% BSA in PBS and incubated for 1 hour at 25°C, followed by three washes with 300 µl of wash buffer. The plate was dried and 100 µl of the samples and the standards were added to each well. Samples and standard were diluted in extraction buffer; the top standard was set to be 100 ng/ml and standard curve was prepared in doubling dilutions; the plate was incubated for 2 hours at 37°C. Samples and standard were washed 6 times with 20 sec soak in between washes and dried. 100µl of the diluted detector antibody mouse monoclonal anti Hsp72 in 0.5%BSA in PBS solution was added to the wells and incubated for 1hour at 37°C. The plate was washed 6 times with the 20 sec soak in between wash and carefully dried. 100µl of the diluted anti-mouse IgG HRP (1/2500) in 0.5% BSA in wash buffer was added to each well and incubated for 1hour at 37°C. The plate was washed 6 times and 100 µl of TMB substrate was added and incubated at 25°C in a plate shaker for about 30 min being careful to check the colour development in between. The reaction was stopped with 1M orthophosphoric acid and the absorbance at 450 nm was recorded.

Extracellular Hsp72 detection by ELISA

HSPA1A release from cells has been detected by an in-house sandwich ELISA previously developed [99]. Briefly plates were coated the with a polyclonal affinity purified sheep anti-HSPA1A in carbonate buffer; plate was washed, and blocked with 0.5% BSA in PBS for 1 hour; plate was washed and 100µl of the samples and the standards were added to each well and incubated for 2 hours. The plate was washed and mouse monoclonal anti HSPA1A (gift from Dr Christensen, Denmark) was added and incubated for 1 hour. The plate was washed and anti-mouse IgG HRP (Sigma) was added and incubated for 1 hour. The plate was washed, TMB substrate was added and incubated in a plate shaker. The reaction was appropriately stopped with 1M orthophosphoric acid and absorbance at 450nm was recorded.

2.10. Statistical analysis

Data were analysed with different analysis methods depending on the assay performed and on the number of variables considered. The statistical tests most used were:

- Student t-test to measure a variable in two groups, and check whether the means and medians are distinct.
- One way ANOVA to measure a variable in three or more groups, and check whether the means and medians are distinct and which groups are different from the other groups. Statistical significance and P value was calculated with Bonferroni post hoc test.
- Two way ANOVA to determine how a response is affected by two factors. For example, when we measure the response of 2 temperatures in different time points. Statistical significance and P value was calculated with Bonferroni post hoc test.

P value as the probability, with a value ranging from zero to one, that the two population of data have the same mean. Differences between groups were considered to be significant when $P<0.05$ and degree of significance are represented on the graphs as * with the following meaning:

*p<0,05, **p<0,01, ***p<0,001, ****p<0,0001

Chapter 3: Cytoplasmic stress response

Introduction

Heat shock proteins (HSPs) are evolutionary conserved intracellular proteins that are known to act as molecular chaperones and are, as a result, cytoprotective. Hsp72, also named HSPA1A by the new proposed nomenclature [3], is a prominent member of the HSP70 family, is strongly heat inducible and, in addition to being intracellular, has been localised to the extracellular environment and the plasma membrane [28, 39, 85, 86]. Outside the cell HSPA1A has been proposed to have several additional functions, including activation of innate and adaptive immune systems [28, 87], as well as having anti-inflammatory activity [86]. It is therefore likely that the translocation of HSPA1A from inside the cell to the extracellular environment will have important consequences.

HSPA1A release from cells has been proposed to involve a passive mechanism from necrotic, and not from healthy or apoptotic, cells [36, 100]. However, several workers have demonstrated that HSPA1A can be released from cells, constitutively or after a specific stress depending on the cell type [16, 42, 43, 92-96]. HSPA1A is known to lack the leader sequence typical of most secreted proteins, suggesting that it does not follow a classical protein secretion pathway. Proposed routes, using various cell systems, for release include via lipid rafts [41, 43], exosome vesicles [18, 35, 96, 101], endo-lysosomes [42, 43], secretory-like granules [94] and ABC family protein transporters [42]. No-one has addressed whether any of these mechanism are exclusive to the cell or conditions used, therefore, a survey of the current available data would suggest that the secretion of HSPA1A from cells is stress and cell type dependent.

HSPA1A can be presented on the cell surface of many tumour cells [102-108] and act as a target for natural killer (NK) cells [18, 109-111]. Surface presentation of HSPA1A on cells has been shown to be associated with particular membrane lipids, enriched in glycosphingolipids and cholesterol which form part of detergent resistant micro-domains (DRMs), also called lipid rafts [35, 39, 112]. Specific lipids that HSPA1A interacts with are the glycosphingolipid globotriaoslyceramide (Gb3) [112] and phosphatidylserine (PS) [35, 39, 113, 114]. The different routes for HSPA1A insertion into the plasma membrane and how that is linked to secretion is not at present fully understood.

In this study we investigated HSPA1A cell surface presentation and secretion after heat stress induced apoptosis and possible mechanisms that control this movement and discuss the significance of different release mechanisms.

Material and Methods

Here below there is a list of the methods used in this work: the methods are fully described in the Material and Methods section.

- ✓ *Cell culture and treatments*
- ✓ *Surface and intracellular HSPA1A by flowcytometry*
- ✓ *Cell viability and proliferation by MTS assay*
- ✓ *Apoptosis analysis analysing Caspase-3 and Caspase-2 detection*
- ✓ *Phosphatidyl-serine (PS) analysis by flowcytometry*
- ✓ *HSPA1A ELISA*
- ✓ *HSPA1A gene expression by real time PCR*
- ✓ *Exosome and microvesicles purification*
- ✓ *Exosome characterization by TEM, Bradford assay, Acethylcholinesterase assay, flowcytometry, western*
- ✓ *Cell cycle analysis*
- ✓ *Statistical analysis*

Results

Elevated temperatures induces apoptosis and then necrosis

We used temperature treatments to induce changes in cell status while also altering HSPA1A production. Cell activity and viability were tested using the MTS assay, caspase-3 activity was used to test apoptosis and propidium iodide (PI) incorporation assay for necrosis. Two hours heat shock treatment shows no effect on temperature on any of the parameters up to 40°C. At 41°C and above cell activity declined while activated caspase-3 increased: that suggests the induction of apoptosis. However at 43°C and above we see an increase in necrosis (Figure 1).

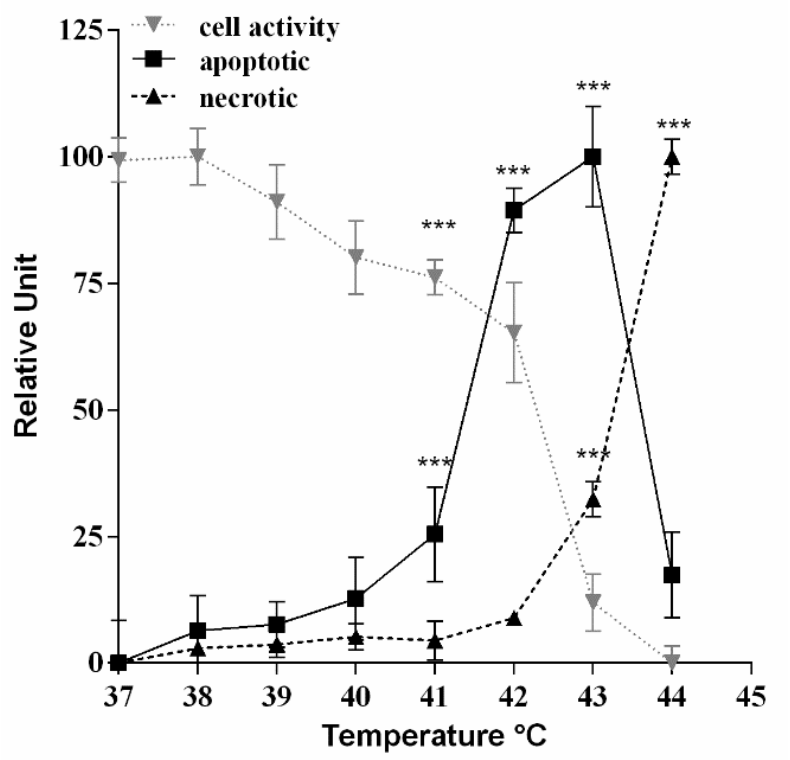

Figure 1: Heat shock treatment determines mode of cell death
Jurkat cells were heat shocked for 2 hours at different temperatures; data n=3 independent experiments are represented a mean ± SD. Cell activity, was measured by MTS assay, apoptosis by Caspase 3 activity and necrosis by PI fluorescence; the relative unit is the expression of a transformation analysis performed with the raw data: in each assay the data from the no treated control cells (37°C) was taken as a reference data in order to obtain a percentage (0% for the necrosis and apoptosis data and 100% for the cell activity datum); statistic performed here was one-way ANOVA with Tukey's post hoc test performed separately in each data set.

Time courses at different temperatures show that necrosis is present at 45°C after 1 hour, and at 42°C only after 3 hours treatment (Figure 2).

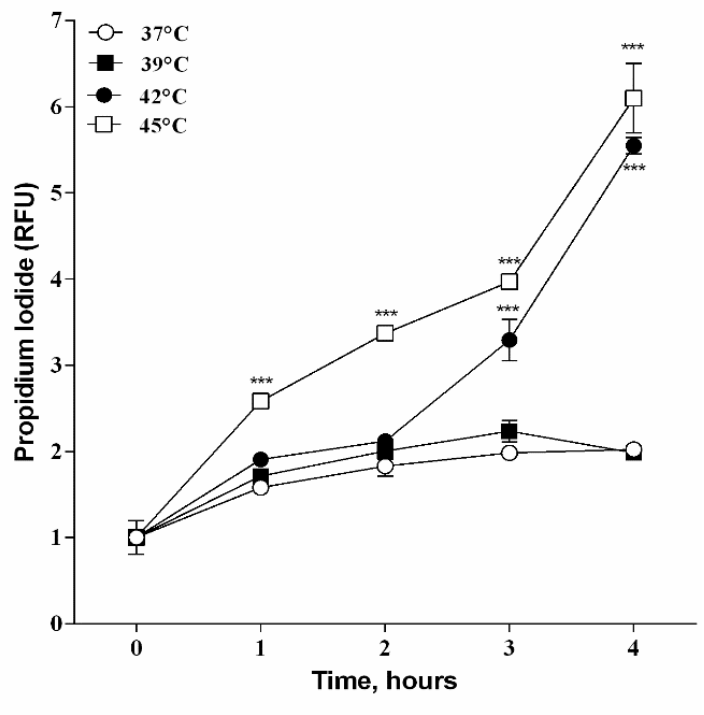

Figure 2: Necrosis after 4 hours heat shock time course

Jurkat cells were heat shocked for 4 hours at four different temperatures (37°C, 39°C, 42°C, 45°C) and necrosis was measured by PI assay; results are expressed as relative fluorescence units (RFU). Statistic performed in all the assays was two-way ANOVA with Bonferroni post hoc test, comparing the data set at 37°C to each temperature in each time point. (*=P<0.05; **=P<0.01;***= P< 0.001).

Apoptosis, detected by active caspase-3 and 2, occurs specifically at 42°C within 1 hour thereafter the activation of both enzymes had similar profiles (Figure 1 C-D); only at 45°C after 4 hours Caspase-2 increase.

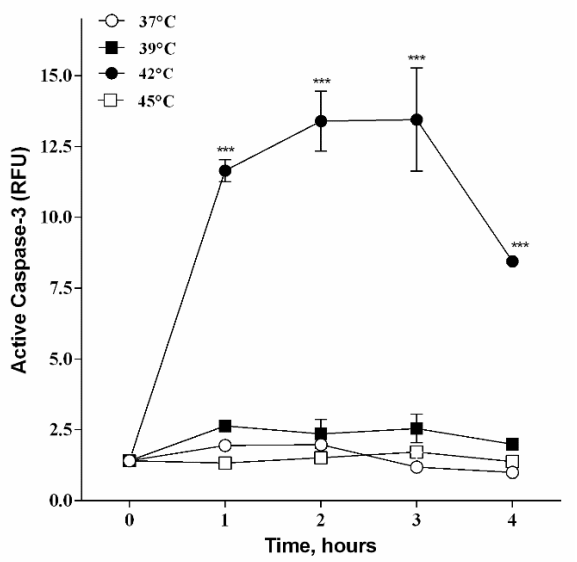

Figure 3: Active Caspase-3 after 4 hours heat time course

Jurkat cells were heat shocked for 4 hours at four different temperatures (37°C, 39°C, 42°C, 45°C) and active Caspase 3 was detected by fluorimetric assay; the results are expressed as relative fluorescence units (RFU). Statistic performed in all the assays was two-way ANOVA with Bonferroni post hoc test, comparing the data set at 37°C to each temperature in each time point. (*=P<0.05; **=P<0.01;***= P< 0.001).

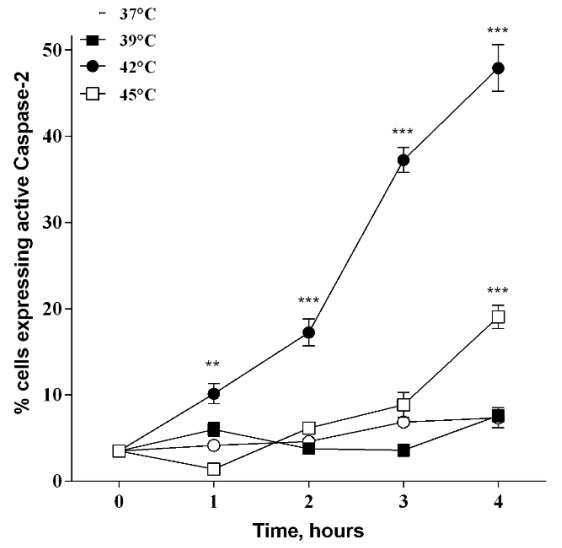

Figure 4: Caspase 2 after 4 hours heat time course

Jurkat cells were heat shocked for 4 hours at four different temperatures (37°C, 39°C, 42°C, 45°C) and caspase 2 activity was measured by flow cytometry; data are represented as percentage of viable (PI negative) cells expressing active Caspase 2; Statistic performed in all the assays was two-way ANOVA with Bonferroni post hoc test, comparing the data set at 37°C to each temperature in each time point. (*=P<0.05; **=P<0.01;***= P< 0.001).

HSPA1A intracellular and extracellular levels are modified with heat shock

We have confirmed that the temperature treatments are giving a normal heat shock response by measuring intracellular HSPA1A. We have also measured extracellular HSPA1A in the same experiments. Neither intracellular HSPA1A (i-HSPA1A) nor extracellular HSPA1A (e-HSPA1A) are altered over time at normal temperatures or by elevation to 39°C (Figure 5-6). e-HSPA1A increased within 2 hours exposure of cells to 42°C and increased further by 4 hours (Fig 6). i-HSPA1A increased after 3 hours at 42°C (Fig 5). Lethal temperature treatment (45°C) results in a decrease in i-HSPA1A and does not affect e-HSPA1A (Figure 5-6).

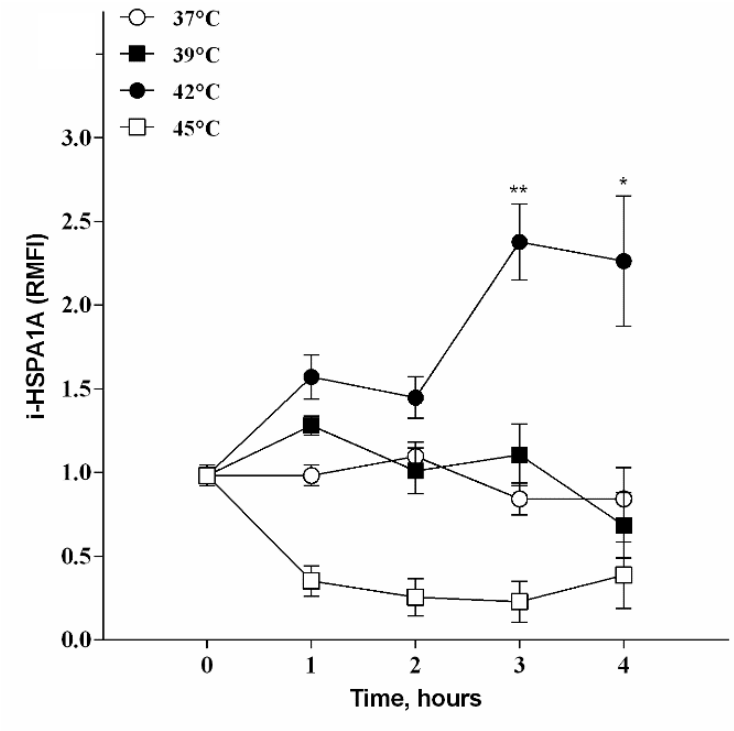

Figure 5: HSPA1A intracellular localization after 4 hours heat shock
Jurkat cells were heat shocked for 4 hours at different temperatures (37°, 39°, 42°, 45°C); data n=3 independent experiments are represented a mean ± SD. Intracellular HSPA1A expression was measured by flow cytometer. Data are represented as relative mean of fluorescence (RMFI) where mean of fluorescence intensities values of each sample was normalised to the non-heat shocked control. Statistical analysis was performed in each data set using two way-ANOVA with Bonferroni post hoc test (***= P< 0.001) comparing the differences between the 0 time in each data set and the difference between the different data set.

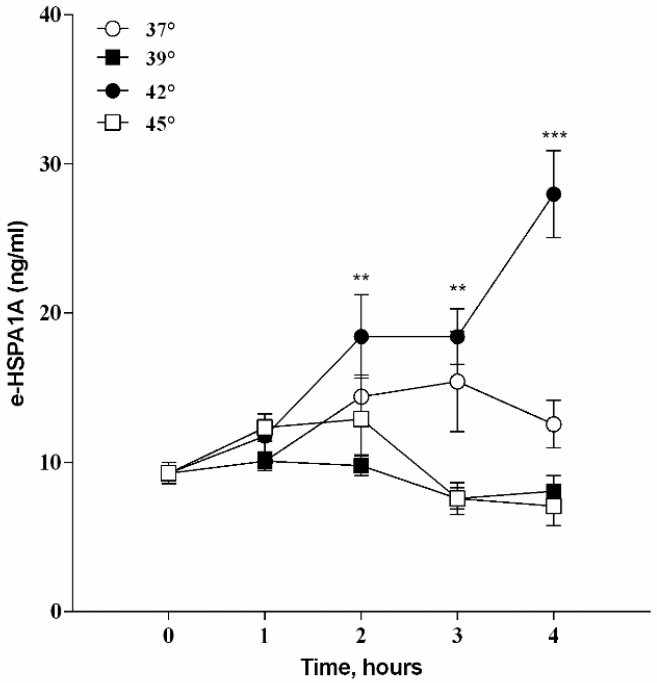

Figure 6: Extracellular HSPA1A after 4 hours heat shock

Jurkat cells were heat shocked for 4 hours at different temperatures (37°, 39°, 42°, 45°C); data n=3 independent experiments are represented a mean ± SD. HSPA1A release was measured by ELISA in cell culture supernatant and concentration was expressed in ng/ml cell suspension. Statistical analysis was performed in each data set using two way-ANOVA with Bonferroni post hoc test (***= P< 0.001) comparing the differences between the 0 time in each data set and the difference between the different data set.

Appearance of surface HSPA1A correlates with PS

Phosphatidilserine (PS) membrane presence, a lipid raft component and also an apoptosis marker, was detected by Annexin V and necrosis was simultaneously tested by PI incorporation. Jurkat cells were not expected to express large levels of surface HSPA1A (s-HSPA1A) at normal growing temperatures: although a small significant population expressing sHSPA1A was observed (Figure 8). Data show that at 42°C there is the highest PS externalization which is concomitant with s-HSPA1A exposure (Figure 7-8). Correlation analysis of the data show that the appearance of s-HSPA1A on Jurkat cells, correlated with PS externalisation between 0-3 hours (r^2 = 0.965) (Figure 8A). These data, together with the previous ones confirms that the cells are committing to apoptotic cell death at a specific temperature (42°C) and that there is a switch of cell death modality at higher temperature (45°C), when the apoptosis markers are mostly not activated necrotic cell death dominates. s-HSPA1A increment, observed in necrotic cells after 3 hours heat shock, is possibly due to membrane leakage and antibody cell internalization.

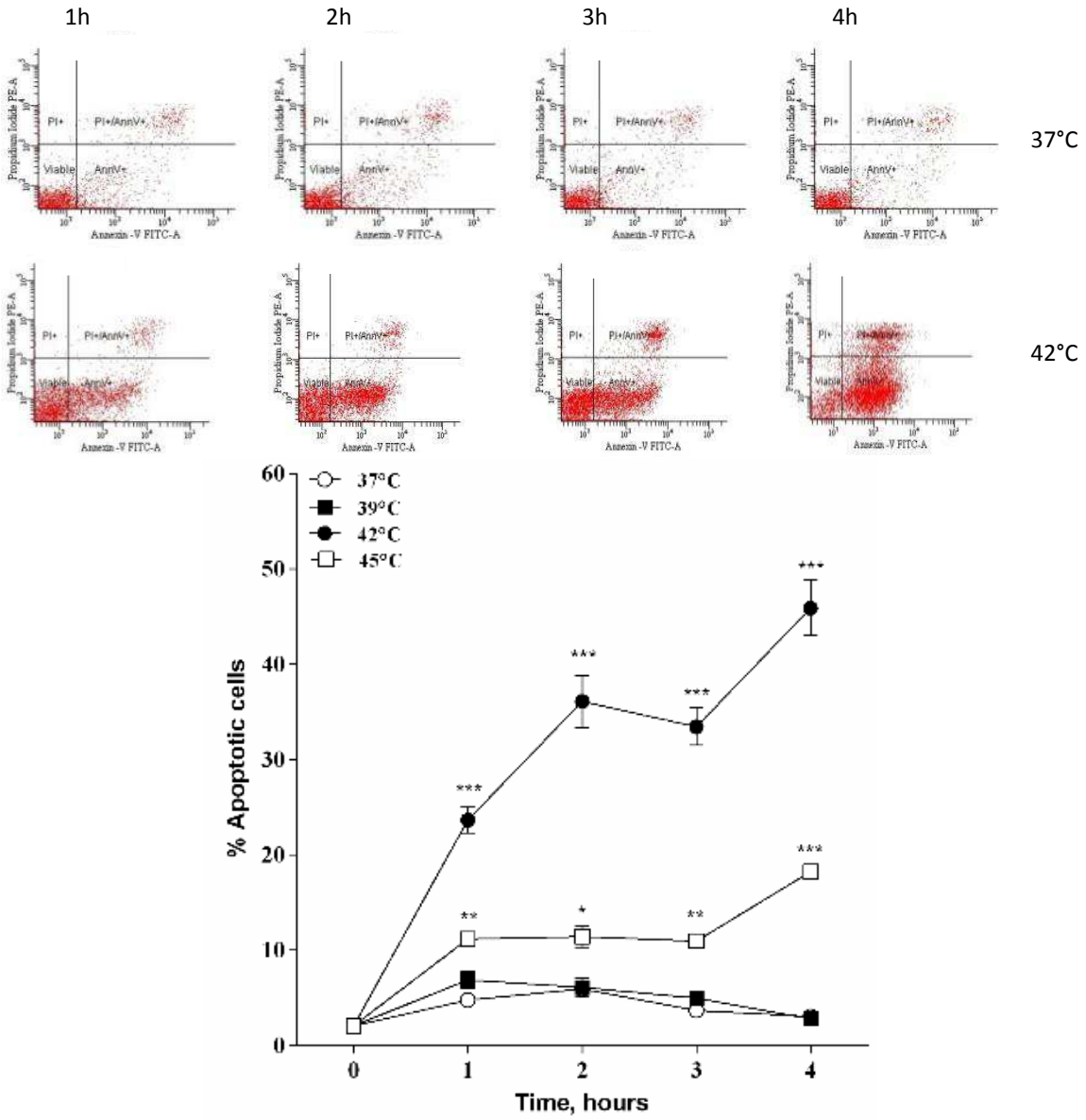

Figure 7: Phosphatidylserine (PS) presentation in heat shock time course

Jurkat cells were treated for 4 hours at four different temperatures (37°C, 39°C, 42°C, and 45°C); data n=3 independent experiments are represented a mean ± SD. Annexin V was measured by flow cytometry, analysing the external phosphatidylserine (PS) expression (RED): data are represented as a percentage of Annexin-V+ /PI- cells; on the right flow cytometric dot plots of the most representative data. Statistical analysis performed was two way-ANOVA with Bonferroni post hoc test (***= P< 0.001) comparing the differences between the 0 time in each data set and the difference between the different data set.

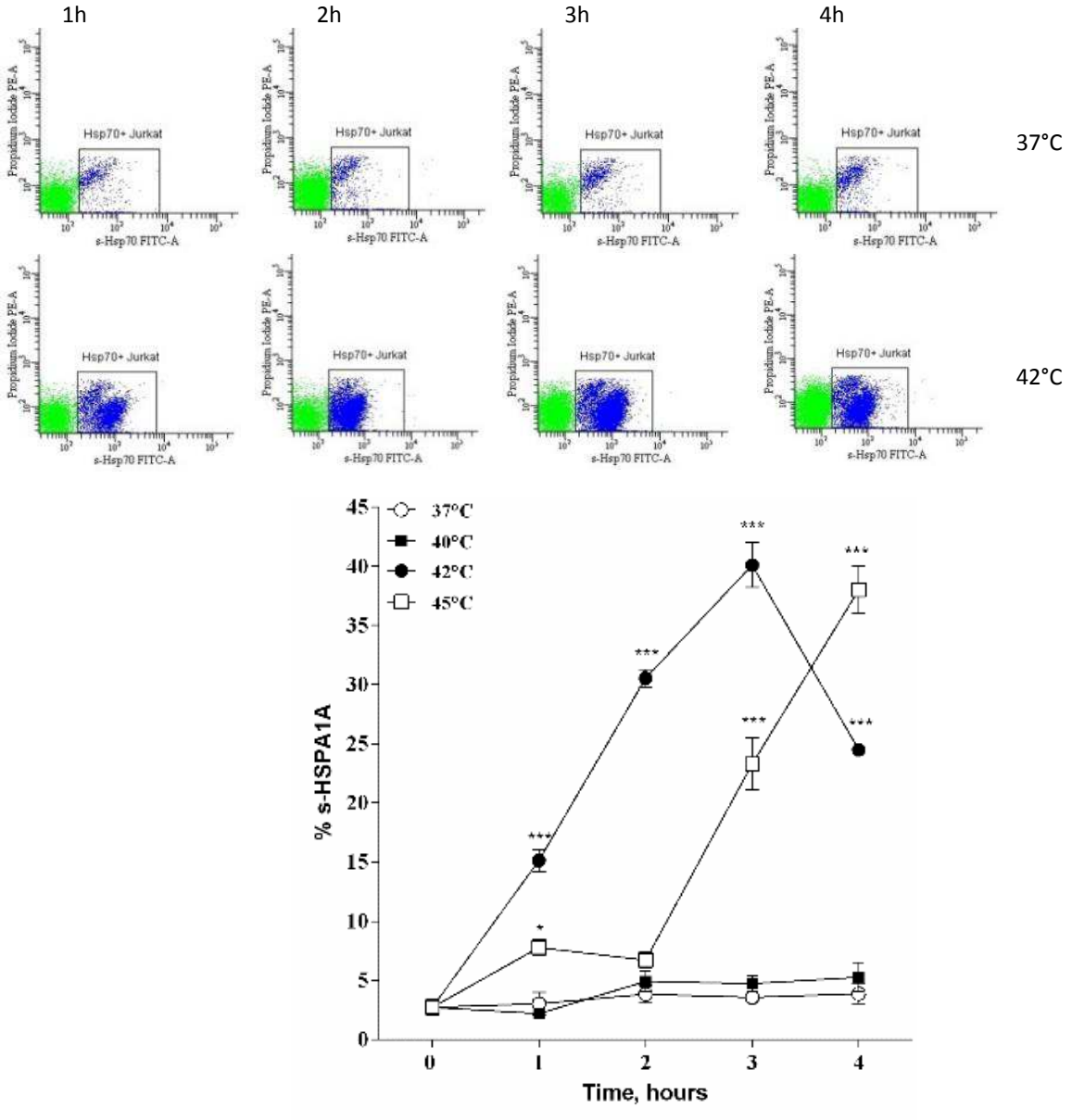

Figure 8: Surface HSPA1A presentation in heat shock time course

Jurkat cells were treated for 4 hours at four different temperatures (37°C, 39°C, 42°C, and 45°C); data n=3 independent experiments are represented a mean ± SD. Flow cytometric data of the s-HSPA1A time course (listed as s-hsp70): data are represented as percentage of viable cells (PI^-) (BLUE and GREEN) expressing surface HSPA1A; on the right flow cytometric dot plots of the most representative data (BLUE only). Statistical analysis performed was two way-ANOVA with Bonferroni post hoc test (***= P< 0.001) comparing the differences between the 0 time in each data set and the difference between the different data set.

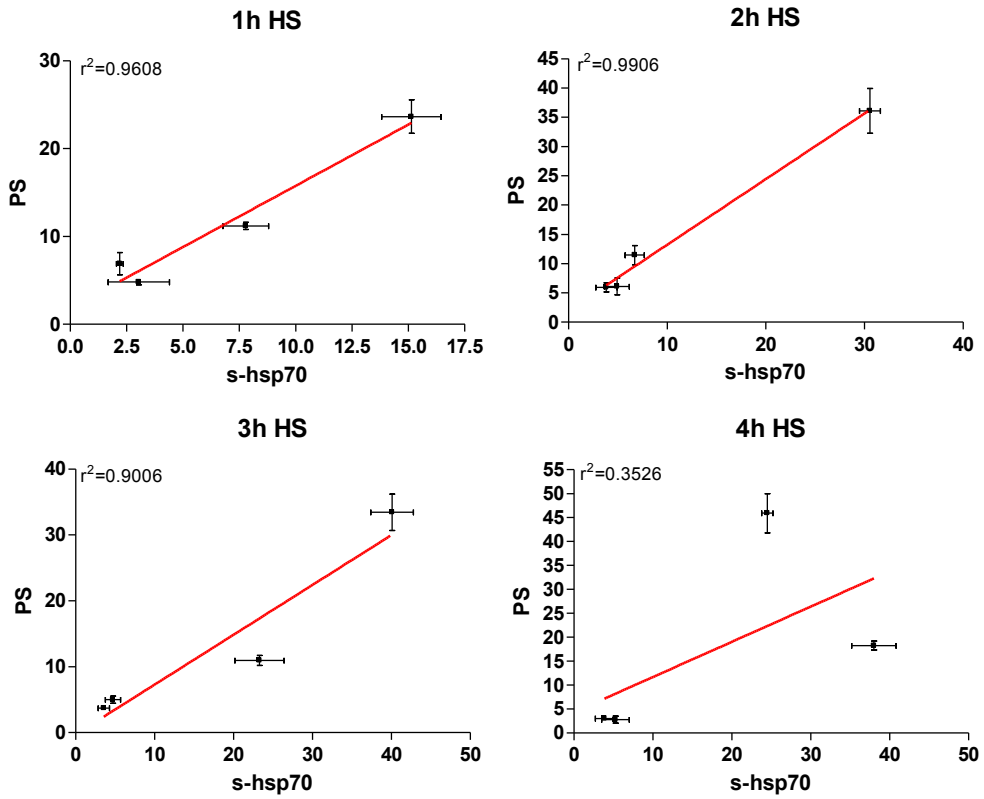

Figure 8A: **Correlation analysis between PS external presentation and surface Hsp72.**
The results show a positive correlation at the first 3 hour of heat shock (R^2 >0.8) but not at the 4th hour (R^2< 0.8). Annexin-V data is represented by the % of cells positive to Annexin-V and negative to PI; the s-Hsp72 data is represented by the % of cells positive to s-Hsp72 and negative to PI.

Surface HSPA1A co-localises with lipid rafts and LAMP-1

Using fluorescence microscopy we investigated three different potential pathways by which HSPA1A could be inserted into the cell membrane: lipid rafts – using an antibody against the penta-saccharide chain of plasma membrane ganglioside-GM1; the endo-lysosomal pathway using an antibody against LAMP-1; and Golgi transport – using an antibody against Golgi, golgin-97. Surface HSPA1A antibody was labelled using the cm.Hsp70.1 antibody. We looked for co-localisation at 2 and 4 hours – times at which we had observed membrane insertion was occurring. The images confirm that apoptosis occurr at 42°C as cells show a typical apoptotic nucleus. The microscopy confirms the flow cytometry data on s-HSPA1A with an increase after 2 hours at 42°C. Surface HSPA1A level decreased between 2 and 4 hours at 42°C. The strongest co-localisation of HSPA1A with GM1 was observed at 42°C at 2 hours treatment (Figure 9). The results show the presence of LAMP-1 on the cell surface at temperatures higher than 37°C. However, it was not possible to co-localise clearly the LAMP-1 expression with HSPA1A on the surface until 4 hours only at 42°C (Figure 10). At no time did HSPA1A co-localize with golgin 97 at any temperature (Figure 11).

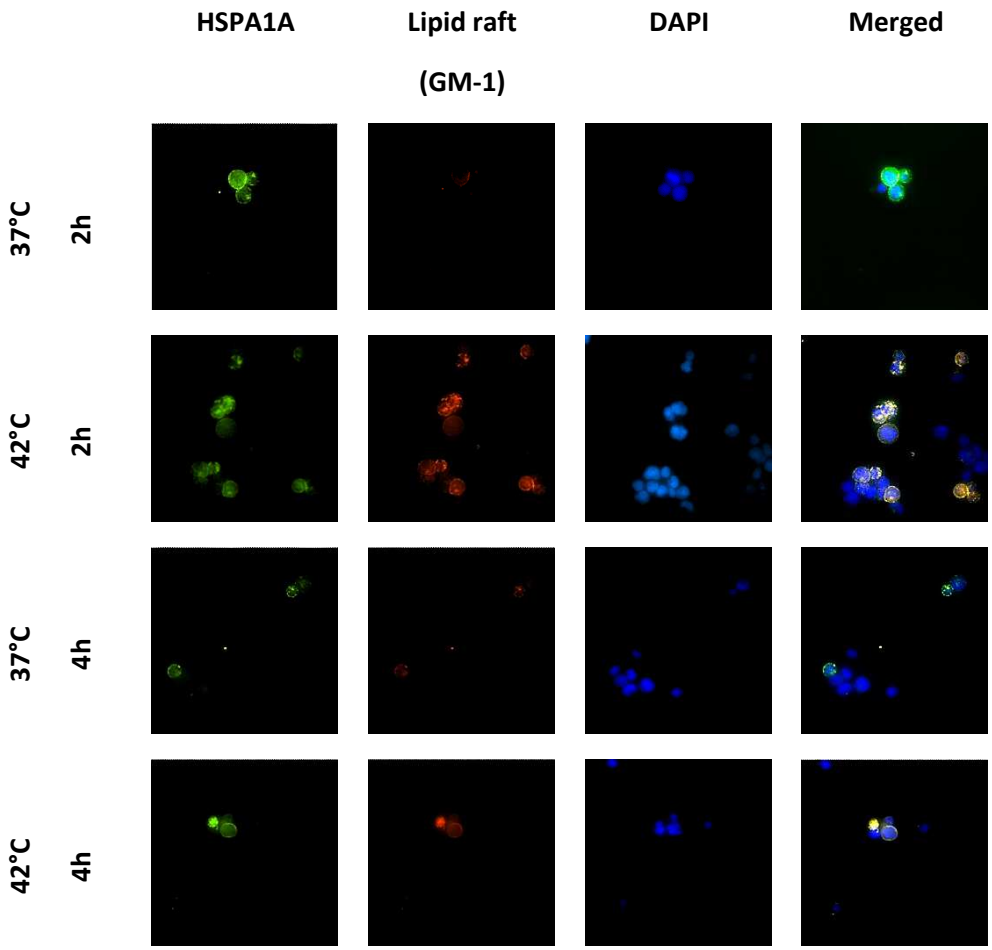

Figure 9: HSPA1A co-localization with lipid rafts after 2 and 4 hours heat shock

Most representative microscopy pictures (at magnification 60X) out of n=3 independent experiments of Jurkat cells heat shocked for 2 hours and 4 hours at 42°C with a control at 37°C, are shown. Single fluorescence images are captured separately and then merged together to analyse co-localization. The colors represent: Blue= Nucleus-DAPI, Red= GM1 (Lipid rafts)-Alexa 555, Green= HSPA1A-FITC, Yellow= when lipid raft and HSPA1A are co-localized.

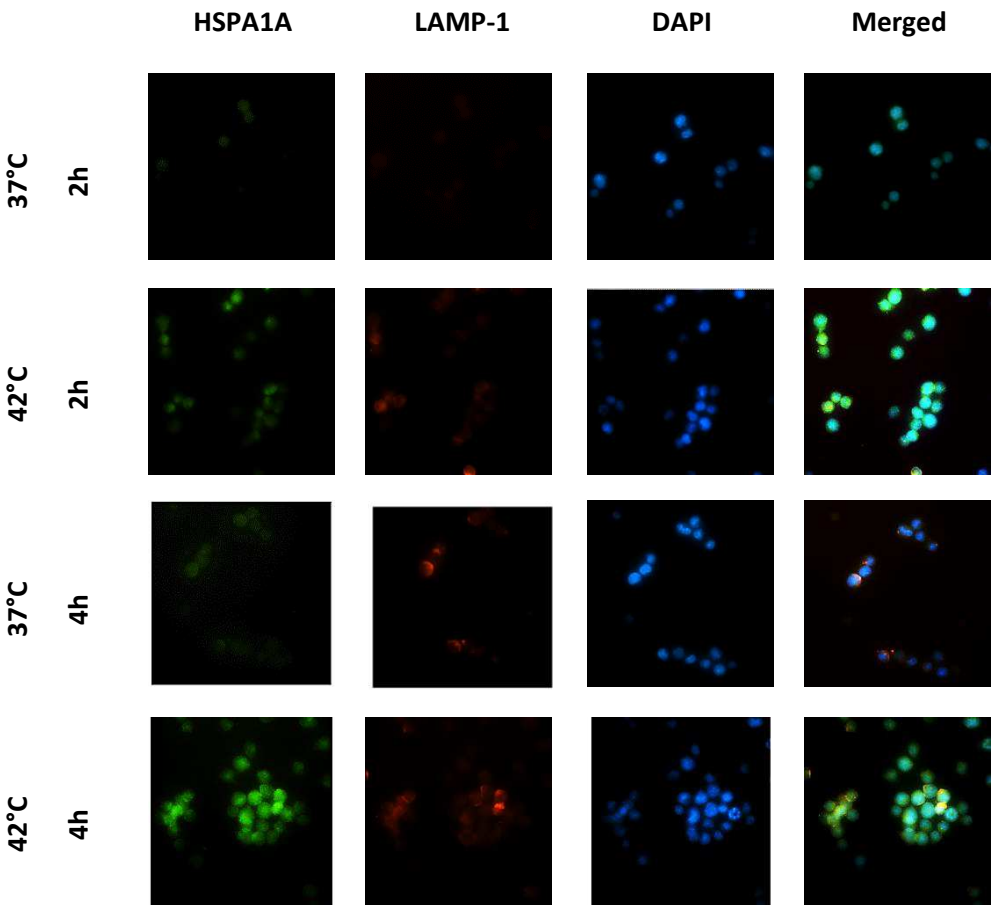

Figure 10: HSPA1A co-localization with surface endo-lysosomes marker after 2 and 4 hours heat shock

Most representative microscopy pictures (at magnification 60X) out of n=3 independent experiments of Jurkat cells heat shocked for 2 hours and 4 hours at 42°C with a control at 37°C, are shown. Single fluorescence images are captured separately and then merged together to analyse co-localization. The colors represent: Blue= Nucleus-DAPI, Red= LAMP-1 (endo-lysosome marker), second antibody IgG-Cy3-conjugated, Green= HSPA1A-FITC, Yellow= when the endo-lysosomal marker and HSPA1A are co-localized.

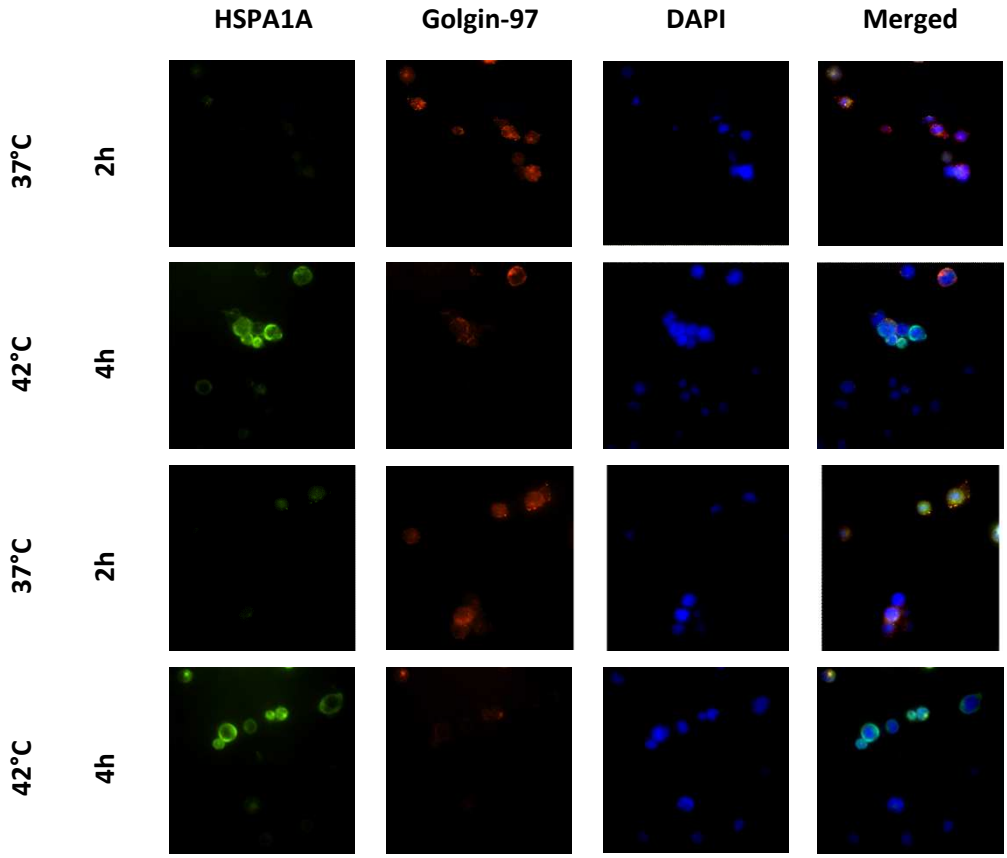

Figure 11: HSPA1A co-localization with Golgi marker after 2 and 4 hours heat shock
Most representative microscopy pictures (at magnification 60X) out of n=3 independent experiments of Jurkat cells heat shocked for 2 hours and 4 hours at 42°C with a control at 37°C, are shown. Single fluorescence images are captured separately and then merged together to analyse co-localization. The colors represent: Blue= Nucleus-DAPI, Red= Golgin 97- second antibody IgG-Cy3-conjugated, Green= HSPA1A-FITC, Yellow= when Golgin-97 and HSPA1A are co-localized.

HSPA1A gene expression is induced with heat shock and heat shock factor- 1 inhibitor KNK347 deplete HSP1A1A up-regulation.

HSPA1A gene expression was tested in the heat shock treatments used: the results confirm the literature and demonstrate an HSPA1A up-regulation with heat shock (P<0.001 at 2hours and 4 hours heat shock) (Figure 12). In addition it was tested the HSPA1A gene expression inhibition with heat shock in order to further test the contribution of the *de-novo* synthesis on the cell surface and outside the cells. The HSPA1A synthesis was inhibited using a N-formyl-3,4-methylenedioxy-benzylidene-γ-butyrolactam (KNK437) that interacts and inactivates the Heat shock factor-1 (*HSF1*). Jurkat cells were treated with 50 µM KNK437 for 1 hour at 37° or 42°C followed by three hours recovery at 37°C. The results show an effective HSPA1A gene expression inhibition with heat shock similar to the non-heat shocked control cells (Figure 12).

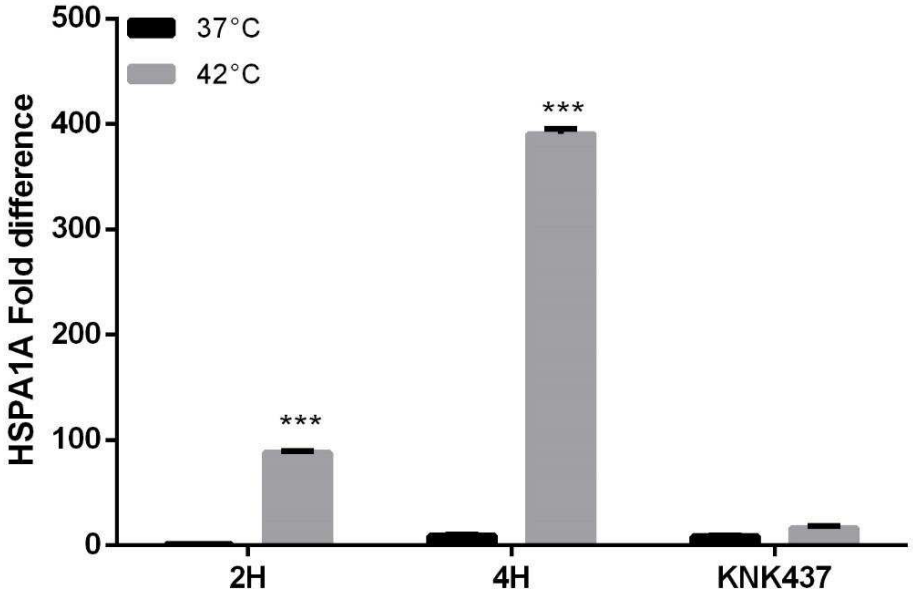

Figure 12: HSPA1A gene expression after 2 and 4 hours heat shock together with treatment with KNK437.

Jurkat cells were treated 1hour with 50µM of KNK437 HSPA1A inhibitor, at different temperatures (37° or 42°C), followed by three hours recovery at 37°C; data n=3 independent experiments are represented a mean ± SD. Gene expression is expressed as fold difference comparing each set of data to the no treated control, who has value of 1. Statistical analysis performed was a two way ANOVA with Bonferroni post hoc test, comparing the difference between the non-treated controls (0 µM) in each temperature set. *=P<0.05; **=P<0.01; ***=P<0.001.

HSPA1A de novo protein synthesis affect protein secretion but not membrane insertion

Once verified the real HSPA1A gene down regulation with KNK347 treatment, surface and extracellular HSPA1A on the cell surface and outside the cells was tested in order to further look the contribution of the HSPA1A *de-novo* synthesis to those mechanisms. The HSPA1A synthesis was inhibited using a N-formyl-3,4-methylenedioxy-benzylidene-γ-butyrolactam (KNK437) that interacts and inactivates the Heat shock factor-1 (*HSF1*). Jurkat cells were treated with 50µM KNK437 for 1 hour at 37° or 42°C followed by three hours recovery at 37°C. Microscopic analysis, cell activity, apoptosis and necrosis assays showed that KNK437 did not induce cell cytotoxicity (Figure 13). The treatment with the *HSF1* inhibitor shows that the membrane HSPA1A exposure is not controlled by the *de novo* synthesis (Figure 14), while the release outside cells as free protein is highly affected by the protein synthesis disruption (Figure 15) and also, to a less degree, the intracellular HSPA1A level (Figure 16).

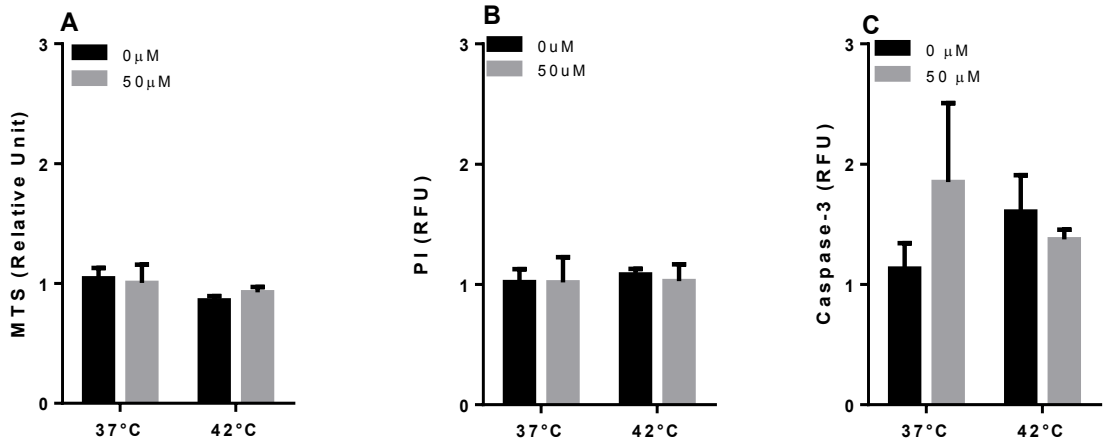

Figure 13: Viability, necrosis and apoptosis analysis of Jurkat after 2 hours heat shock together with KNK347.

Jurkat cells were treated 1hour with 50µM of KNK437 HSPA1A inhibitor, at different temperatures (37° or 42°C), followed by three hours recovery at 37°C; data n=3 independent experiments are represented a mean ± SD. **(A)** MTS assay: the results are expressed as relative units, comparing the each sample to the MTS value of a no treated control. **(B)** Necrosis analysis by PI fluorescence: the results are expressed as relative units, comparing the each sample to the PI value of a no treated control. **(C)** Caspase-3 fluorimetric analysis the results are expressed as relative units, comparing the each sample to the fluorescence value of a no treated control. Statistical analysis performed was a two way ANOVA with Bonferroni post hoc test, comparing the difference between the non-treated controls (0 µM) in each temperature set. *=P<0.05; **=P<0.01; ***=P<0.001.

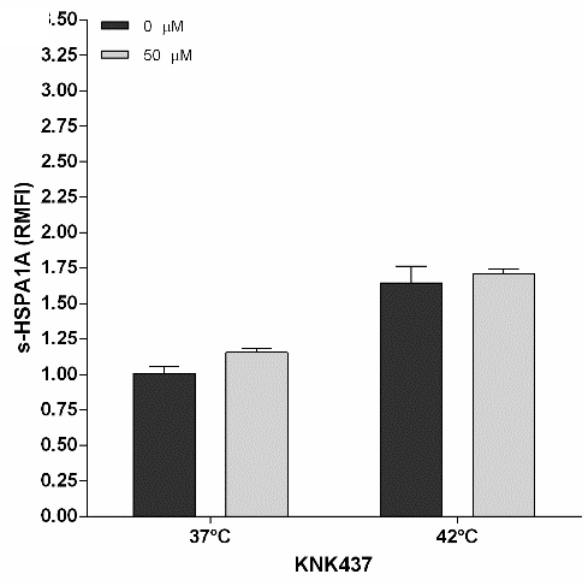

Figure 14: HSPA1A gene expression inhibition and effect on s-HSPA1A

Jurkat cells were treated 1hour with 50µM of KNK437 HSPA1A inhibitor, at different temperatures (37° or 42°C), followed by three hours recovery at 37°C; data n=3 independent experiments are represented a mean ± SD. Surface HSPA1A (s-HSPA1A), measured by flow cytometry: data are represented as RMFI where mean of fluorescence intensities values of each sample was normalised to the non-heat shocked control. Statistical analysis performed was a two way ANOVA with Bonferroni post hoc test, comparing the difference between the non-treated controls (0 µM) in each temperature set. *=P<0.05; **=P<0.01; ***=P<0.001.

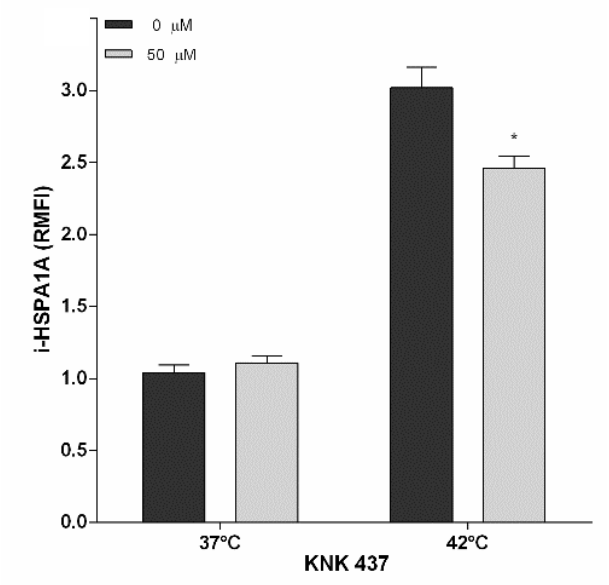

Figure 15: HSPA1A gene expression inhibition and effect on i-HSPA1A

Jurkat cells were treated 1hour with 50µM of KNK437 HSPA1A inhibitor, at different temperatures (37° or 42°C), followed by three hours recovery at 37°C; data n=3 independent experiments are represented a mean ± SD. Intracellular HSPA1A (i-HSPA1A) measured by flow cytometry: data are represented as RMFI where mean of fluorescence intensities values of each sample was normalised to the non-heat shocked control. Statistical analysis performed was a two way ANOVA with Bonferroni post hoc test, comparing the difference between the non-treated controls (0 µM) in each temperature set. *=P<0.05; **=P<0.01; ***=P<0.001.

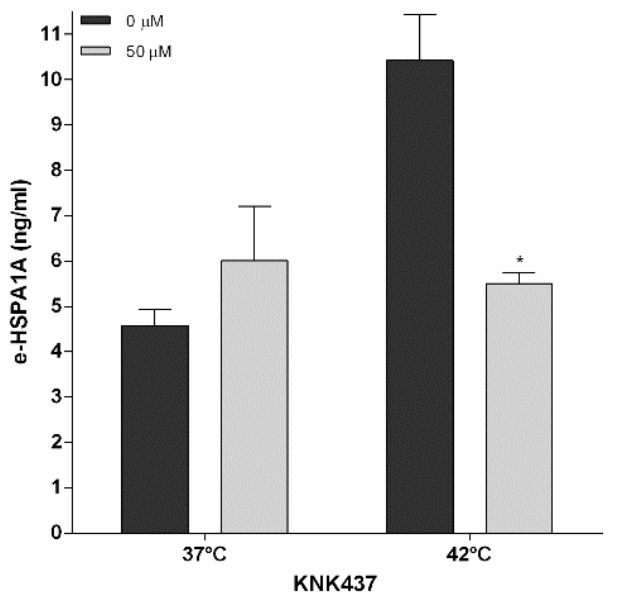

Figure 16: HSPA1A gene expression inhibition and effect on e-HSPA1A

Jurkat cells were treated 1hour with 50µM of KNK437 HSPA1A inhibitor, at different temperatures (37° or 42°C), followed by three hours recovery at 37°C; data n=3 independent experiments are represented a mean ± SD. Extracellular HSPA1A (e-HSPA1A) measured by ELISA in tissue culture supernatant and expressed in ng/ml. Statistical analysis performed was a two way ANOVA with Bonferroni post hoc test, comparing the difference between the non-treated control (0 µM) in each temperature set. *=P<0.05; **=P<0.01; ***=P<0.001.

Exosome secretion rate did not increase significantly but internal exosome HSPA1A increase

We next tested exosome secretion from heat shocked Jurkat cells and the presence of membrane and intra-luminal HSPA1A on purified exosomes. Exosomes were purified by differential ultracentrifugation and analysed by flowcytometry to test surface antigens and western blot on lysed and sonicated exosomes to test internal exosome content. The image acquired by TEM show that the purified vesicles are within the defined size range for exosomes (Figure 17).

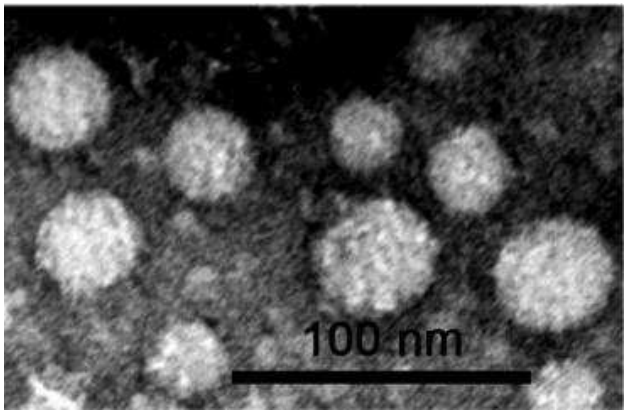

Figure 17: Exosome analysis and HSPA1A localization following heat shock treatment
Jurkat cells were heat shocked at 42°C for 2 and 4 hours, a control was left a 37°C and exosomes were purified; data n=3 independent experiments are represented a mean ± SD. A representative sample of exosomes purified were visualised by TEM.

The results show that exosome production does not significantly change with heat shock as tested by total protein quantification by Bradford assay, acetyl cholinesterase assay (Figure 18), CD81 exosome surface expression by flowcytometry (Figure 19) and western blot (Figure 20).

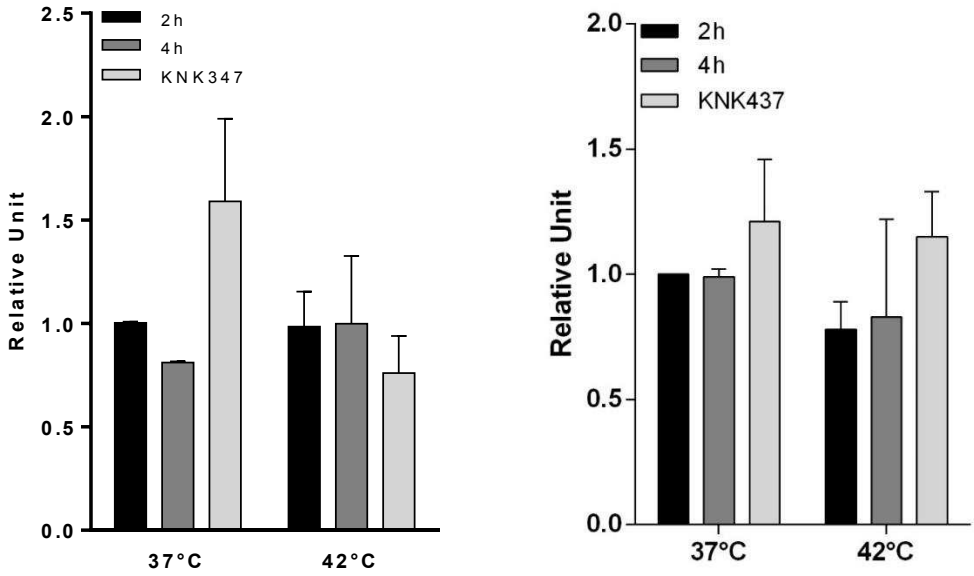

Figure 18: Exosome protein content following heat shock treatment
Jurkat cells were heat shocked at 42°C for 2 and 4 hours, a control was left a 37°C and exosomes were purified; data n=3 independent experiments are represented a mean ± SD. Exosome protein content was analysed by Bradford assay (left) and acetylcholinesterase assay (right). Statistical analysis was two way ANOVA with Bonferroni post hoc test, comparing the non-treated samples with the treated samples at different temperatures. *=P<0.05; **=P<0.01; ***=P<0.001.

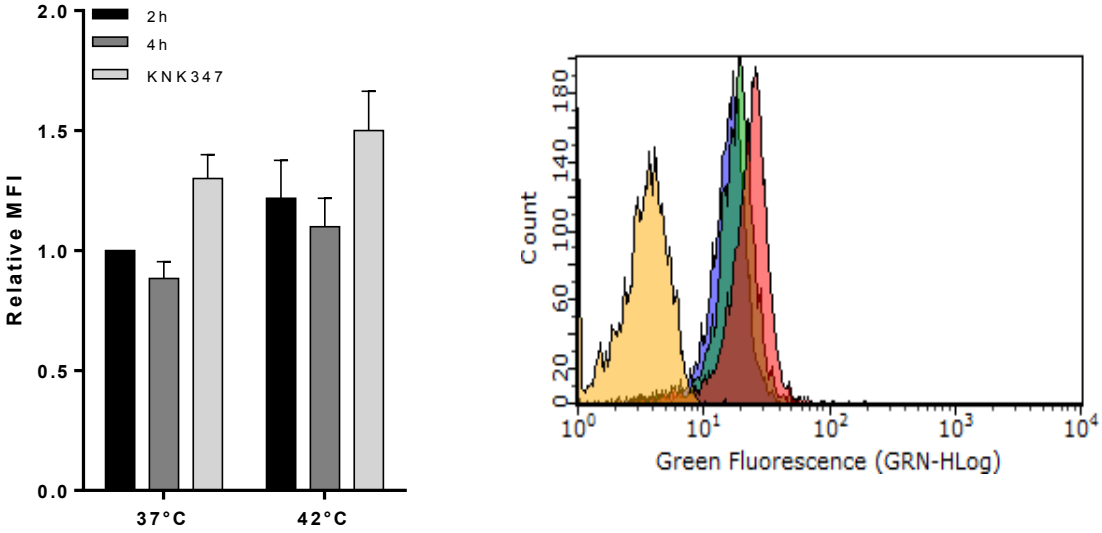

Figure 19: Exosome CD81 analysis following heat shock treatment

Jurkat cells were heat shocked at 42°C for 2 and 4 hours, a control was left a 37°C and exosomes were purified; data n=3 independent experiments are represented a mean ± SD. Surface CD81 was measured by flowcytometry using 4µm latex beads as a support for exosome flow cytometric analysis; mean of fluorescence values from samples were normalised with the control non treated sample, therefore the data are represented as relative mean of fluorescence intensities (RMFI); below each graph a representative flow cytometric hystogram.

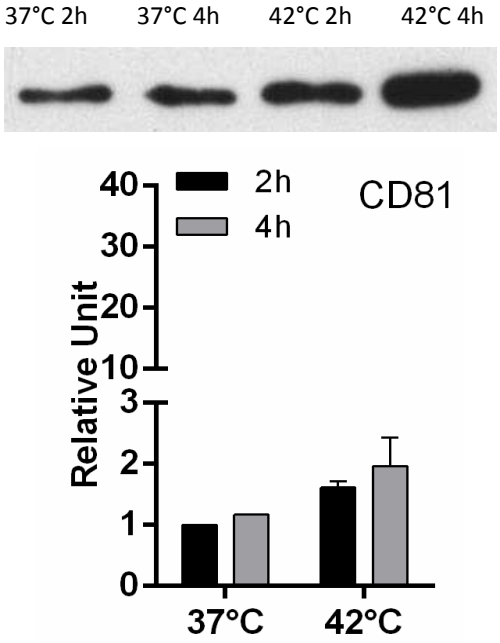

Figure 20: Exosome CD81 content on sonicated samples

Western blot on exosomes purified from heat shock and control cells was performed and CD81 was tested on lysed and sonicated samples. Densitometric results are summarised below. Statistical analysis was two way ANOVA with Bonferroni post hoc test, comparing the non-treated samples with the treated samples at different temperatures. *=P<0.05; **=P<0.01; ***=P<0.001.

Exosomal membrane HSPA1A, tested by flowcytometry, does not change in heat shock cells as tested by flowcytometry (Figure 21). However, total HSPA1A content in lysed and sonicated exosomes, tested by western blot, increase with heat shock (Figure 22), suggesting that the HSPA1A, carried by these exosomes, is intra-luminal. Exosomes isolated from cells treated with KNK437 have the same level of intra luminal HSPA1A content of the no-treated heat shocked samples, demonstrating that exosome HSPA1A loading and release is *de novo* synthesis independent (Figure 23).

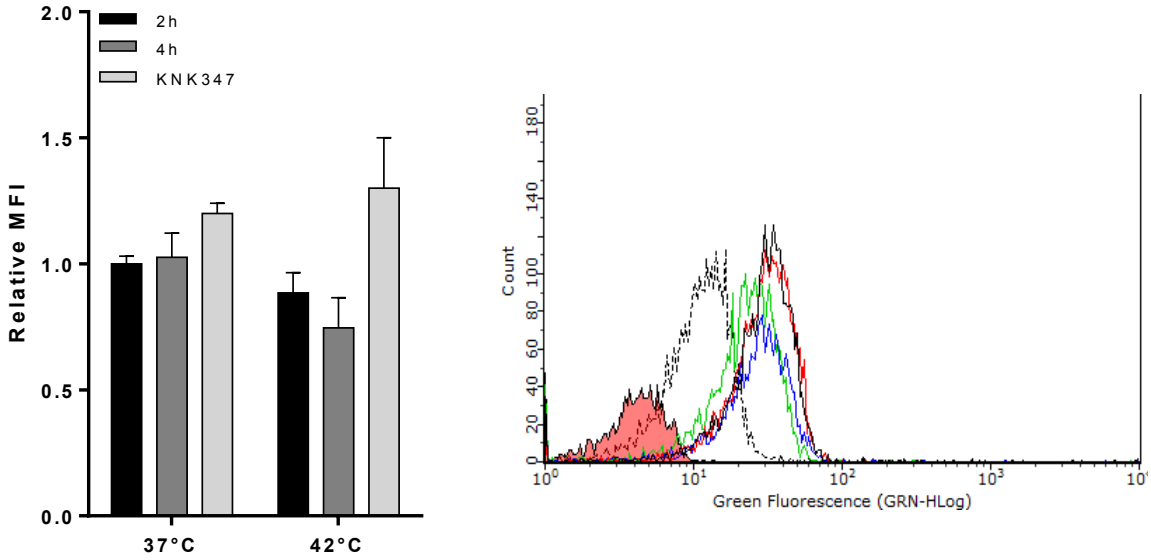

Figure 21: Exosome s-HSPA1A analysis following heat shock treatment
Jurkat cells were heat shocked at 42°C for 2 and 4 hours, a control was left a 37°C and exosomes were purified; data n=3 independent experiments are represented a mean ± SD. HSPA1A was measured by flowcytometry using 4µm latex beads as a support for exosome flow cytometric analysis; mean of fluorescence values from samples were normalised with the control non treated sample, therefore the data are represented as relative mean of fluorescence intensities (RMFI); below each graph a representative flow cytometric hystogram. Statistical analysis was two way ANOVA with Bonferroni post hoc test, comparing the non-treated samples with the treated samples at different temperatures. *=P<0.05; **=P<0.01; ***=P<0.001.

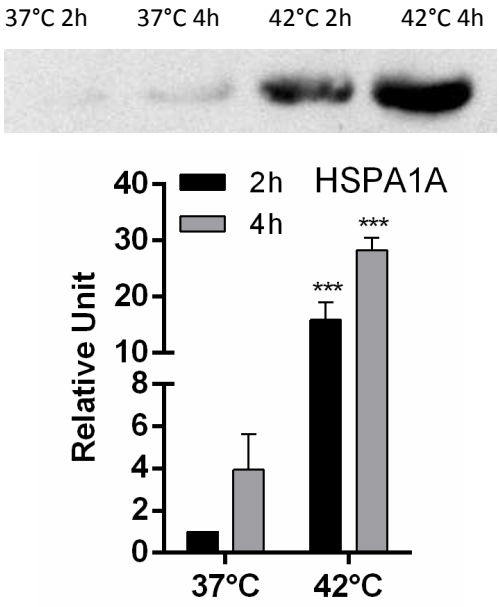

Figure 22: Exosome HSPA1A content on sonicated samples

Western blot on exosomes purified from heat shock and control cells was performed and HSPA1A was tested on lysed and sonicated samples. Densitometric results are summarised below. Statistical analysis was two way ANOVA with Bonferroni post hoc test, comparing the non-treated samples with the treated samples at different temperatures. *=P<0.05; **=P<0.01; ***=P<0.001.

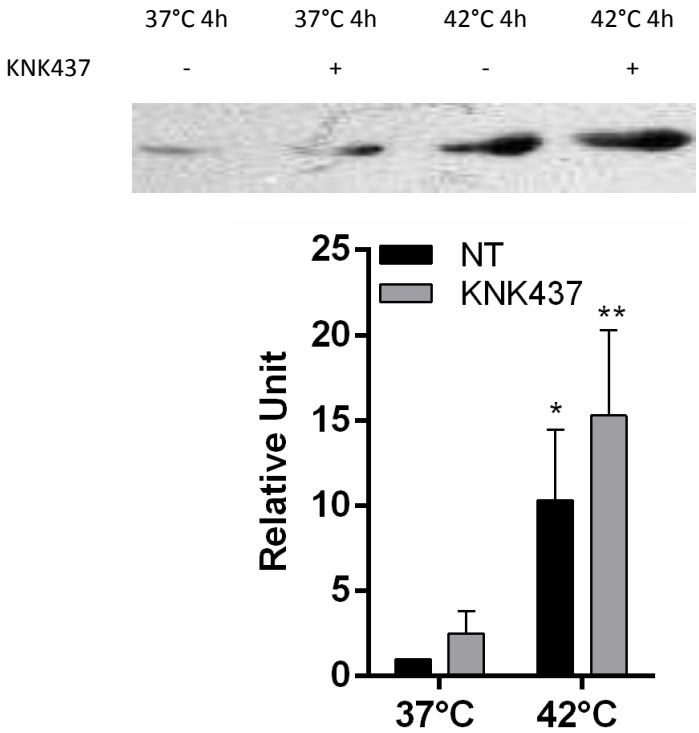

Figure 23: Exosome content on sonicated cells treated with KNK437

Western blot on exosomes purified from heat shocked cells treated with the KNK437 inhibitor was performed and HSPA1A was tested on lysed and sonicated samples. Densitometric results are summarised below. Statistical analysis was two way ANOVA with Bonferroni post hoc test, comparing the non-treated samples with the treated samples at different temperatures. *=P<0.05; **=P<0.01; ***=P<0.001.

Purified microvesicles from stressed cells don't increase their release rate with heat shock

We further tested the microvesicles purified from Jurkat cells after heat shock and checked the total protein content and the s-HSPA1A content. We decided to analyse only the surface content of the vesicles, because the microvesicle biogenesis is associated with plasma membrane. The results show by Bradford and by acetylcholinesterase assays that there is no change in the release rate of microvesicles. The results also show that s-HSPA1A does not increase on microvesicle's surface after heat shock.

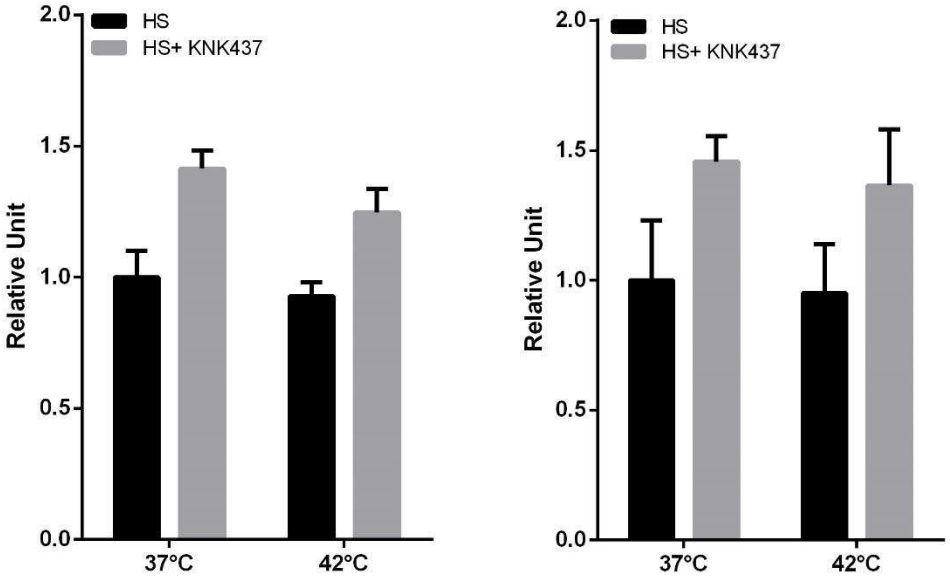

Figure 24: Microvesicles protein content following heat shock treatment

Jurkat cells were heat shocked at 42°C for 2 and 4 hours, a control was left a 37°C and microvesicles were purified; data n=3 independent experiments are represented a mean ± SD. Microvesicles protein content was analysed by Bradford assay (left) and acetylcholinesterase assay (right). Statistical analysis was two way ANOVA with Bonferroni post hoc test, comparing the non-treated samples with the treated samples at different temperatures. *=P<0.05; **=P<0.01; ***=P<0.001.

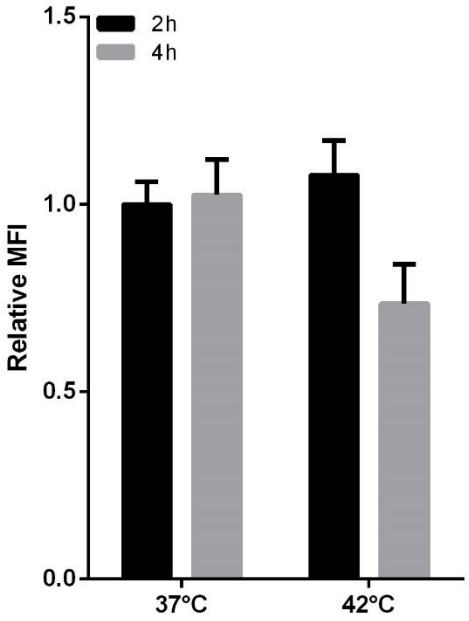

Figure 25: Microvesicles s-HSPA1A analysis following heat shock treatment
Jurkat cells were heat shocked at 42°C for 2 and 4 hours, a control was left a 37°C and microvesicles were purified; data n=3 independent experiments are represented a mean ± SD. HSPA1A was measured by flowcytometry using 4µm latex beads as a support for microvesicles flow cytometric analysis; mean of fluorescence values from samples were normalised with the control no treated sample, therefore the data are represented as relative mean of fluorescence intensities (RMFI). Statistical analysis was two way ANOVA with Bonferroni post hoc test, comparing the non-treated samples with the treated samples at different temperatures. *=P<0.05; **=P<0.01; ***=P<0.001.

Exosomes purified from stressed cells activate immunocompetent cells

Purified exosomes were used to perform functional studies: in detail 100µg/nl of the purified exosomes were co-cultured with U937, a monocitic cell line. In certain conditions these cells have the ability to activate and transform to active macrophages. Therefore this co treatment was performed to test the ability of purified exosome to stimulate or abrogate immune response. U937 cell cycle analysis was performed and G1 arrest was analysed in detail as a sign of macrophage differentiation. Preliminary experiments were made in order to have a positive control that activate macrophages. Phorbol myristate acetate (PMA) was used at concentration of 100ng/ml at different times and 18h of activation was chosen as the best treatment that induce macrophage activation (Figure 26). Microscopy images show activated and transformed macrophages (Figure 27).

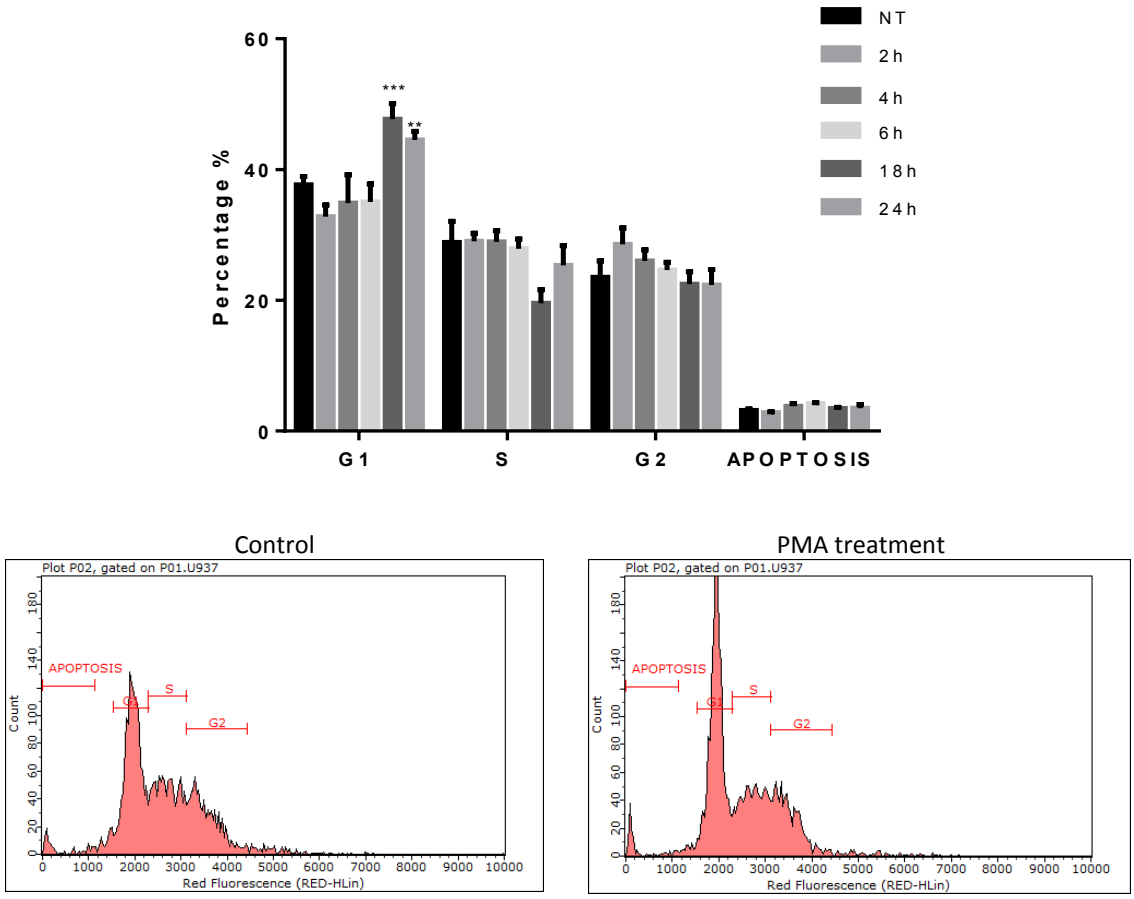

Figure 26: PMA treatment on U937 activation at different times.

U937 cells were treated with 100ng/ml PMA at different incubation times and cell cycle analysis was performed by flowcytometry. The graph above represent the percentage of the cells in each phase of the cell cycle. The hystograms below are the two representative samples of a cell clycle analysis of a normal U937 sample and a PMA activated sample. Statistical analysis was two way ANOVA with Bonferroni post hoc test, comparing the non-treated samples with the treated samples at different temperatures. *=P<0.05; **=P<0.01; ***=P<0.001.

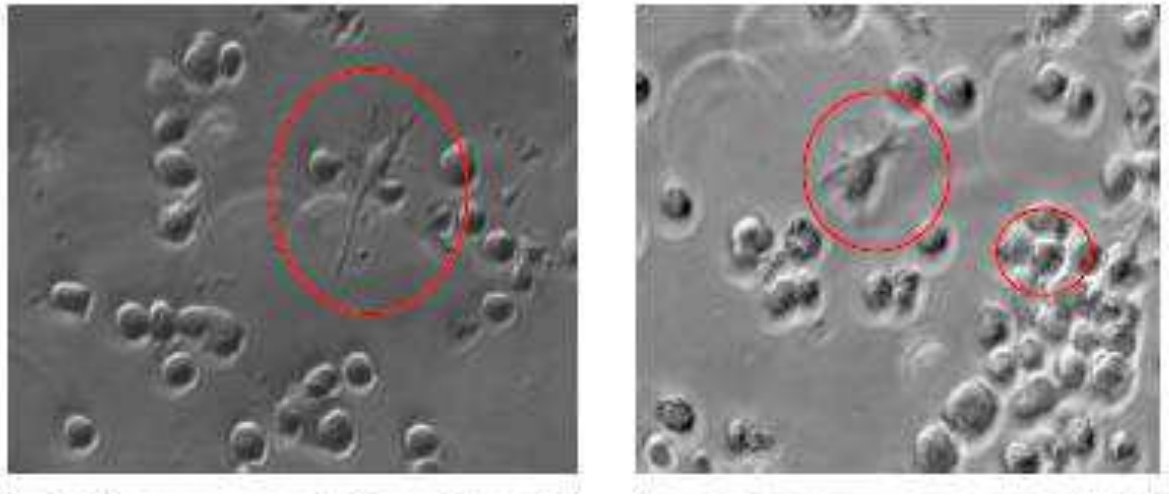

Figure 27: activated U937 cells after PMA treatment for 18 h
The images are two representative examples of U937 cells treated with 100ng/ml PMA for 18 hours. The cells circled are activated macrophages with their typical hairy shape.

Microvesicles and exosomes purified from controls and heat shocked cells were used to treat U937 cells. The results show that microvesicle treatment does not induce any macrophage differentiation (Figure 28), while exosome treatment slightly induce macrophage differentiation only when using exosomes from heat shock cells (P<0,05) (Figure 29).

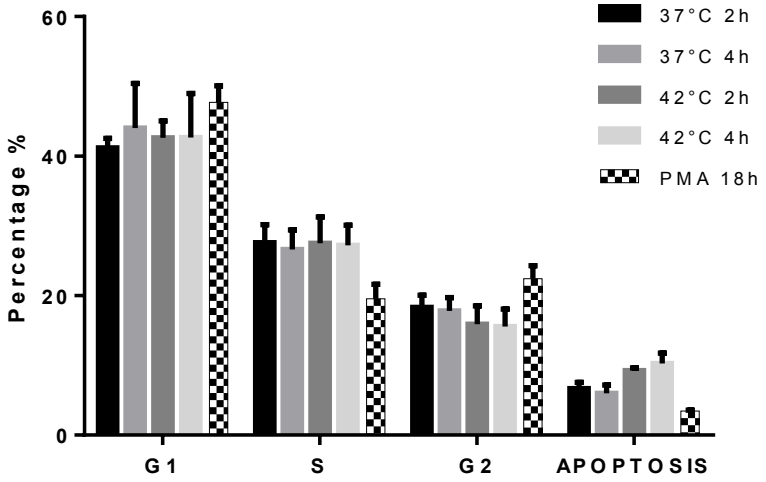

Figure 28: U937 cell cycle profile after treatment with purified Microvesicles.
U937 cells were treated with 100ng/ml of microvesicles for 4 hours and cell cycle analysis was performed by flowcytometry; the results are represented as percentage of cells at a certain stage of the cell cycle. Statistical analysis was two way ANOVA with Bonferroni post hoc test, comparing the non-treated samples with the treated samples at different temperatures. *=P<0.05; **=P<0.01; ***=P<0.001.

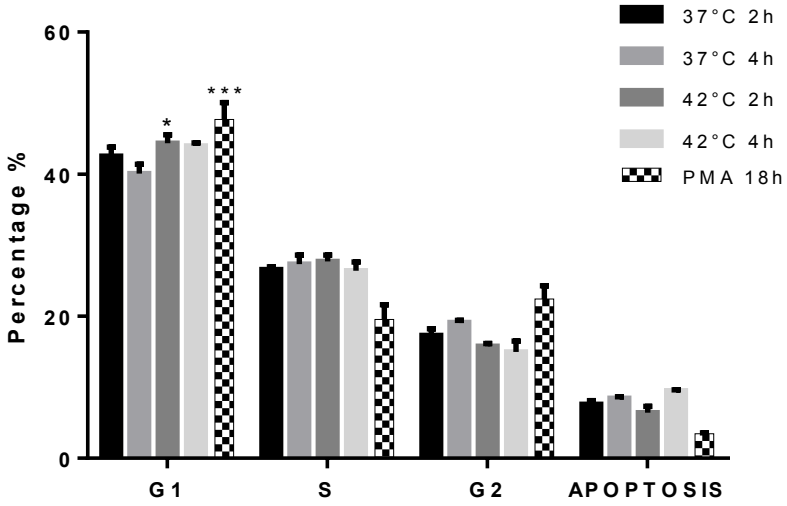

Figure 29: U937 cell cycle profile after treatment with purified Exosomes.
U937 cells were treated with 100ng/ml of exosomes for 4 hours and cell cycle analysis was performed by flowcytometry; the results are represented as percentage of cells at a certain stage of the cell cycle. Statistical analysis was two way ANOVA with Bonferroni post hoc test, comparing the non-treated samples with the treated samples at different temperatures. *=P<0.05; **=P<0.01; ***=P<0.001.

Discussion

We initially address 2 paradigms that appear in the literature: firstly that HSPA1A is secreted from necrotic and not apoptotic cells; secondly, that HSPA1A secretory pathways are stress and cell specific. In this study we investigated HSPA1A cell surface presentation and secretion after heat stress induced apoptosis and the potential mechanisms involved.

Many studies reported that HSPA1A is only released by necrotic cells [115-120]; however some of these studies that have been using extreme cell treatments such as ionising irradiation or acrylamide treatment [36, 100]. On the other hand, only recently there are some studies regarding membrane expression of HSPA1A in apoptotic cells [121-125].

The data presented in this paper, obtained by carefully selected temperature treatments, clearly confirm that surface presentation and secretion of HSPA1A occurs also when cells are apoptotic. Regarding the kinetics of heat-induced cell death, our results confirm previous literature which show that, after an heat shock treatment (40°C and 43°C) up to 30 min there is a minimal effect on cell survival [126], while longer heat shock times at this temperature range showed apoptosis and necrosis increase [127]. Previous studies show that surface HSPA1A function, either initiated by mitochondrial disruption or direct surface stress, is to stabilize the plasma membrane integrity, although such function failed to prevent apoptosis induced by lethal Photo Dynamic Therapy treatment [128]. This could be also the reason why surface HSPA1A could be found when apoptosis was initiated by heat shock treatment. HSPA1A surface appearance in apoptotic cells could be part of an activation pathway initiated by the plasma membrane that could be a heat-stress sensor [129].

We next consider possible mechanisms for HSPA1A translocation and the relationship between HSPA1A insertion into the plasma membrane and its exposure to the external surface and secretion.

HSPA1A has been shown to interact with the membrane lipids forming ion conductance pathways within artificial lipid bilayers [113, 114]. The resulting hypothesis is that HSPA1A associated with PS might be carried to the outer membrane surface as PS flips during apoptosis in association with lipid raft structures [35]. We found a clear correlation between the appearance of HSPA1A and PS at the cell surface in the first 3 hours of treatment, consistent with this suggestion. Our data also confirm that the protein inserts into lipid raft structures, through the colocalisation of HSPA1A with lipid raft marker GM-1, in agreement with literature [35, 41, 43, 130, 131]. This is in line with recent findings where they recently showed that HSPA1A, within unilamellar liposomes, selectively interacts with negatively charged phospholipids, particularly phosphatidylserine (PS), and inserts into the lipid bilayer [39, 123]. HSPA1A display a preference for less fluid lipid environments and

the region embedded into the lipid membrane was mapped toward the C-terminus end of the molecule [39]. Komarova et al. found, within the C-term of the HSPA1A protein, a sequence composed of 20 amino acids necessary for the protein to penetrate the membrane of live cells [123]. After insertion in the membrane bilayer, HSPA1A forms high-molecular weight oligomers [39]. Therefore HSPA1A may associate and insert into the plasma membrane through an oligomerization process. In non-stressed cells, PS is located to the inner side of the plasma membrane as the ATP-dependent aminophospholipid translocase [132]. Under stress there is an activation of the ATP and Ca2+ dependent phospholipid scramblase leading PS to translocate to the outer plasma membrane [133], providing a phagocytic "eat-me" signal thus making an early marker of apoptosis [134]. However, PS positivity does not necessarily mean that cells are apoptotic, as HSPA1A/ PS membrane-positive tumor cells are viable [135]. In addition, viable T cells also have been found to present PS on the outer leaflet following activation [136]. The presence of Hsps temporarily or permanently LR membrane-associated could be useful for the membrane stabilization and for the folding of membrane proteins [129]. Our study show for the first time that the correlation between surface HSPA1A and PS after heat shock treatment occurs at early stages of apoptosis, as demonstrated by caspases activation as well as PS externalization. Hence, in our cellular model, HSPA1A membrane association could be an important signal for cellular communication, rather than for self-survival.

Furthermore we showed a colocalisation of HSPA1A with the appearance of the endo-lysosomal marker LAMP-1 on the membrane, observed at 42°C at later time points. The event occurs when cells are late apoptotic: we could hypothesise that in apoptotic cells, HSPA1A translocation can involve secretory lysosomes, as demonstrated previously in different cell models [42]The lack of co-localisation with golgin 97, a Golgi marker, confirms that membrane HSPA1A movement does not involve the classical protein secretion pathway, as demonstrated broadly by the literature [39, 42, 43].

To address the hypothesis that HSPA1A could be released via a non-classical pathway, we then tested free extracellular HSPA1A by ELISA and exosomal HSPA1A by Flow Cytometry and Western-blot. The results show that, after heat shock, free extracellular HSPA1A increase as well as total exosomal HSPA1A protein, accounting for the membrane and the intra-luminal HSPA1A protein; on the other hand exosomal membrane HSPA1A, did not increase. In contrast, some literature showed HSPA1A being released within extracellular vesicles (ECV) still inserted into the lipid bilayer [40]. Nevertheless, our data is in line with some literature showing an exosome intraluminal HSPA1A release from lymphocytes [54], while adherent cells HSPA1A release is vesicles-free [42]. Since secreted HSPA1A is a leaderless protein, therefore it doesn't go through the ER-Golgi

compartments, it is exported by an alternative mechanism called the non-classical secretory pathway. Our data suggest that free-extracellular HSPA1A could be released via exocytosis of secretory lysosomes as described previously for another leader-less protein, IL-1β [137], considering that HSPA1A has been reported previously in the lysosome lumen [5]. On the other hand the HSPA1A, transported inside the exosome lumen rather than being inserted into the vesicle membrane, could be the result of another alternative non-classical secretory pathway. Indeed, exosomes forms inside intracellular compartment, by budding off inside endosomes and not by direct shedding of cytoplasmic contents from the plasma membrane like other extracellular vesicles [138].

We further explored the role of PS in HSPA1A translocation, using a series of experiments that induce HSPA1A movement in combination with KNK437, a compound that inhibits *de novo* HSPA1A synthesis through heat shock factor 1 (HSF1) inhibition [139, 140]. Our data demonstrates that *de novo* synthesis is required for intracellular HSPA1A increase and for its secretion in stress conditions, as free protein in the extracellular space. Instead *de novo* HSPA1A synthesis is not required for HSPA1A plasma membrane exposure and for exosome-mediated release.

All together the new findings demonstrate that cells exploit differential HSPA1A surface presentation and secretion pathways, and these distinct presentations could be part of a cellular crosstalk.

The cellular crosstalk was demonstrated by the functional studies performed. Treatment of U937 cells with exosomes from heat-stressed Jurkat cells induce macrophage activation: this is partly in line with previous literature that show that membrane associate HSPA1A in extracellular vesicles induce macrophage activation [35]. Our cellular model has the HSPA1A mainly transported in the exosome lumen as other cellular models [101] but differently from this study, the exosomes induce an immune response although the immune response is mild. The results also suggest that cells can communicate different levels of stress by expressing HSPA1A in different ways.

Chapter 4: Endoplasmic Reticulum stress response

Introduction

The Unfolded Protein Response (UPR) is the system by which the Endoplasmic Reticulum (ER) responds to endogenous or exogenous stress [141, 142] and is activated by the accumulation of misfolded proteins in the reticulum lumen [143]. Recent studies revealed the role of the UPR in neoplastic transformation, where it promotes cell survival in hypoxic environment. This effect consists in attenuation of pro-apoptotic signals, cellular metabolism change and neo-angiogenesis stimulation. The activation of UPR may promote cell survival or stimulate apoptosis, depending on the context. Its activation in tumor cells plays a protective role against cell death caused by ER stress.

This response takes place via the activation of three ER transmembrane receptors: Pancreatic ER kinase (PERK), Activating Transcription Factor 6 (ATF6) and Inositol - Requiring Enzyme 1 (IRE1).

UPR molecular pathway has been studied in several tumor models and its activation has been repeatedly shown. Its role has been defined as fundamental for cell survival in tumor microenvironment. In addition UPR activation has been demonstrated also in inflammation-mediated oncogenesis [144]. UPR has been shown to be activated in hematological malignancies such as Acute Myeloid Leukemia (AML) [145], Acute B-Lymphoblastic Leukemia (B-ALL), Chronic Lymphocytic Leukemia (CLL). In AML patients IRE1α/XBP1 is often up-regulated together with grp78 and this relate to good prognosis [146].

There is no literature regarding the role of heat shock in term of UPR activation in lymphocytes; the only work done in this direction show that heat shock response (HSR) activated by heat shock, can relieve stress in UPR-deficient cells by affecting multiple ER activities [147]. The aim of the work is to analyze the UPR pathway and test how heat shock stress influence endoplasmic reticulum stress and the unfolded protein response in Jurkat cells. We tested the main UPR genes involved in activation: grp78, ATF6 and, CHOP. Grp78 is an endoplasmic reticulum chaperone and is usually located inside cells; however may works demonstrated that it could be found on the cell surface of different cancer cells [142, 148-150], also leukemic cells [142, 151]. We then tested the cell surface expression of grp78 with heat shock. There is few literature regarding the role of grp78 in extracellular vesicles such as exosomes and microvesicles. Melanoma exosomes could contain surface grp78 [152] as well as exosomes from ovarian cancer [153]. Therefore microvesicles and exosome surface grp78 has been tested by flowcytometry to check whether translocation of this endoplasmic reticulum chaperone could occur after heat shock.

Material and Methods

Here below there is a list of the methods used in this work: the methods are fully described in the Material and Methods section.

- ✓ *Jurkat cell culture and treatments*
- ✓ *Real time PCR gene expression analysis of UPR genes*
- ✓ *Surface Grp78 detection in cells and extracellular vesicles by flowcytometry*
- ✓ *Exosome and microvesicles purification*
- ✓ *Statistical analysis*

Results

Endoplasmic reticulum stress markers are activated in Stressed Jurkat cells

We tested the gene expression of protein involved in the *Unfolded Protein Response pathway (UPR)* to explore the response of the endoplasmic reticulum to heat shock in this cellular model. Jurkat cells were left at 37°C or treated at 42°C for 2 hours and 4 hours according the previous experiments settings. *Grp78*, *CHOP* and *ATF6* were chosen as markers of the UPR pathway and their gene expression was tested. *Grp78* gene expression decreased with heat shock both at 2 and 4 hours treatments (P<0,001) (Figure 1). *CHOP* gene expression decreased as well as *grp78*, however its decrease is maximal with 2 hours heat shock (P<0,0001) and minimal at 4 hours (p<0,05) (Figure 2). On the other hand *ATF6* expression did not change with 2 hours heat shock and increased only slightly after 4 hours heat shock (Figure 3).

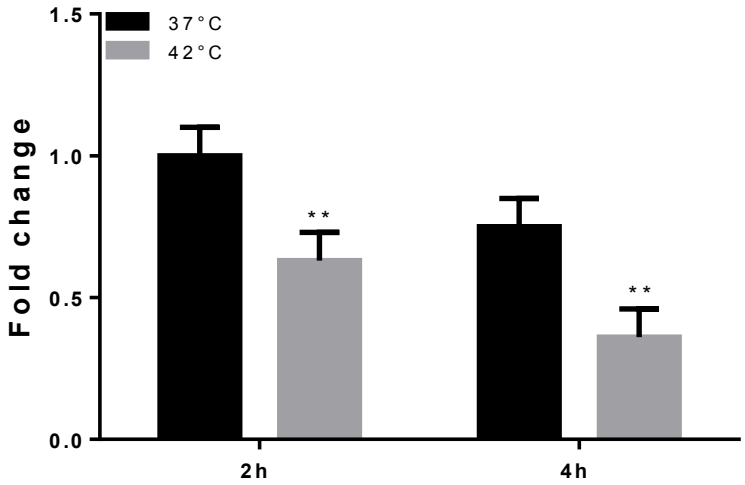

Figure1: Expression of *grp78* in heat shocked Jurkat cells.
Jurkat cells are heat shocked for 2 and 4 hours and *grp78* gene expression was tested; the results are expressed as fold change of expression mean ± standard deviation of the heat shocked samples, compared to the no treated control, setting 1 as a reference value of the control. Statistical analysis was two way ANOVA with Bonferroni post hoc test, comparing the non-treated samples with the treated samples at different temperatures. *=P<0.05; **=P<0.01; ***=P<0.001.

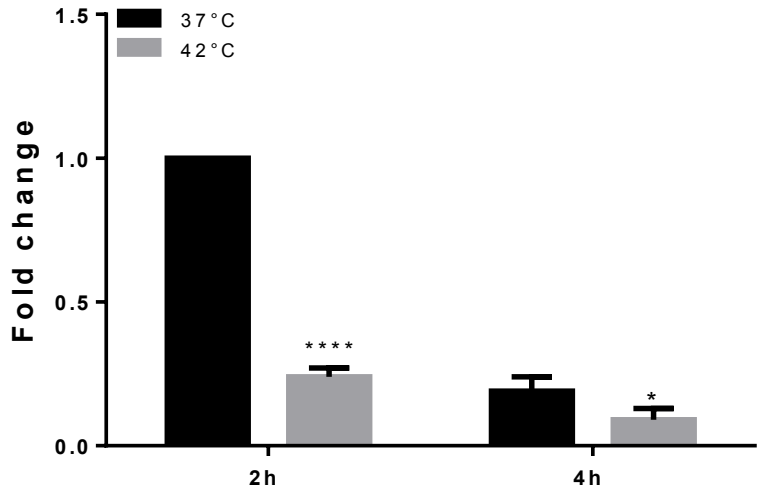

Figure 2: Expression of *CHOP* in heat shocked Jurkat cells.
Jurkat cells are heat shocked for 2 and 4 hours and *CHOP* gene expression was tested; the results are expressed as fold change of expression mean ± standard deviation of the heat shocked samples, compared to the no treated control, setting 1 as a reference value of the control. Statistical analysis was two way ANOVA with Bonferroni post hoc test, comparing the non-treated samples with the treated samples at different temperatures. *=P<0.05; **=P<0.01; ***=P<0.001.

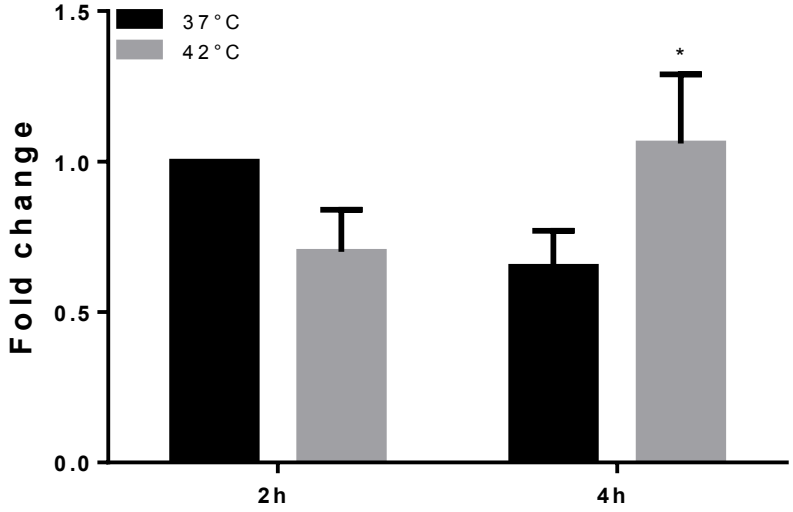

Figure 3: Expression of *ATF6* in heat shocked Jurkat cells.
Jurkat cells are heat shocked for 2 and 4 hours and *ATF6* gene expression was tested; the results are expressed as fold change of expression mean ± standard deviation of the heat shocked samples, compared to the no treated control, setting 1 as a reference value of the control. Statistical analysis was two way ANOVA with Bonferroni post hoc test, comparing the non-treated samples with the treated samples at different temperatures. *=P<0.05; **=P<0.01; ***=P<0.001.

Surface Grp78 protein expression change with heat shock

We next tested the protein expression of grp78; grp78 is normally present inside cells although it has been previously demonstrated to be present on the surface of some cancer cells. Flowcytometric results show that cell surface grp78 increased in stressed cells (2 hours treatment, P<0,001) (Figure 4). On the other hand microvesicles and exosome surface analysis demonstrated that grp78 is not present on the surface of these vesicles neither in normal nor stressed cells (Figure 5.6).

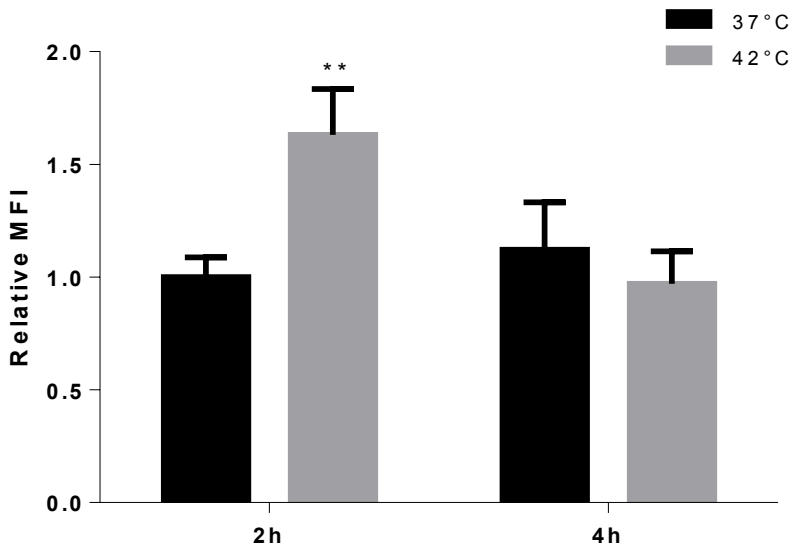

Figure 4: grp78 surface expression on stressed Jurkat cells.
Jurkat cells were heat shocked at 42°C for 2 and 4 hours, a control was left a 37°C and surface grp78 was tested by flowcytometry; data n=3 independent experiments are represented a mean ± SD. Mean of fluorescence values from samples were normalised with the control no treated sample, therefore the data are represented as relative mean of fluorescence intensities (RMFI). Statistical analysis was two way ANOVA with Bonferroni post hoc test, comparing the non-treated samples with the treated samples at different temperatures. *=P<0.05; **=P<0.01; ***=P<0.001.

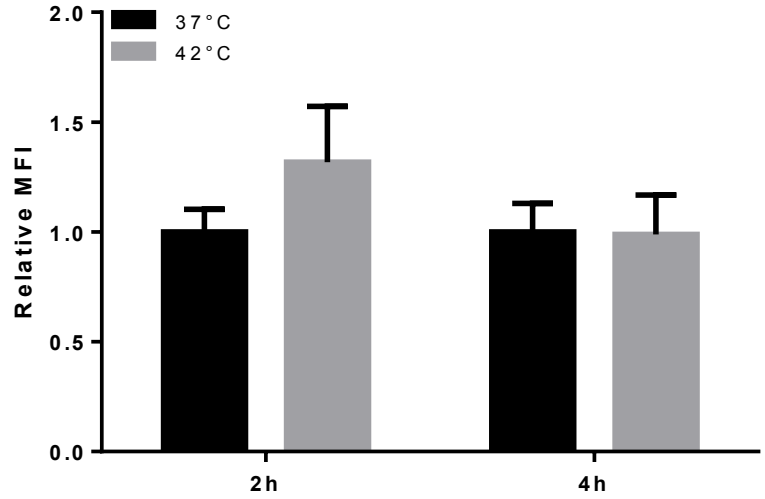

Figure 5: grp78 surface expression on purified microvesicles from stressed Jurkat cells
Jurkat cells were heat shocked at 42°C for 2 and 4 hours, a control was left a 37°C and microvesicles were purified; data n=3 independent experiments are represented a mean ± SD. Surface grp78 was measured by flowcytometry using 4µm latex beads as a support for microvesicles flow cytometric analysis; mean of fluorescence values from samples were normalised with the control no treated sample, therefore the data are represented as relative mean of fluorescence intensities (RMFI). Statistical analysis was two way ANOVA with Bonferroni post hoc test, comparing the non-treated samples with the treated samples at different temperatures. *=P<0.05; **=P<0.01; ***=P<0.001.

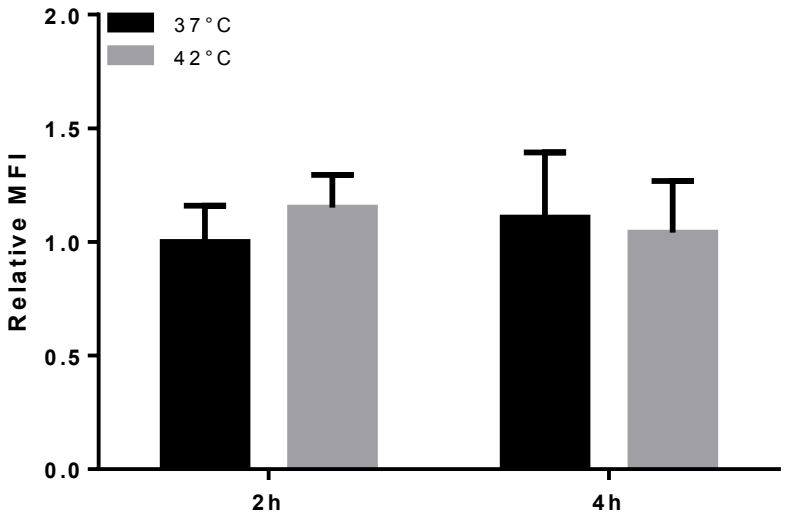

Figure 6: grp78 surface expression on purified exosomes from stressed Jurkat cells
Jurkat cells were heat shocked at 42°C for 2 and 4 hours, a control was left a 37°C and exosomes were purified; data n=3 independent experiments are represented a mean ± SD. Surface grp78 was measured by flowcytometry using 4µm latex beads as a support for microvesicles flow cytometric analysis; mean of fluorescence values from samples were normalised with the control no treated sample, therefore the data are represented as relative mean of fluorescence intensities (RMFI). Statistical analysis was two way ANOVA with Bonferroni post hoc test, comparing the non-treated samples with the treated samples at different temperatures. *=P<0.05; **=P<0.01; ***=P<0.001.

Discussion

The results summarised in this chapter is part of a preliminary work that aimed to look in detail UPR activation in heat shocked Jurkat cells and see whether heat shock could influence plasma membrane exosome and microvesicles grp78 expression. Gene expression analysis of the three main genes involved in UPR pathway, grp78, CHOP and ATF6 show that Grp78 and CHOP are reduced after heat shock, while AFT6 is only mildly induced after 4 hours heat shock. There is no literature regarding the role of heat shock in term of UPR activation in lymphocytes; the only work done in this direction show that heat shock response (HSR) activated by heat shock, can relieve stress in UPR-deficient cells by affecting multiple ER activities [147]. Literature analysing heat shock Jurkat and UPR studied the protein expression by bi-dimensional protein electrophoresis, and showed that heat treatment of human Jurkat cells led to an activation of PERK pathway with an increase in grp78 protein expression, together with protein ubiquitination increase, suggesting that heat treatment reduce protein expression and activated UPR, concomitant with protein hyper-ubiquitination in ER [154]. The data from the literature and the ones obtained here cannot be directly linked becaused they analyse two different aspect of UPR activation: one looks at the protein expression and the other to the gene expression.

The other aspect that has been investigated here was the translocation of the endoplasmic reticulum chaperone grp78 to the plasma membrane in the same way the cytoplasmic HSPA1A does. Indeed literature show in some cancer model a surface translocation of grp78 on the plasma membrane where it assume novel functions that regulate signalling, proliferation, apoptosis and immunity [142, 148-153]. Our results demonstrate a grp78 presence outside Jurkat cells and an increase after heat shock which in turn is not correspondent to a gene expression increase. This could be due to a translocation of the grp78 already present inside the cells in the same way happens with HSPA1A.

We then looked at surface grp78 in microvesicles and exosome from heat shocked Jurkat cells. The aim was to see whether this external plasma membrane expression could be extended to extracellular vesicles, like exosomes and microvesicles. There is few literature regarding the role of grp78 in extracellular vesicles such as exosomes and microvesicles. Melanoma exosomes could contain surface grp78 [152] as well as exosomes from ovarian cancer [153]. Surface grp78 in microvesicles and exosomes is low and is maintained low after the heat shock demonstrating that extracellular vesicles are not involved in surface presentation of UPR protein grp78, at least in this cellular model.

Chapter 5: A haematological model to study UPR: the Myelodysplastic Syndrome

Introduction

Myelodysplastic syndromes (MDS) are some of the most prevalent haematological malignancies, and are defined as clonal stem-cell disorders characterized by ineffective haematopoiesis in one or more of the lineages of the bone marrow. Although distinct morphological subgroups exist, the natural history of the syndromes is progression from cytopaenias to myeloid leukaemia [155]. MDS in children might be associated with inherited bone marrow-failure syndromes that is commonly present with a deficiency in a single lineage and over time frequently terminate in MDS or acute myeloid leukaemia AML: standard classification distinguish MDS from AML on the basis of a blast count of 20-30%. Although the peripheral cytopaenias become progressively worse as the disease persists, most cases of MDS are characterized by a cellular bone marrow with active cell turnover and cell division. As the disease progresses, the percentage of blasts in the bone marrow increases, and cytogenetic abnormalities arise.

To date, the role of UPR pathway in myelodysplastic syndromes has not been investigated. There are few data referring to the evolution of the MDS, the acute myeloid leukaemia (AML). Literature show that in AML, as in other malignancies, the UPR pathway is altered as a consequence of ER stress and overload. In particular CHOP and IRE1α pathway are altered [156] and there is an increase in the expression of the most important proteins involved in the pathway, XBP1, CHOP, grp78 and ATF6 [145, 146, 157, 158].

ER-associated degradation (ERAD) machinery is strictly associated with UPR because it helps to adapt cells to proteotoxic stress in the ER and therefore is critical for the life and death decision in cells under stress. HERP proteins are a family of ER membrane proteins, and are involved in ERAD protein degradation of glycosylated and nonglycosylated HRD1 substrates [159]. To date there is no literature showing the involvement of HERP in the pathogenesis of the MDS disease and no data on its deregulation in this pathology.

Regulation of Herp has been recently hypothesised by computational analysis done in other disease models: this regulation mechanism could involve the action of a long non-coding RNA, the XLOC_006043 [160].

The work therefore aimed to explore cytoplasmic HSPA1A chaperone expression and mainly the the UPR gene expression in MDS patients comparing a group of them with a group of healthy controls; the work analysed the main genes involved in the three pathways: grp78, CHOP, XBP1,

and ATF6. In addition HERPUD-2, the gene that codify for HERP-2 protein and the long non-coding RNA XLOC_006043 had been added to the investigation as previous works in other experimental models associated Herpud-2 expression with UPR activation [159] and the long non-coding RNA could upstream regulate the Herpud gene expression [160].

The other aspect that has been investigate here in this disease model, is the secretion of extracellular vesicles and their potential ability to modulate immune response or contribute to disease spreading from the bone marrow niche to the whole organism. A very recent study showed that extracellular vesicles, in particular exosomes increase in many haematological malignancies, like AML, but not in MDS patients [161]. Acute myeloid leukemia (AML) cell lines and patient-derived blasts release exosomes: these AML exosomes produce proangiogenic changes in nearby cells by participating to the suppression of residual hematopoietic function that precedes widespread leukemic invasion of the bone marrow directly and indirectly via stromal components [162]. To test this we purified extracellular vesicles, tested the total content and used for functional studies of immune response regulation.

Materials and Methods

Here below there is a list of the methods used in this work: the methods are fully described in the Material and Methods section.

- ✓ *Blood cell collection*
- ✓ *Real time PCR gene expression analysis of UPR genes*
- ✓ *Exosome and microvesicles purification*
- ✓ *Functional studies on exosomes purified*
- ✓ *Statistical analysis*

Results

HSPA1A gene expression and UPR gene expression was tested in blood samples from a group of healthy people (CTRL n=4) and patients with myelodysplastic syndrome (MDS n=4). The main UPR gene were analysed: *grp78, CHOP, ATF6, s-XBP1*. *HERPUD-2* and a long non - coding RNA *XLOC_006043* was also tested based on the literature which show in some pathological models that UPR could be controlled or interact with HERPUD-2 and the long non-coding RNA could control this process [160].

HSPA1A and UPR gene expression in patients with myelodisplastic syndrome (MDS)

HSPA1A gene expression show a significant increase in MDS patients compared with CTRL (P<0,05) (Figure1). However the highest activation of stress related genes was observed in UPR genes. While *grp78* gene expression remain unchanged between the two groups of patients (Figure 2), *CHOP*, *ATF6* and *s-XBP1* gene expression markedly increased in MDS patients compared with healthy controls (P< 0,0001 in *CHOP* and *s-XBP1* genes and P<0,01 in *ATF6*) (Figure 3-4-5).

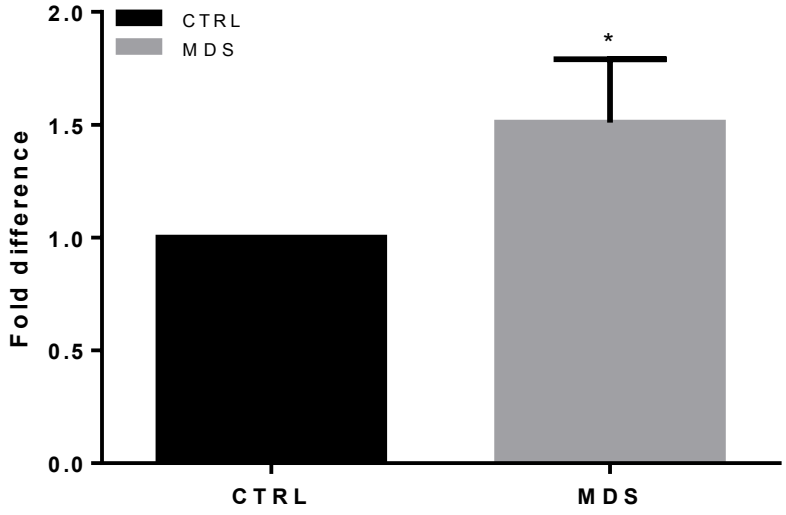

Figure 1: *HSPA1A* gene expression in control and MDS patients
The results are expressed as fold change of expression mean ± standard deviation in the pathological tissues compared to control tissue (CTRL), setting 1 as a reference value of the control. The degree of significance is defined by the value of the resulting *p*: the data are significantly different if the value of $p < 0.05$; the degree of significance increases with decreasing value of *p*. *p* values are significant at $p < 0.05$ = *, $p < 0.01$ = **, $p < 0.001$ = ***, $p < 0.0001$ = ****.

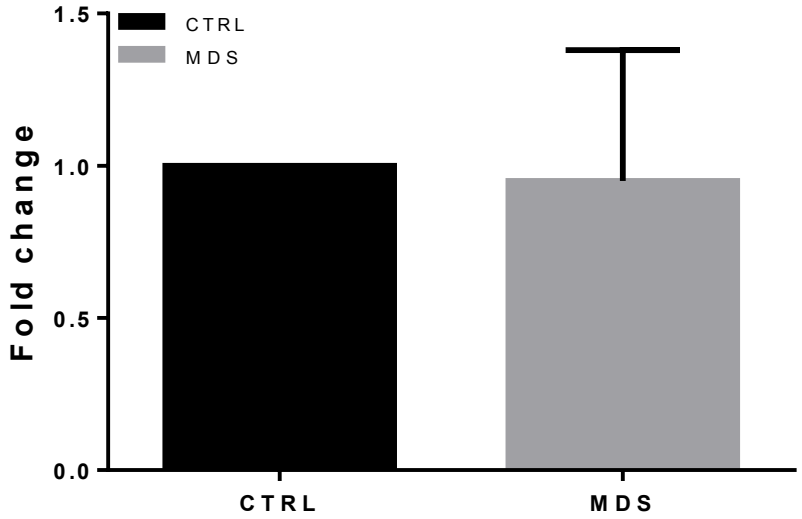

Figure 2: *grp78* gene expression in control and MDS patients

The results are expressed as fold change of expression mean ± standard deviation in the pathological tissues compared to control tissue (CTRL), setting 1 as a reference value of the control. The degree of significance is defined by the value of the resulting *p*: the data are significantly different if the value of $p < 0.05$; the degree of significance increases with decreasing value of *p*. *p* values are significant at $p < 0.05$ = *, $p < 0.01$ = **, $p < 0.001$ = ***, $p < 0.0001$ = ****.

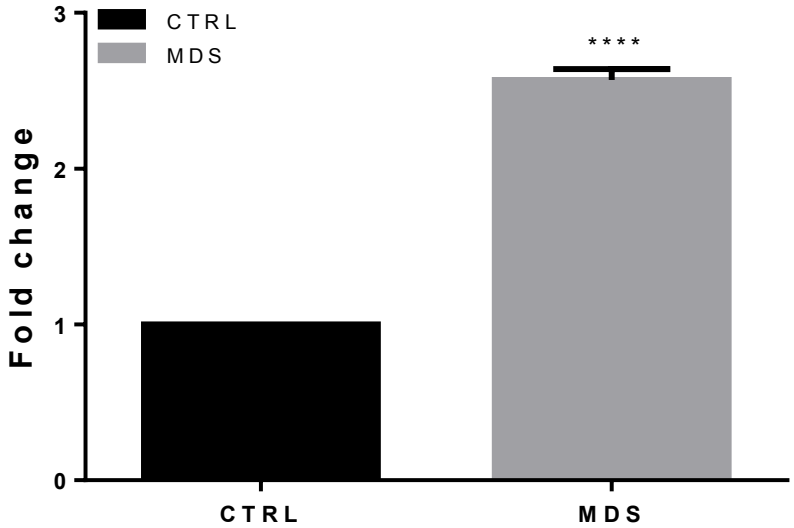

Figure 3: *CHOP* gene expression in control and MDS patients

The results are expressed as fold change of expression mean ± standard deviation in the pathological tissues compared to control tissue (CTRL), setting 1 as a reference value of the control. The degree of significance is defined by the value of the resulting *p*: the data are significantly different if the value of $p < 0.05$; the degree of significance increases with decreasing value of *p*. *p* values are significant at $p < 0.05$ = *, $p < 0.01$ = **, $p < 0.001$ = ***, $p < 0.0001$ = ****.

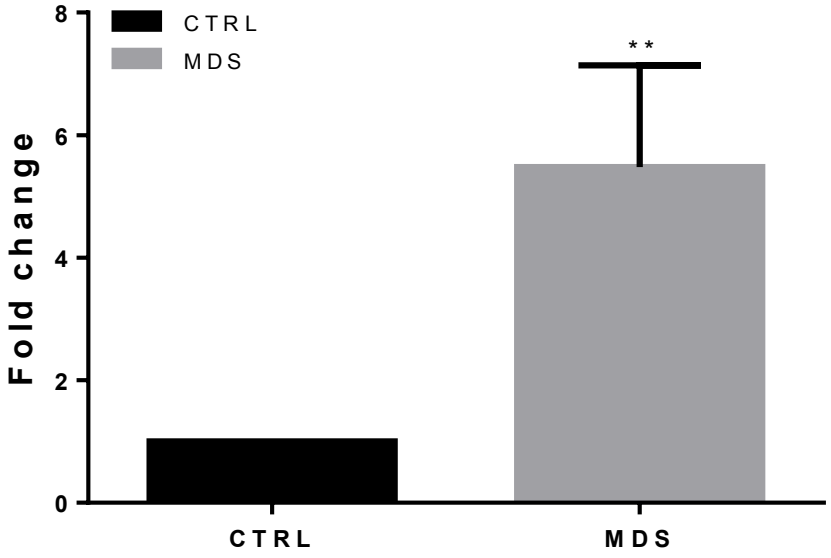

Figure 4: *ATF6* gene expression in control and MDS patients

The results are expressed as fold change of expression mean ± standard deviation in the pathological tissues compared to control tissue (CTRL), setting 1 as a reference value of the control. The degree of significance is defined by the value of the resulting *p*: the data are significantly different if the value of $p < 0.05$; the degree of significance increases with decreasing value of *p*. *p* values are significant at $p < 0.05$ = *, $p < 0.01$ = **, $p < 0.001$ = ***, $p < 0.0001$ = ****.

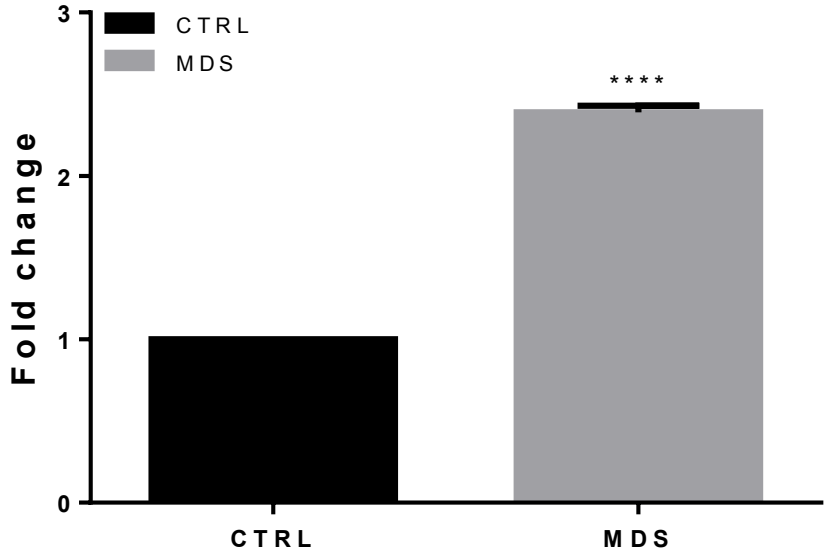

Figure 5: *s-XBP1* gene expression in control and MDS patients

The results are expressed as fold change of expression mean ± standard deviation in the pathological tissues compared to control tissue (CTRL), setting 1 as a reference value of the control. The degree of significance is defined by the value of the resulting *p*: the data are significantly different if the value of $p < 0.05$; the degree of significance increases with decreasing value of *p*. *p* values are significant at $p < 0.05$ = *, $p < 0.01$ = **, $p < 0.001$ = ***, $p < 0.0001$ = ****.

HERPUD 2 gene expression and the long non-coding RNA XLOC_006043 are highly modified in MDS patients

HERPUD-2 gene expression show a high increase in MDS patients compared to the healthy control group (CTRL) (P<0,0001) (Figure 6). However the long non-coding RNA XLOC_006043 markedly decrease its expression in MDS group (P<0,05) (Figure 7).

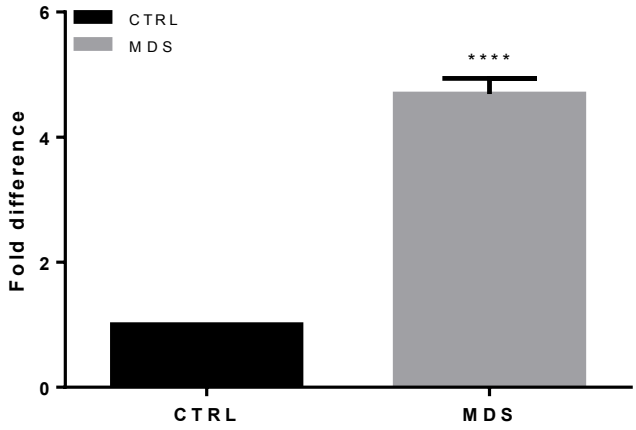

Figure 6: *HERPUD-2* gene expression in control and MDS patients
The results are expressed as fold change of expression mean ± standard deviation in the pathological tissues compared to control tissue (CTRL), setting 1 as a reference value of the control. The degree of significance is defined by the value of the resulting *p*: the data are significantly different if the value of $p < 0.05$; the degree of significance increases with decreasing value of *p*. *p* values are significant at $p < 0.05$ = *, $p < 0.01$ = **, $p < 0.001$ = ***, $p < 0.0001$ = ****.

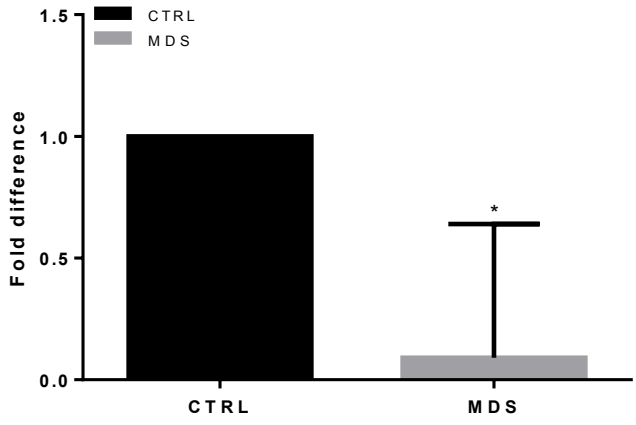

Figure 7: *XLOC_006043* gene expression in control and MDS patients
The results are expressed as fold change of expression mean ± standard deviation in the pathological tissues compared to control tissue (CTRL), setting 1 as a reference value of the control. The degree of significance is defined by the value of the resulting *p*: the data are significantly different if the value of $p < 0.05$; the degree of significance increases with decreasing value of *p*. *p* values are significant at $p < 0.05$ = *, $p < 0.01$ = **, $p < 0.001$ = ***, $p < 0.0001$ = ****.

Exosome and microvesicles release in MDS patients

Exosome and microvesicles release was tested in the two groups analysed. Plasma from patients was collected and exosomes were purified from the plasma using an in house developed kit. The Bradford analysis performed in the purified vesicles show that the total content of exosomes and microvesicles does not change in MDS patients compared with the control group (CTRL) (Figure 8 A-B).

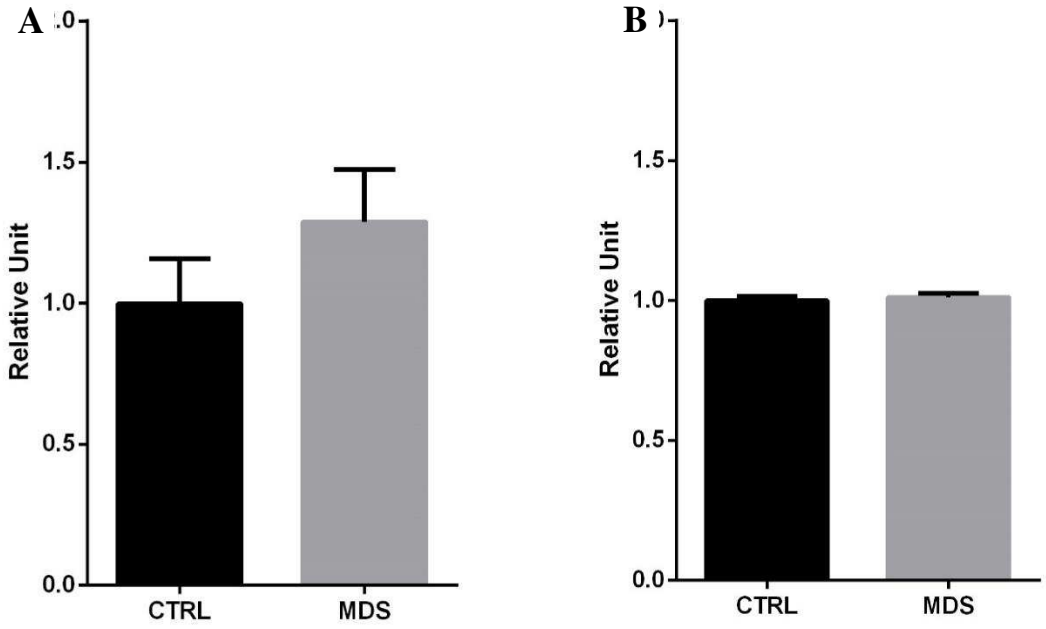

Figure 8: Bradford Assay on exosomes and microvesicles from haematological samples
Protein content was analysed by Bradford assay in exosomes **(A)** and microvesicles **(B)** and values are expressed as relative unit comparing the healthy control group (CTRL) with MDS group setting the CTRL to 1. Statistical analysis was two way ANOVA with Bonferroni post hoc test, comparing the non-treated samples with the treated samples at different temperatures. *=P<0.05; **=P<0.01; ***=P<0.001.

Exosomes purified from MDS patients stimulate macrophage differentiation

Total plasma and purified exosomes were used to perform functional studies: in detail 100μg/nl of the plasma or purified exosomes were co-cultured with U937, a monocitic cell line. These cells have the ability to activate and transform to active macrophages. Therefore this co treatment was performed to test the ability of extracellular vesicles from MDS patients to stimulate or abrogate immune response. U937 cell cycle analysis was performed and G1 arrest was analysed in detail as a sign of macrophage differentiation. Total plasma was also used to check whether the immune response modulation was effectively due to extracellular vesicles. U937 co-treatment with total plasma show no effect on their activation (Figure 9), while MDS exosome treatment to U937 show a G1 increase when compared to the no-treated control (NT, $P<0,0001$) and celles treated with exosomes from healthy patients (CTRL $P<0,0001$), demonstrating that monocytes underwent to macrophage differentiation, even higher than PMA activation; (Figure 10).

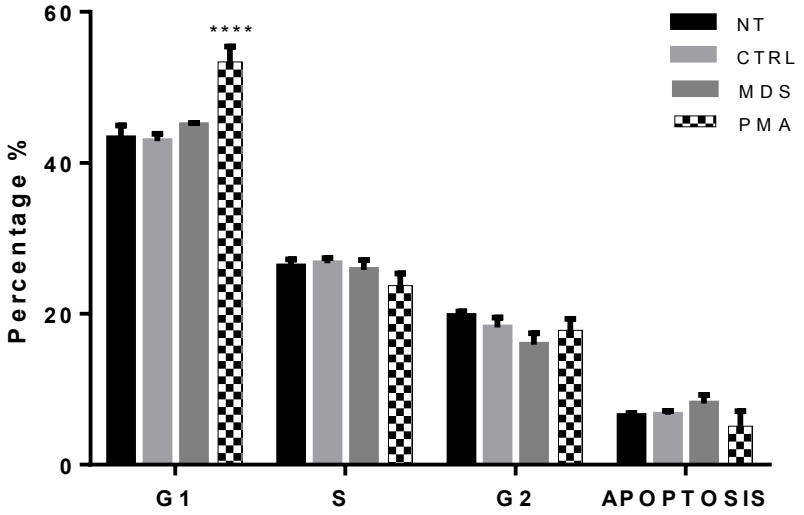

Figure 9: Cell cycle analysis after U937 treatment with PLASMA from CTRL and MDS
U937 cells were treated with 100ng/ml of PLASMA for 4 hours and cell cycle analysis was performed by flowcytometry; the results are represented as percentage of cells at a certain stage of the cell cycle. Statistical analysis was two way ANOVA with Bonferroni post hoc test, comparing the non-treated samples with the treated samples at different temperatures. *=P<0.05; **=P<0.01; ***=P<0.001.

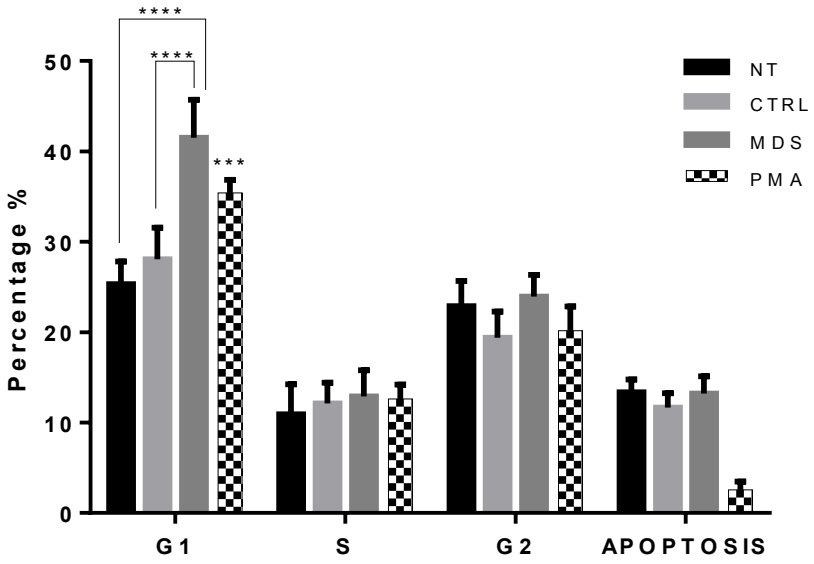

Figure 10: Cell cycle of treatment of U937 cell with EXOSOMES from patients CTRL and MDS
U937 cells were treated with 100ng/ml of EXOSOMES for 4 hours and cell cycle analysis was performed by flowcytometry; the results are represented as percentage of cells at a certain stage of the cell cycle. Statistical analysis was two way ANOVA with Bonferroni post hoc test, comparing the non-treated samples with the treated samples at different temperatures. *=P<0.05; **=P<0.01; ***=P<0.001.

Lymphocyte activation is influenced by exosome treatment

HUT78, a T-Helper lymphocyte cell line was chosen as a second cellular model for functional studies, to check whether exosome treatment could induce or suppress lymphocyte activation. Cell cycle analysis by flowcytometry was performed an increase in lymphocyte activation is expressed as G1 increase, while a lymphocyte suppression is expressed as lymphocyte apoptosis increase. Moreover it was tested CD25 surface expression by flowcytometry: CD 25 surface expression is indeed a sign of lymphocyte activation. The results from the cell cycle analysis show that MDS exosomes significantly induce lymphocyte activation when compared to the no treated control (NT, P<0,0001) and when compared to the sample treated with exosomes from healthy patients (CTRL, P<0,0001) (Figure 11). CD25 surface analysis show that both exosomes from CTRL and MDS are able to induce CD25 on the cell surface (P<0,001) but there is no difference between the two groups in terms of CD25 surface exposure (Figure 12).

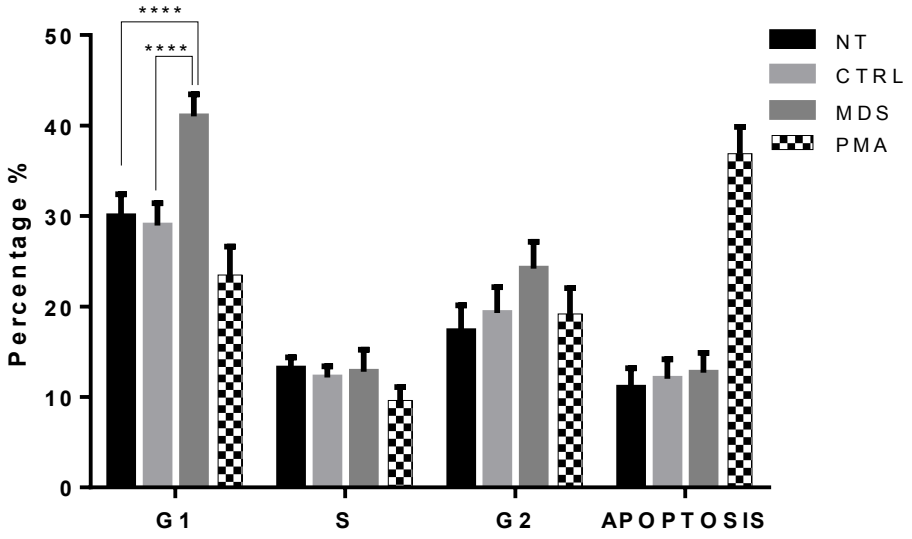

Figure 11: HUT78 cell cycle analysis following treatment with exosomes from healthy patients and MDS patients.

HUT78 cells were treated with 100ng/ml of EXOSOMES for 4 hours and cell cycle analysis was performed by flowcytometry; the results are represented as percentage of cells at a certain stage of the cell cycle. Statistical analysis was two way ANOVA with Bonferroni post hoc test, comparing the non-treated samples with the treated samples at different temperatures. *=P<0.05; **=P<0.01; ***=P<0.001.

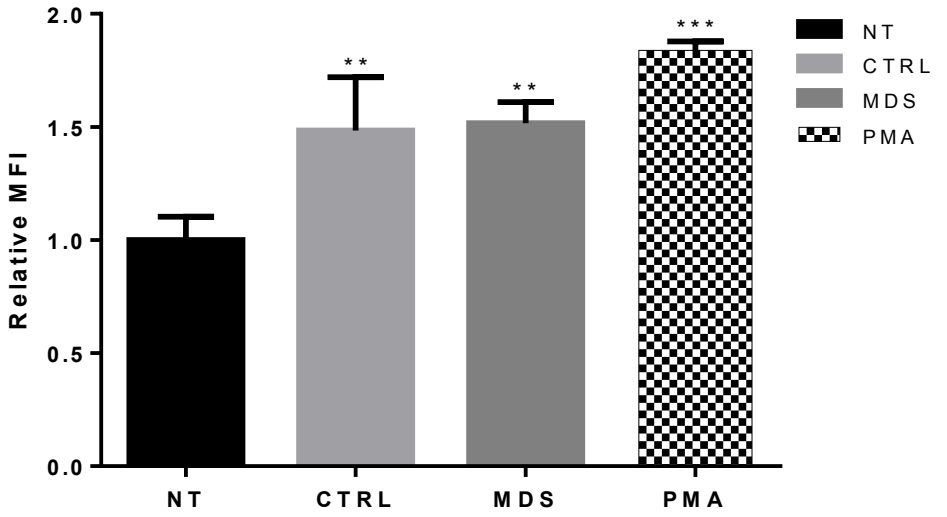

Figure 12: CD25 surface presentation after treatment with Exosomes from healthy patients (CTRL) and MDS patients (MDS).
HUT78 cells were treated with 100ng/ml of EXOSOMES for 4 hours and cell cycle analysis was performed by flowcytometry; the results are represented as percentage of cells at a certain stage of the cell cycle. Statistical analysis was one way ANOVA with Bonferroni post hoc test, comparing the non-treated samples with the treated samples at different temperatures. *=P<0.05; **=P<0.01; ***=P<0.001.

Discussion

The work presented here highlight a number of relevant data regarding the Myelodysplastic Sindrome (MDS). First of all, we looked at the cytoplasmic chaperone HSPA1A gene expression and found it increases slightly in MDS patients compared with healthy controls. This is in line with literature which shows an intracellular expression and gene overexpression of different heat shock proteins including Hsp72 (or HSPA1A) in bone marrow of patients with myelodysplastic syndrome (MDS) especially in advanced disease, providing resistance to induction of apoptosis, suggesting that Hsps could be implicated in the progression of MDS to acute myeloid leukaemia [163].

Furthermore we found an altered expression profile of UPR genes in Myelodysplastic syndrome (MDS), compared with controls (CTRL). The increase of ATF6 in cancer samples is in line with literature [157]. Grp78 represents the main target of ATF6 activation and plays an important role in protein folding and assembly, in the regulation of ER Ca^{2+} levels, and finally in the control of stress transmembrane sensors activation [78]. Several studies indicate that, among the different over expressed proteins following UPR activation, Grp78 plays a crucial role in tumor proliferation,

survival, metastasis and resistance to a wide variety of therapies [78], and its induction in tumor cells protects them from apoptosis and from the organism immune response [75, 164, 165]. Our result which show that grp78 in MDS is not different from controls need to take into consideration that MDS is not defined as proper malignant disease, is rather a premalignant form of myeloid leukaemia. The induction of CHOP in MDS patients represent also an important data: although its function in oncogenesis has not been clearly established yet, many studies show that CHOP induction in response to a prolonged ER stress, cause apoptosis of pre-malignant cells, thus preventing the tumor progression. In KRAS-induced mouse models, CHOP deletion increases the incidence of malignant lung tumors, suggesting its oncosuppressive role [74]. Therefore, as MDS is a premalignant disease, CHOP induction is reasonable, as the induction of apoptosis is a control mechanism for disease proliferation and when this mechanism is lost the disease progress to leukemia. It is also important to remind that CHOP mRNA half-life is short, and it is therefore necessary to promote cell death, an increase of CHOP expression by far more high level than what translated at the end of the process [166]. XBP1 increased in MDS patients; this is in line with most of the literature that show its induction in cancer and in particular in AML [145, 146, 157]. However the role of XBP1s in neoplastic transformation has not yet been fully elucidated and literature is controversial. Some studies highlight the importance of the IRE1/XBP1 axis for cell survival and growth in hypoxic environment. Fujimoto et al., demonstrate that XBP1 depletion reduces tumor formation, increasing the sensitivity of cells to hypoxia [81]. On the other hand, other studies show an oncosuppressive role of IREα-XBP1 axis: it was detected in many human tumor types, mutations of IRE1α, some of which result in a loss of kinase and/or endo-ribonucleasic activity [83]. These mutations may be responsible for XBP1 splicing inhibition and consequently a reduction of XBP1s.

ER-associated degradation (ERAD) machinery is strictly associated with UPR: this mechanism of protein degradation helps cells to adapt to proteotoxic stress in the ER and therefore is critical for the life and death decision in cells under stress. To test this pathway we decided to test the HERP family proteins that are involved in endoplasmic reticulum membrane transport [159]. In particular, literature show that Herp-1 is inducible, while Herp-2 is a constitutive expressed protein; Herp has been suggested to improve ER-folding, decrease ER protein load, and participate in ER-associated degradation (ERAD) of proteins [167]. Many studies show that Herp family proteins are present before and after the UPR pathway. Herp are regulated by two of the branches of the UPR pathway: PERK mediated and IRE1/ATF6 mediated [168]; Herp is involved in the protein retrotraslocation that occur during ERAD formation [159]: this event induce UPR activation. ER stress increase the production of proteins involved in UPR and also of ER chaperones and Herp [169] Outinen P.A. et al.; 1998]. The gene that encode for the protein is called HERPUD-2: this gene is over expressed in

MDS patients as expected from a disease model where UPR is activated. Therefore this finding is in line with literature.

Recent computational analysis done in other disease models hypothesised that HERPUD expression is regulated by long non-coding RNA (lncRNA): in detail this regulation mechanism could involve the action of a long non-coding RNA, the XLOC_006043 [160]. For this reason this lncRNA has been tested and the results show that is inversely correlated with HERPUD-2 expression, therefore it decrease in MDS patients. Hence it could be hypothesised that the lncRNA could negatively regulate HERPUD-2 expression and its downregulation could induce HERPUD-2 expression. Further analysis are needed to clarify the nature of the relationship between the two genes.

The other aspect that has been investigated in this chapter is the extracellular vesicle release in MDS patients and the potential role of these vesicles purified in modulation of the immune response. The results here show that total exosome content did not change in MDS compared to controls. This is in line with literature that show no change in exosomal production in MDS whereas an increase in AML patients [161]. Extracellular vesicles indeed contain markers of the disease, in detail the AML marker CD34 [170] but could also contain molecules that could conversely induce or suppress immune response. Leukemic exosomes could improve vaccine efficacy compared to tumor lysate loaded dendritic cells [171, 172]; on the other hand different cellular models show that exosomes could have an immunosuppressive role [173]. For this reason we tested two different model of immune modulation: in detail we used the monocytes U937 to test immune activation through their transformation to macrophages, and T-helper lymphocytes activation or suppression through the HUT 78 cell line. Our results show that MDS exosomes have the ability to induce immune response and promote the differentiation of U937 to macrophages in similar manner PMA does. MDS induce less strongly T-helper lymphocytes as G1 peack increase but not CD25 surface expression. From this results it could be hypothesized that MDS exosomes could induce innate immune response rather than cell-mediated immune response and that the immunosuppression role of exosomes is not present in the premalignant disease MDS.

Conclusions

The work aimed to explore the cytoplasmic stress and the endoplasmic reticulum stress in haematological malignancies and explore possible ways of cellular communication of stress to distant cells. The work was performed *in vitro* using a cell line of leukemic malignant cells. More work has been done *in vivo*, collecting samples from a haematological disease which is in a pre-malignant state, the Myelodysplastic Syndrome (MDS). We chose to analyse a pre-malignant state because there is no literature about it, while only few data are already collected for malignant haematological diseases such as acute lymphoid leukaemia or acute myeloid leukaemia and it could be interesting to compare the two state in relation to cytoplasmic stress response and endoplasmic reticulum stress response. We chose to start out investigation studying a family of proteins that more than others are sensitive to stress: the chaperones. These proteins are responsible for protein folding, hence fundamental for a correct growth and cell division: in the absence of chaperones, cells including cancer ones, could not divide. Chaperone location is crucial also for other cellular mechanisms such as immune system modulation, disease progression, and spreading, for this reason could represent useful targets in cancer treatment. Understanding these mechanisms, specially looking at pre malignant state and see differences between advanced malignant state could represent an important step, for a better definition of cancer pathogenesis, and also in the future, for the development of customized therapies.

Dealing with cytoplasmic stress is crucial for cell survival or death. When stress is low cells adopt different strategies to cope with it and get over it, but when the stress is too high cells inevitably go to cell death. Communication of cell death is important for the microenvironment and for distant cells and stressed or dying cells could be a good danger signal for the whole organism.

The work presented here demonstrate that cells exploit differential HSPA1A surface presentation and secretion pathways, and these distinct presentations could be part of a cellular crosstalk. The results also suggest that cells can communicate different levels of stress by expressing HSPA1A in different ways. The quickest signals of stress are the *de-novo* synthesis-independent mechanisms, the membrane HSPA1A exposition in a lipid raft environment and HSPA1A exosomal loading. Membrane exposition signal appears at the early phases of the heat stress: the protein already present inside the cells become associated with PS, with heat stress it flips out with the lipid and oligomerize. The presence of HSPA1A in the membrane could facilitate the membrane stabilization, the folding of membrane proteins and help to recover from the shock. However these cells express the classical apoptotic markers, demonstrating that this signal does not prevent cells to die, but could be an important message to the neighbour cells. Another *de-novo* synthesis-independent

process is the HSPA1A exosomal loading and release outside cells that may also be a stress signal but, differently from HSPA1A membrane insertion, could target distant cells. Indeed, it has been recently described that intercellular chaperone transmission, mediated by exosomes, improve proteostasis in other cells [174]. While exosome release occurs independently from *de-novo* HSPA1A synthesis, the free extracellular HSPA1A is dependent on the HSF1, suggesting that the new synthesised HSPA1A could act as a second level of stress severity. The presence of LAMP1 at later time points suggests that HSPA1A may be released via a secretory lysosome pathway. At more severe stresses such as higher temperatures or longer times the cells die by necrosis, and release all the intracellular products which are potent stimulators of the immune system. This could be the third and more powerful level of danger signal.

Here below a proposed model of HSPA1A translocation dependent on stress intensity.

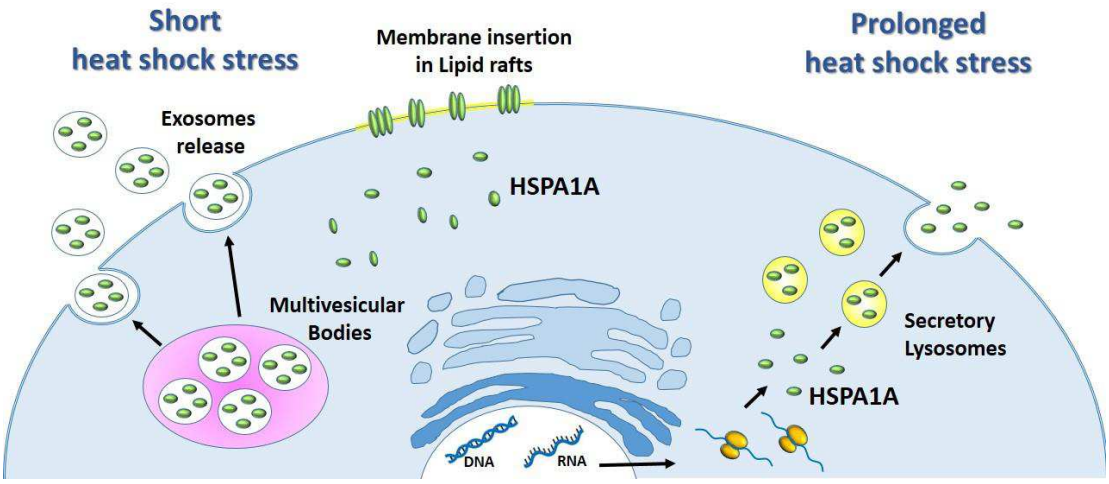

Figure 1: Proposed model of HSPA1A translocation in response to different degrees of stress

We next moved to analyze the endoplasmic reticulum stress and the cellular response that is usually activated, the unfolded protein response (UPR). Normal cells exposed to high levels stress have an activated UPR that could lead to cell death via apoptosis; on the other hand, in cancer cells, a slight activation of the UPR determines cell survival. Hence different degree of stress determine a different cellular response that could determine cell survival or death. The *in-vitro* model demonstrated a UPR activation under stress, but more interesting the in-vivo model of MDS a premalignant hematological disease, show an up-regulation of the cytoplasmic HSPA1A and also all the proteins related to UPR pathway. Exosomes secreted from these cells are able, differently from healthy cells, to activate macrophage differentiation and lymphocyte activation, demonstrating

that their composition must be different from the normal ones. Further studies need to be performed characterizing the extracellular vesicles isolated, but from these data, it is possible to hypothesize that MDS cells are stressed cells, as they have both (cytoplasmic and ER) stress pathway activated, and they secrete extracellular vesicles with immune modulatory functions.

In conclusion there are two aspects that need to be considered: first of all, the danger model of Matzinger [27, 175], proposes that endogenous danger signals, including HSPA1A and HMGB1, are released outside the cells and, stimulates aspects the immune response. The original model stated that this release could occur only by necrotic cells. However our study demonstrates an HSPA1A secretion from apoptotic cells, as well as previously demonstrated for HMGB1 [122]. Therefore, the paradigm that danger signals are only released from necrotic cells should be refined in a more carefully defined danger model, incorporating apoptotic secretion.

Secondly, De Maio has recently coined the new concept of Stress Observation System [176]. According to this model, cells are able to secrete extracellular vesicles with different composition and membrane inserted proteins, depending on the stress applied: these vesicles may be recognised by a variety of cell types and may trigger different responses. In line with this theory, our results show that HSPA1A and grp78 can be embedded in the plasma membrane, secreted as a free protein, or intra-vesicular, and each format could possess a specific systemic function and could be a part of an assessment of the stress conditions [176].

It is intriguing to hypothesise cells perceive the amount of stress in the environment and respond differently to the severity of the stress. This different response in term of signal delivery is useful for the neighbour and distant cells for protein homeostasis, for cell stress adaptation and for immune system modulation.

REFERENCES

1. Lianos, G.D., et al., *The role of heat shock proteins in cancer.* Cancer Lett, 2015. **360**(2): p. 114-8.
2. Srivastava, P., *Interaction of heat shock proteins with peptides and antigen presenting cells: Chaperoning of the innate and adaptive immune responses.* Annual Review of Immunology, 2002. **20**: p. 395-425.
3. Kampinga, H.H., et al., *Guidelines for the nomenclature of the human heat shock proteins.* Cell Stress & Chaperones, 2009. **14**(1): p. 105-111.
4. Trieb, K., et al., *Heat shock protein 72 expression in chondrosarcoma correlates with differentiation.* Journal of Cancer Research and Clinical Oncology, 2000. **126**(11): p. 667-670.
5. Gyrd-Hansen, M., J. Nylandsted, and M. Jaattela, *Heat shock protein 70 promotes cancer cell viability by safeguarding lysosomal integrity.* Cell Cycle, 2004. **3**(12): p. 1484-1485.
6. Nylandsted, J., K. Brand, and M. Jaattela, *Heat shock protein 70 is required for the survival of cancer cells*, in *Mechanisms of Cell Death Ii*. 2000. p. 122-125.
7. Volloch, V.Z. and M.Y. Sherman, *Oncogenic potential of Hsp72.* Oncogene, 1999. **18**(24): p. 3648-3651.
8. Schett, G., et al., *Activation of Fas inhibits heat-induced activation of HSF1 and up-regulation of hsp70.* Faseb Journal, 1999. **13**(8): p. 833-842.
9. Beere, H.M. and D.R. Green, *Stress management - heat shock protein-70 and the regulation of apoptosis.* Trends in Cell Biology, 2001. **11**(1): p. 6-10.
10. Garrido, C., et al., *Mechanisms of cytochrome c release from mitochondria.* Cell Death and Differentiation, 2006. **13**(9): p. 1423-1433.
11. Mosser, D.D., et al., *The chaperone function of hsp70 is required for protection against stress-induced apoptosis.* Molecular and Cellular Biology, 2000. **20**(19): p. 7146-7159.
12. Milleron, R.S. and S.B. Bratton, *Heat shock induces apoptosis independently of any known initiator caspase-activating complex.* Journal of Biological Chemistry, 2006. **281**(25): p. 16991-17000.
13. Gurbuxani, S., et al., *Selective depletion of inducible HSP70 enhances immunogenicity of rat colon cancer cells.* Oncogene, 2001. **20**(51): p. 7478-7485.
14. Multhoff, G., et al., *A Stress-Inducible 72-Kda Heat-Shock Protein (Hsp72) Is Expressed on the Surface of Human Tumor-Cells, but Not on Normal-Cells.* International Journal of Cancer, 1995. **61**(2): p. 272-279.
15. Gehrmann, M., et al., *Membrane-bound heat shock protein 70 in acute myeloid leukemia: a tumor-specific recognition structure for the cytolytic activity of autologous natural killer cells.* Haematologica, 2003. **88**(4): p. 474-476.
16. Barreto, A., et al., *Stress-induced release of HSC70 from human tumors.* Cellular Immunology, 2003. **222**(2): p. 97-104.
17. Gross, C., et al., *Heat shock protein 70-reactivity is associated with increased cell surface density of CD94/CD56 on primary natural killer cells.* Cell Stress & Chaperones, 2003. **8**(4): p. 348-360.
18. Gastpar, R., et al., *Heat shock protein 70 surface-positive tumor exosomes stimulate migratory and cytolytic activity of natural killer cells.* Cancer Research, 2005. **65**(12): p. 5238-5247.
19. Krause, S.W., et al., *Treatment of colon and lung cancer patients with ex vivo heat shock protein 70-peptide-activated, autologous natural killer cells: a clinical phase I trial.* Clinical Cancer Research, 2004. **10**(11): p. 3699-3707.
20. Stangl, S., et al., *Control of metastasized pancreatic carcinomas in SCID/beige mice with human IL-2/TKD-activated NK cells.* Journal of Immunology, 2006. **176**(10): p. 6270-6276.

21. Sondermann, H., et al., *Characterization of a receptor for heat shock protein 70 on macrophages and monocytes.* Biological Chemistry, 2000. **381**(12): p. 1165-1174.
22. Arnold-Schild, D., et al., *Cutting edge: Receptor-mediated endocytosis of heat shock proteins by professional antigen-presenting cells.* Journal of Immunology, 1999. **162**(7): p. 3757-3760.
23. Binder, R.J., et al., *Saturation, competition, and specificity in interaction of heat shock proteins (hsp) gp96, hsp90, and hsp70 with CD11b(+) cells.* Journal of Immunology, 2000. **165**(5): p. 2582-2587.
24. Binder, R.J., N.E. Blachere, and P.K. Srivastava, *Heat shock protein-chaperoned peptides but not free peptides introduced into the cytosol are presented efficiently by major histocompatibility complex I molecules.* Journal of Biological Chemistry, 2001. **276**(20): p. 17163-17171.
25. Srivastava, P.K., et al., *Heat shock proteins come of age: Primitive functions acquire new roles in an adaptive world.* Immunity, 1998. **8**(6): p. 657-665.
26. Wells, A.D. and M. Malkovsky, *Heat shock proteins, tumor immunogenicity and antigen presentation: an integrated view.* Immunology Today, 2000. **21**(3): p. 129-132.
27. Matzinger, P., *The danger model: A renewed sense of self.* Science, 2002. **296**(5566): p. 301-305.
28. Williams, J.H.H. and H.E. Ireland, *Sensing danger - Hsp72 and HMGB1 as candidate signals.* Journal of Leukocyte Biology, 2008. **83**(3): p. 489-492.
29. Tytell, M., et al., *Cytoprotection by Hsps elevated via hyperthermia or direct administration of the proteins.* Cell Stress & Chaperones, 2000. **5**(5): p. 499-499.
30. Guzhova, I., et al., *In vitro studies show that Hsp70 can be released by glia and that exogenous Hsp70 can enhance neuronal stress tolerance.* Brain Research, 2001. **914**(1-2): p. 66-73.
31. Tytell, M., *Release of heat shock proteins (Hsps) and the effects of extracellular Hsps on neural cells and tissues.* International Journal of Hyperthermia, 2005. **21**(5): p. 445-455.
32. Pastukhov, Y.F., et al., *Lipopolysaccharide-free 70-kDa heat shock protein has hypotherimic and somnogenic effects.* Dokl Biol Sci, 2005. **402**.
33. Kustanova, G.A., et al., *Protective effect of exogenous 70-kDa heat shock protein during endotoxic shock (sepsis).* Dokl Biol Sci, 2006. **411**.
34. Lancaster, G.I. and M.A. Febbraio, *Exosome-dependent trafficking of HSP70 - A novel secretory pathway for cellular stress proteins.* Journal of Biological Chemistry, 2005. **280**(24): p. 23349-23355.
35. Vega, V.L., et al., *Hsp70 translocates into the plasma membrane after stress and is released into the extracellular environment in a membrane-associated form that activates macrophages.* Journal of Immunology, 2008. **180**(6): p. 4299-4307.
36. Saito, K., Y. Dai, and K. Ohtsuka, *Enhanced expression of heat shock proteins in gradually dying cells and their release from necrotically dead cells.* Experimental Cell Research, 2005. **310**(1): p. 229-236.
37. Basu, S., et al., *Necrotic but not apoptotic cell death releases heat shock proteins, which deliver a partial maturation signal to dendritic cells and activate the NF-kappa B pathway.* International Immunology, 2000. **12**(11): p. 1539-1546.
38. Arispe, N. and A. De Maio, *ATP and ADP modulate a cation channel formed by Hsc70 in acidic phospholipid membranes.* Journal of Biological Chemistry, 2000. **275**(40): p. 30839-30843.
39. Armijo, G., et al., *Interaction of heat shock protein 70 with membranes depends on the lipid environment.* Cell Stress & Chaperones, 2014. **19**(6): p. 877-886.
40. De Maio, A., et al., *Hsp70 is present in extracellular vesicles rich in GM1 and cholesterol.* Inflammation Research, 2007. **56**: p. S87-S87.

41. Broquet, A.H., et al., *Expression of the molecular chaperone Hsp70 in detergent-resistant microdomains correlates with its membrane delivery and release.* Journal of Biological Chemistry, 2003. **278**(24): p. 21601-21606.
42. Mambula, S.S. and S.K. Calderwood, *Heat shock protein 70 is secreted from tumor cells by a nonclassical pathway involving lysosomal endosomes.* Journal of Immunology, 2006. **177**(11): p. 7849-7857.
43. Hunter-Lavin, C., et al., *Hsp70 release from peripheral blood mononuclear cells.* Biochemical and Biophysical Research Communications, 2004. **324**(2): p. 511-517.
44. Wang, R.B., et al., *HSP70 enhances macrophage phagocytosis by interaction with lipid raft-associated TLR-7 and upregulating p38 MAPK and PI3K pathways.* Journal of Surgical Research, 2006. **136**(1): p. 58-69.
45. Triantafilou, M., et al., *Cell surface molecular chaperones as endogenous modulators of the innate immune response.* Novartis Found Symp, 2008. **291**.
46. Vigh, L., et al., *Membrane-regulated stress response: A theoretical and practical approach*, in *Molecular Aspects of the Stress Response: Chaperones, Membranes and Networks*. 2007. p. 114-131.
47. Bang, C. and T. Thum, *Exosomes: new players in cell-cell communication.* Int J Biochem Cell Biol, 2012. **44**(11): p. 2060-4.
48. Denzer, K., et al., *Exosome: from internal vesicle of the multivesicular body to intercellular signaling device.* J Cell Sci, 2000. **113 Pt 19**: p. 3365-74.
49. Yin, W., et al., *Immature dendritic cell-derived exosomes: a promise subcellular vaccine for autoimmunity.* Inflammation, 2013. **36**(1): p. 232-40.
50. Kalra, H., et al., *Vesiclepedia: a compendium for extracellular vesicles with continuous community annotation.* PLoS Biol, 2012. **10**(12): p. e1001450.
51. Pan, B.T., et al., *Electron microscopic evidence for externalization of the transferrin receptor in vesicular form in sheep reticulocytes.* J Cell Biol, 1985. **101**(3): p. 942-8.
52. Harding, C., J. Heuser, and P. Stahl, *Endocytosis and intracellular processing of transferrin and colloidal gold-transferrin in rat reticulocytes: demonstration of a pathway for receptor shedding.* Eur J Cell Biol, 1984. **35**(2): p. 256-63.
53. Bausero, M.A., et al., *Alternative mechanism by which IFN-gamma enhances tumor recognition: Active release of heat shock protein 72.* Journal of Immunology, 2005. **175**(5): p. 2900-2912.
54. Clayton, A., et al., *Induction of heat shock proteins in B-cell exosomes.* Journal of Cell Science, 2005. **118**(16): p. 3631-3638.
55. Giampietri, C., et al., *Cancer Microenvironment and Endoplasmic Reticulum Stress Response.* Mediators Inflamm, 2015. **2015**: p. 417281.
56. Kozutsumi, Y., et al., *The presence of malfolded proteins in the endoplasmic reticulum signals the induction of glucose-regulated proteins.* Nature, 1988. **332**(6163): p. 462-4.
57. Wek, R.C., H.Y. Jiang, and T.G. Anthony, *Coping with stress: eIF2 kinases and translational control.* Biochem Soc Trans, 2006. **34**(Pt 1): p. 7-11.
58. Harding, H.P., et al., *Regulated translation initiation controls stress-induced gene expression in mammalian cells.* Mol Cell, 2000. **6**(5): p. 1099-108.
59. Marciniak, S.J., et al., *CHOP induces death by promoting protein synthesis and oxidation in the stressed endoplasmic reticulum.* Genes Dev, 2004. **18**(24): p. 3066-77.
60. Wang, X.Z., et al., *Cloning of mammalian Ire1 reveals diversity in the ER stress responses.* Embo j, 1998. **17**(19): p. 5708-17.
61. Chen, X., J. Shen, and R. Prywes, *The luminal domain of ATF6 senses endoplasmic reticulum (ER) stress and causes translocation of ATF6 from the ER to the Golgi.* J Biol Chem, 2002. **277**(15): p. 13045-52.
62. Lee, K., et al., *IRE1-mediated unconventional mRNA splicing and S2P-mediated ATF6 cleavage merge to regulate XBP1 in signaling the unfolded protein response.* Genes Dev, 2002. **16**(4): p. 452-66.

63. Calfon, M., et al., *IRE1 couples endoplasmic reticulum load to secretory capacity by processing the XBP-1 mRNA.* Nature, 2002. **415**(6867): p. 92-6.
64. Yoshida, H., et al., *XBP1 mRNA is induced by ATF6 and spliced by IRE1 in response to ER stress to produce a highly active transcription factor.* Cell, 2001. **107**(7): p. 881-91.
65. Li, H., et al., *Mammalian endoplasmic reticulum stress sensor IRE1 signals by dynamic clustering.* Proc Natl Acad Sci U S A, 2010. **107**(37): p. 16113-8.
66. Ishiwata-Kimata, Y., et al., *BiP-bound and nonclustered mode of Ire1 evokes a weak but sustained unfolded protein response.* Genes Cells, 2013. **18**(4): p. 288-301.
67. Fels, D.R. and C. Koumenis, *The PERK/eIF2alpha/ATF4 module of the UPR in hypoxia resistance and tumor growth.* Cancer Biol Ther, 2006. **5**(7): p. 723-8.
68. Bobrovnikova-Marjon, E., et al., *PERK promotes cancer cell proliferation and tumor growth by limiting oxidative DNA damage.* Oncogene, 2010. **29**(27): p. 3881-95.
69. Wang, M. and R.J. Kaufman, *The impact of the endoplasmic reticulum protein-folding environment on cancer development.* Nat Rev Cancer, 2014. **14**(9): p. 581-97.
70. Ozcan, U., et al., *Loss of the tuberous sclerosis complex tumor suppressors triggers the unfolded protein response to regulate insulin signaling and apoptosis.* Mol Cell, 2008. **29**(5): p. 541-51.
71. Kang, Y.J., M.K. Lu, and K.L. Guan, *The TSC1 and TSC2 tumor suppressors are required for proper ER stress response and protect cells from ER stress-induced apoptosis.* Cell Death Differ, 2011. **18**(1): p. 133-44.
72. Yeung, B.H., et al., *Glucose-regulated protein 78 as a novel effector of BRCA1 for inhibiting stress-induced apoptosis.* Oncogene, 2008. **27**(53): p. 6782-9.
73. Babour, A., et al., *A surveillance pathway monitors the fitness of the endoplasmic reticulum to control its inheritance.* Cell, 2010. **142**(2): p. 256-69.
74. Huber, A.L., et al., *p58(IPK)-mediated attenuation of the proapoptotic PERK-CHOP pathway allows malignant progression upon low glucose.* Mol Cell, 2013. **49**(6): p. 1049-59.
75. Reddy, R.K., et al., *Endoplasmic reticulum chaperone protein GRP78 protects cells from apoptosis induced by topoisomerase inhibitors: role of ATP binding site in suppression of caspase-7 activation.* J Biol Chem, 2003. **278**(23): p. 20915-24.
76. Fu, Y. and A.S. Lee, *Glucose regulated proteins in cancer progression, drug resistance and immunotherapy.* Cancer Biol Ther, 2006. **5**(7): p. 741-4.
77. Zhang, J., et al., *Association of elevated GRP78 expression with increased lymph node metastasis and poor prognosis in patients with gastric cancer.* Clin Exp Metastasis, 2006. **23**(7-8): p. 401-10.
78. Bifulco, G., et al., *Endoplasmic reticulum stress is activated in endometrial adenocarcinoma.* Gynecol Oncol, 2012. **125**(1): p. 220-5.
79. Ghosh, R., et al., *Transcriptional regulation of VEGF-A by the unfolded protein response pathway.* PLoS One, 2010. **5**(3): p. e9575.
80. Auf, G., et al., *Inositol-requiring enzyme 1alpha is a key regulator of angiogenesis and invasion in malignant glioma.* Proc Natl Acad Sci U S A, 2010. **107**(35): p. 15553-8.
81. Fujimoto, T., et al., *Overexpression of human X-box binding protein 1 (XBP-1) in colorectal adenomas and adenocarcinomas.* Anticancer Res, 2007. **27**(1a): p. 127-31.
82. Kan, Z., et al., *Diverse somatic mutation patterns and pathway alterations in human cancers.* Nature, 2010. **466**(7308): p. 869-73.
83. Ghosh, R., et al., *Allosteric inhibition of the IRE1alpha RNase preserves cell viability and function during endoplasmic reticulum stress.* Cell, 2014. **158**(3): p. 534-48.
84. Niederreiter, L., et al., *ER stress transcription factor Xbp1 suppresses intestinal tumorigenesis and directs intestinal stem cells.* J Exp Med, 2013. **210**(10): p. 2041-56.
85. Pockley, A.G., S.K. Calderwood, and G. Multhoff, *The atheroprotective properties of Hsp70: a role for Hsp70-endothelial interactions?* Cell Stress & Chaperones, 2009. **14**(6): p. 545-553.

86. van Eden, W., et al., *A case of mistaken identity: HSPs are no DAMPs but DAMPERs.* Cell Stress & Chaperones, 2012. **17**(3): p. 281-292.
87. Henderson, B. and A.G. Pockley, *Molecular chaperones and protein-folding catalysts as intercellular signaling regulators in immunity and inflammation.* Journal of Leukocyte Biology, 2010. **88**(3): p. 445-462.
88. Calderwood, S.K., et al., *Heat shock proteins in cancer: chaperones of tumorigenesis.* Trends in Biochemical Sciences, 2006. **31**(3): p. 164-172.
89. Ciocca, D.R. and S.K. Calderwood, *Heat shock proteins in cancer: diagnostic, prognostic, predictive, and treatment implications.* Cell Stress & Chaperones, 2005. **10**(2): p. 86-103.
90. Sherman, M. and G. Multhoff, *Heat shock proteins in cancer*, in *Stress Responses in Biology and Medicine: Stress of Life in Molecules, Cells, Organisms, and Psychosocial Communities*, P.K.T.S.K. Csermely, Editor. 2007. p. 192-201.
91. Dempsey, N.C., et al., *Differential heat shock protein localization in chronic lymphocytic leukemia.* J Leukoc Biol, 2010. **87**(3): p. 467-76.
92. Bausero, M.A., et al., *Alternative mechanism by which IFN-gamma enhances tumor recognition: active release of heat shock protein 72.* J Immunol, 2005. **175**(5): p. 2900-12.
93. Davies, E.L., et al., *Heat shock proteins form part of a danger signal cascade in response to lipopolysaccharide and GroEL.* Clinical and Experimental Immunology, 2006. **145**(1): p. 183-189.
94. Evdonin, A.L., et al., *The release of Hsp70 from A431 carcinoma cells is mediated by secretory-like granules.* European Journal of Cell Biology, 2006. **85**(6): p. 443-455.
95. Guzhova, I., et al., *In vitro studies show that Hsp70 can be released by glia and that exogenous Hsp70 can enhance neuronal stress tolerance.* Brain Res, 2001. **914**(1-2): p. 66-73.
96. Lancaster, G.I. and M.A. Febbraio, *Exosome-dependent trafficking of HSP70: a novel secretory pathway for cellular stress proteins.* J Biol Chem, 2005. **280**(24): p. 23349-55.
97. Multhoff, G., et al., *A 14-mer Hsp70 peptide stimulates natural killer (NK) cell activity.* Cell Stress & Chaperones, 2001. **6**(4): p. 337-344.
98. Thery, C., et al., *Isolation and characterization of exosomes from cell culture supernatants and biological fluids.* Curr Protoc Cell Biol, 2006. **Chapter 3**: p. Unit 3.22.
99. Ireland, H.E. and J.H. Williams, *Measuring Hsp72 (HSPA1A) by indirect sandwich ELISA.* Methods Mol Biol, 2011. **787**: p. 145-53.
100. Basu, S., et al., *Necrotic but not apoptotic cell death releases heat shock proteins, which deliver a partial maturation signal to dendritic cells and activate the NF-kappa B pathway.* Int Immunol, 2000. **12**(11): p. 1539-46.
101. Clayton, A., et al., *Induction of heat shock proteins in B-cell exosomes.* J Cell Sci, 2005. **118**(Pt 16): p. 3631-8.
102. Kaur, J., et al., *Cell surface expression of 70 kDa heat shock protein in human oral dysplasia and squamous cell carcinoma: correlation with clinicopathological features.* Oral Oncology, 1998. **34**(2): p. 93-98.
103. Kleinjung, T., et al., *Heat shock protein 70 (Hsp70) membrane expression on head-and-neck cancer biopsy-a target for natural killer (NK) cells.* Int J Radiat Oncol Biol Phys, 2003. **57**(3): p. 820-6.
104. Korbelik, M., J.H. Sun, and I. Cecic, *Photodynamic therapy-induced cell surface expression and release of heat shock proteins: Relevance for tumor response.* Cancer Research, 2005. **65**(3): p. 1018-1026.
105. Multhoff, G., et al., *A Stress-Inducible 72-Kda Heat-Shock Protein (Hsp72) Is Expressed on the Surface of Human Tumor-Cells, but Not on Normal-Cells.* International Journal of Cancer 1995. **61**(2): p. 272-279.
106. Sapozhnikov, A.M., et al., *Translocation of cytoplasmic HSP70 onto the surface of EL-4 cells during apoptosis.* Cell Proliferation, 2002. **35**(4): p. 193-206.

107. Sapozhnikov, A.M., et al., *Spontaneous apoptosis and expression of cell surface heat shock proteins in cultured EL-4 lymphoma cells.* Cell Proliferation, 1999. **32**(6): p. 363-378.
108. Steiner, K., et al., *High HSP70-membrane expression on leukemic cells from patients with acute myeloid leukemia is associated with a worse prognosis.* Leukemia, 2006. **20**(11): p. 2076-2079.
109. Botzler, C., et al., *Definition of extracellular localized epitopes of Hsp70 involved in an NK immune response.* Cell Stress & Chaperones, 1998. **3**(1): p. 6-11.
110. Gehrmann, M., et al., *Membrane-bound heat shock protein 70 (Hsp70) in acute myeloid leukemia: a tumor specific recognition structure for the cytolytic activity of autologous NK cells.* Haematologica, 2003. **88**(4): p. 474-6.
111. Multhoff, G., et al., *Heat shock protein 70 (Hsp70) stimulates proliferation and cytolytic activity of natural killer cells.* Exp Hematol, 1999. **27**(11): p. 1627-36.
112. Gehrmann, M., et al., *Tumor-specific Hsp70 plasma membrane localization is enabled by the glycosphingolipid Gb3.* PLoS ONE, 2008. **3**(4).
113. Arispe, N., M. Doh, and A. De Maio, *Lipid interaction differentiates the constitutive and stress-induced heat shock proteins Hsc70 and Hsp70.* Cell Stress & Chaperones, 2002. **7**(4): p. 330-338.
114. Arispe, N., et al., *Hsc70 and Hsp70 interact with phosphatidylserine on the surface of PC12 cells resulting in a decrease of viability.* Faseb Journal, 2004. **18**(14): p. 1636-1645.
115. Rock, K.L., J.-J. Lai, and H. Kono, *Innate and adaptive immune responses to cell death.* Immunological Reviews, 2011. **243**: p. 191-205.
116. Seong, S.Y. and P. Matzinger, *Hydrophobicity: an ancient damage-associated molecular pattern that initiates innate immune responses.* Nature Reviews Immunology, 2004. **4**(6): p. 469-478.
117. Chen, G.Y. and G. Nunez, *Sterile inflammation: sensing and reacting to damage.* Nature Reviews Immunology, 2010. **10**(12): p. 826-837.
118. Green, D.R., *The End and After: How Dying Cells Impact the Living Organism.* Immunity, 2011. **35**(4): p. 441-444.
119. Green, D.R., et al., *Immunogenic and tolerogenic cell death.* Nature Reviews Immunology, 2009. **9**(5): p. 353-363.
120. Nunez, G., *Intracellular sensors of microbes and danger.* Immunological Reviews, 2011. **243**: p. 5-8.
121. Feng, H.P., et al., *Stressed apoptotic tumor cells stimulate dendritic cells and induce specific cytotoxic T cells.* Blood, 2002. **100**(12): p. 4108-4115.
122. Fucikova, J., et al., *High hydrostatic pressure induces immunogenic cell death in human tumor cells.* International Journal of Cancer, 2014. **135**(5): p. 1165-1177.
123. Komarova, E.Y., et al., *The discovery of Hsp70 domain with cell-penetrating activity.* Cell Stress & Chaperones, 2015. **20**(2): p. 343-354.
124. Panzarini, E., et al., *Rose Bengal Acetate PhotoDynamic Therapy (RBAc-PDT) Induces Exposure and Release of Damage-Associated Molecular Patterns (DAMPs) in Human HeLa Cells.* Plos One, 2014. **9**(8).
125. Panzarini, E., et al., *In vitro and in vivo clearance of Rose Bengal Acetate-PhotoDynamic Therapy-induced autophagic and apoptotic cells.* Experimental Biology and Medicine, 2013. **238**(7): p. 765-778.
126. Hahn, G.M. and G.C. Li, *Thermotolerance and heat shock proteins in mammalian cells.* Radiation research, 1982. **92**(3): p. 452-7.
127. Mambula, S.S. and S.K. Calderwood, *Heat induced release of Hsp70 from prostate carcinoma cells involves both active secretion and passive release from necrotic cells.* International Journal of Hyperthermia, 2006. **22**(7): p. 575-585.
128. Jalili, A., et al., *Effective photoimmunotherapy of murine colon carcinoma induced by the combination of photodynamic therapy and dendritic cells.* Clinical Cancer Research, 2004. **10**(13): p. 4498-4508.

129. Torok, Z., et al., *Plasma membranes as heat stress sensors: From lipid-controlled molecular switches to therapeutic applications.* Biochimica Et Biophysica Acta-Biomembranes, 2014. **1838**(6): p. 1594-1618.
130. Triantafilou, K., et al., *Fluorescence recovery after photobleaching reveals that LPS rapidly transfers from CD14 to hsp70 and hsp90 on the cell membrane.* Journal of Cell Science, 2001. **114**(13): p. 2535-2545.
131. Triantafilou, M., et al., *Mediators of innate immune recognition of bacteria concentrate in lipid rafts and facilitate lipopolysaccharide-induced cell activation.* Journal of Cell Science, 2002. **115**(12): p. 2603-2611.
132. Pomorski, T., et al., *Tracking down lipid flippases and their biological functions.* J Cell Sci, 2004. **117**(Pt 6): p. 805-13.
133. Schlegel, R.A. and P. Williamson, *Phosphatidylserine, a death knell.* Cell Death Differ, 2001. **8**(6): p. 551-63.
134. Tyurin, V.A., et al., *Oxidatively modified phosphatidylserines on the surface of apoptotic cells are essential phagocytic 'eat-me' signals: cleavage and inhibition of phagocytosis by Lp-PLA2.* Cell Death Differ, 2014. **21**(5): p. 825-35.
135. Segawa, K., J. Suzuki, and S. Nagata, *Constitutive exposure of phosphatidylserine on viable cells.* Proc Natl Acad Sci U S A, 2011. **108**(48): p. 19246-51.
136. Fischer, K., et al., *Antigen recognition induces phosphatidylserine exposure on the cell surface of human CD8+ T cells.* Blood, 2006. **108**(13): p. 4094-101.
137. Eder, C., *Mechanisms of interleukin-1β release.* Immunobiology, 2009. **214**(7): p. 543-553.
138. Vlassov, A.V., et al., *Exosomes: Current knowledge of their composition, biological functions, and diagnostic and therapeutic potentials.* Biochimica Et Biophysica Acta-General Subjects, 2012. **1820**(7): p. 940-948.
139. Yokota, S., M. Kitahara, and K. Nagata, *Benzylidene lactam compound, KNK437, a novel inhibitor of acquisition of thermotolerance and heat shock protein induction in human colon carcinoma cells.* Cancer Research, 2000. **60**(11): p. 2942-2948.
140. Koishi, M., et al., *The effects of KNK437, a novel inhibitor of heat shock protein synthesis, on the acquisition of thermotolerance in a murine transplantable tumor in vivo.* Clinical Cancer Research, 2001. **7**(1): p. 215-219.
141. Schroder, M. and R.J. Kaufman, *The mammalian unfolded protein response.* Annu Rev Biochem, 2005. **74**: p. 739-89.
142. Zhao, S., et al., *The role of c-Src in the invasion and metastasis of hepatocellular carcinoma cells induced by association of cell surface GRP78 with activated alpha2M.* BMC Cancer, 2015. **15**: p. 389.
143. Dorner, A.J., L.C. Wasley, and R.J. Kaufman, *Increased synthesis of secreted proteins induces expression of glucose-regulated proteins in butyrate-treated Chinese hamster ovary cells.* J Biol Chem, 1989. **264**(34): p. 20602-7.
144. Kitamura, M., *Biphasic, bidirectional regulation of NF-kappaB by endoplasmic reticulum stress.* Antioxid Redox Signal, 2009. **11**(9): p. 2353-64.
145. Schardt, J.A., B.U. Mueller, and T. Pabst, *Activation of the unfolded protein response in human acute myeloid leukemia.* Methods Enzymol, 2011. **489**: p. 227-43.
146. Schardt, J.A., et al., *Activation of the unfolded protein response is associated with favorable prognosis in acute myeloid leukemia.* Clin Cancer Res, 2009. **15**(11): p. 3834-41.
147. Liu, Y. and A. Chang, *Heat shock response relieves ER stress.* Embo j, 2008. **27**(7): p. 1049-59.
148. Yerushalmi, R., et al., *Cell surface GRP78: A potential marker of good prognosis and response to chemotherapy in breast cancer.* Oncol Lett, 2015. **10**(4): p. 2149-2155.
149. Toyoda, K., et al., *Grp78 Is Critical for Amelogenin-Induced Cell Migration in a Multipotent Clonal Human Periodontal Ligament Cell Line.* J Cell Physiol, 2016. **231**(2): p. 414-27.
150. Yao, X., et al., *Cell Surface GRP78 Accelerated Breast Cancer Cell Proliferation and Migration by Activating STAT3.* PLoS One, 2015. **10**(5): p. e0125634.

151. Shin, B.K., et al., *Global profiling of the cell surface proteome of cancer cells uncovers an abundance of proteins with chaperone function.* J Biol Chem, 2003. **278**(9): p. 7607-16.
152. Xiao, D., et al., *Identifying mRNA, microRNA and protein profiles of melanoma exosomes.* PLoS One, 2012. **7**(10): p. e46874.
153. Taylor, D.D., C. Gercel-Taylor, and L.P. Parker, *Patient-derived tumor-reactive antibodies as diagnostic markers for ovarian cancer.* Gynecol Oncol, 2009. **115**(1): p. 112-20.
154. Zhang, X., et al., *Endoplasmic reticulium protein profiling of heat-stressed Jurkat cells by one dimensional electrophoresis and liquid chromatography tandem mass spectrometry.* Cytotechnology, 2015.
155. Corey, S.J., et al., *Myelodysplastic syndromes: the complexity of stem-cell diseases.* Nat Rev Cancer, 2007. **7**(2): p. 118-29.
156. Aveic, S., et al., *Targeting BAG-1: a novel strategy to increase drug efficacy in acute myeloid leukemia.* Exp Hematol, 2015. **43**(3): p. 180-190.e6.
157. Schardt, J.A., et al., *Unfolded protein response suppresses CEBPA by induction of calreticulin in acute myeloid leukaemia.* J Cell Mol Med, 2010. **14**(6b): p. 1509-19.
158. Haefliger, S., et al., *Protein disulfide isomerase blocks CEBPA translation and is up-regulated during the unfolded protein response in AML.* Blood, 2011. **117**(22): p. 5931-40.
159. Huang, C.H., et al., *Role of HERP and a HERP-related protein in HRD1-dependent protein degradation at the endoplasmic reticulum.* J Biol Chem, 2014. **289**(7): p. 4444-54.
160. Sun, P.R., et al., *Genome-wide profiling of long noncoding ribonucleic acid expression patterns in ovarian endometriosis by microarray.* Fertil Steril, 2014. **101**(4): p. 1038-46.e7.
161. Caivano, A., et al., *High serum levels of extracellular vesicles expressing malignancy-related markers are released in patients with various types of hematological neoplastic disorders.* Tumour Biol, 2015. **36**(12): p. 9739-52.
162. Huan, J., et al., *Coordinate regulation of residual bone marrow function by paracrine trafficking of AML exosomes.* Leukemia, 2015. **29**(12): p. 2285-95.
163. Michalopoulou, S., et al., *Expression and inducibility of cytoprotective heat shock proteins in the bone marrow of patients with myelodysplastic syndrome: correlation with disease progression.* Haematologica, 2006. **91**(12): p. 1714-6.
164. Bernstein, H., et al., *Activation of the promoters of genes associated with DNA damage, oxidative stress, ER stress and protein malfolding by the bile salt, deoxycholate.* Toxicol Lett, 1999. **108**(1): p. 37-46.
165. Jamora, C., G. Dennert, and A.S. Lee, *Inhibition of tumor progression by suppression of stress protein GRP78/BiP induction in fibrosarcoma B/C10ME.* Proc Natl Acad Sci U S A, 1996. **93**(15): p. 7690-4.
166. Zinszner, H., et al., *CHOP is implicated in programmed cell death in response to impaired function of the endoplasmic reticulum.* Genes Dev, 1998. **12**(7): p. 982-95.
167. Slodzinski, H., et al., *Homocysteine-induced endoplasmic reticulum protein (herp) is up-regulated in parkinsonian substantia nigra and present in the core of Lewy bodies.* Clin Neuropathol, 2009. **28**(5): p. 333-43.
168. Ma, Y. and L.M. Hendershot, *Herp is dually regulated by both the endoplasmic reticulum stress-specific branch of the unfolded protein response and a branch that is shared with other cellular stress pathways.* J Biol Chem, 2004. **279**(14): p. 13792-9.
169. Althausen, S. and W. Paschen, *Homocysteine-induced changes in mRNA levels of genes coding for cytoplasmic- and endoplasmic reticulum-resident stress proteins in neuronal cell cultures.* Brain Res Mol Brain Res, 2000. **84**(1-2): p. 32-40.
170. Hong, C.S., et al., *Isolation and characterization of CD34+ blast-derived exosomes in acute myeloid leukemia.* PLoS One, 2014. **9**(8): p. e103310.
171. Gu, X., et al., *Improved vaccine efficacy of tumor exosome compared to tumor lysate loaded dendritic cells in mice.* Int J Cancer, 2015. **136**(4): p. E74-84.
172. Yao, Y., et al., *Dendritic cells pulsed with leukemia cell-derived exosomes more efficiently induce antileukemic immunities.* PLoS One, 2014. **9**(3): p. e91463.

173. Hedlund, M., et al., *Thermal- and oxidative stress causes enhanced release of NKG2D ligand-bearing immunosuppressive exosomes in leukemia/lymphoma T and B cells.* PLoS One, 2011. **6**(2): p. e16899.
174. Takeuchi, T., et al., *Intercellular chaperone transmission via exosomes contributes to maintenance of protein homeostasis at the organismal level.* Proceedings of the National Academy of Sciences of the United States of America, 2015. **112**(19): p. E2497-E2506.
175. Matzinger, P., *An innate sense of danger.* Seminars in Immunology, 1998. **10**(5): p. 399-415.
176. De Maio, A., *Extracellular heat shock proteins, cellular export vesicles, and the Stress Observation System: a form of communication during injury, infection, and cell damage. It is never known how far a controversial finding will go! Dedicated to Ferruccio Ritossa.* Cell Stress Chaperones, 2011. **16**(3): p. 235-49.